MOLECULAR PROBES FOR STUDYING HEME TOXICITY AND TOLERANCE IN GRAM POSITIVE PATHOGENS

By

Laura Anzaldi Mike

Dissertation

Submitted to the Faculty of the

Graduate School of Vanderbilt University

in partial fulfillment of the requirements

for the degree of

DOCTOR OF PHILOSOPHY

in

Microbiology and Immunology

December, 2013

Nashville, Tennessee

Approved:	Date:
Eric P. Skaar	08/29/13
D. Borden Lacy	08/29/13
Timothy L. Cover	08/29/13
David W. Wright	08/29/13
Gary A. Sulikowski	08/29/13

To Chris,

my beloved husband and best friend

ACKNOWLEDGMENTS

More than anything, I would like to first acknowledge my mentor, Dr. Eric Skaar. He is an example of what a mentor should be. He has taught me how to think and write and work as a scientist. He has been exceptionally encouraging and supportive of my ideas and endeavors both in and out of the lab, as well as a source of great advice. He provides a contagious source of energy and enthusiasm to the laboratory, which has produced a fun and exciting training environment.

Next, I would like to thank each of the members of the Skaar lab, past and present, who have mentored me, made school a joy, and been great friends. This includes: Dr. Devin Stauff, Dr. Michelle Reniere, Amanda McCoy, Sheg Aranmolate, Dr. Indriati Hood, Keith Adams, Dr. Ahmed Attia, Susan Dickey, Dr. Thomas Kehl-Fie, Kathryn Haley, Dr. Neal Hammer, Amanda Hirsch, Lorenzo Olive, Dr. Allison Farrand, Dr. Catherine Wakeman, Kyle Becker, Jessica Moore Hooten, Ben Gu, Dr. Jim Cassat, Dr. Brittany Mortensen, Julie Lemen, Matt Surdel, Dr. Mike Noto, Shawn Albert, Lillian Johnson, and Lisa Lojek. Devin (DLS), Sheg (OA), Thomas (TKF), Lorenzo (LQO), and Jessica (JMH) have all contributed to work presented here and I have acknowledged their contributions throughout my thesis with their initials. I would like to thank Amanda McCoy for generating the Skaar lab transposon library. I would also like to thank Kathryn Haley, who generously shared purified IsdG for use as a protein standard. I would also like to thank a former rotation student, Shawn Barton, for his work transducing SaeRS-regulated genes into *S. aureus* strain Newman. I would like to thank Jim Cassat who has also worked on the ‘882 project, although none of our work together made it into my dissertation. Finally I would like to thank my running buddy Brittany for being a consistent source of joy and consolation.

I would be amiss not to recognize the indelible mark Devin has made on my training and research. Devin’s hard work and diligence during his graduate work formed the foundation for what I have described here. Beyond that, Devin patiently taught me many of my bench skills.

Most people who know Devin recognize that he is not only intelligent, but also an excellent teacher and mentor. That is exemplified by the fact that as a professor at Grove City College, his own undergraduate trainees have directly contributed to work described here. Devin and two of his students, Jacob Choby (JC) and Paul Brinkman (PB), have been critical to the success of the *B. anthracis* project.

Working in the field of chemical biology is a highly interdisciplinary field and as such I have had the good fortune to have great collaborators. Dr. Friedrich Götz shared his *hemB*::*ermC* strain. Daniel Dorset and the Vanderiblt HTS facility guided our high-throughput screening efforts. Xenogen shared the pXen-1 plasmid with us. Dr. Carrie Jones and her lab assisted with the formulation of our compounds for use in mice. Dr. Brian Hachey and M. Lisa Manier in the Mass Spectrometry Resource Core assisted with the HPLC-MS quantitation. Nicholas Vitko (NPV) and Dr. Anthony Richardson from UNC-Chapel Hill contributed to our studies on central metabolism. Sarah Sullivan (SS) and Dr. Jennifer DuBois performed direct quantification of heme by MS. Dr. Chia Lee kindly shared *S. aureus* strain Newman Δ*saeRS* and *saeS*::P18L. Dr. Taeok 'Ted' Bae shared anti-SaeQ antibodies. I would like to thank Dr. Maria Hadjifrangiskou for sharing purified QseB and Dr. Suzanne Walker for sharing targocil. Finally, I would like to thank Dr. Paul Dunman for his help with *S. aureus* microarrays.

Dr. Gary Sulikowski and two of his lab members, Brendan Dutter (BFD) and Dr. Paul Reid deserve special recognition. I have collaborated very closely with Dr. Sulikowski and first Paul, then Brendan. Without their help this thesis would have never come to fruition. They have developed all of the synthetic chemistry involved in this project as well as contributed intellectually to the project. I have benefited greatly from having Dr. Sulikowski as a mentor and a member of my committee.

Other professors who have been kind enough to serve on my committee include my chair, Dr. Borden Lacy, Dr. Timothy Cover, Dr. David Wright and Dr. Eric Skaar. I thank each of them for the time they have taken to provide guidance and advice. From the former Microbiology &

Immunology department I would like to thank our former chair Dr. Jacek Hawiger for his dedication to training young scientists, our former education coordinator Jean Teadwell, and Mark Hughes for his help surrounding travel. From the new Department of Pathology, Microbiology & Immunology I would like to thank our chair Dr. Sam Santoro for his support, Matt Bruckse for his assistance regarding meeting attendance, and the graduate education office, especially Lorie Franklin and Audrey Patrick. My graduate education has also been enriched by training opportunities through the Vanderbilt Institute for Chemical Biology (VICB). I would like to specifically thank Dr. Michelle Sulikowski and Amanda Renick for their support. I would also like to thank the Biomedical Research Education & Training (BRET) office for their assistance, especially Dr. Lindsay Meyers, Dr. Michelle Grundy, Dr. Jim Patton, and Dr. Roger Chalkley.

I was supported by the Immunobiology of Blood and Vascular Systems training grant from the NIAID, NIH grant T32 HL069765. This work was supported by the Searle Scholars Program, NIH grant U54 AI057157-06 from Southeastern Regional Center of Excellence for Emerging Infections and Biodefense, the Burroughs Wellcome Fund, and NIH AI069233 and AI073843. The HTS was supported by a pilot grant from the VICB.

To my friends in Nashville and elsewhere, who have encouraged me and shown me love – thank you. Most of all, I want to thank my family for supporting me throughout all of my education. My parents have always done their best to encourage my academic pursuits and I would not be here today without their love and support. I thank my husband Chris for patiently standing by my side for these five years. Thank you for all the sacrifices you have made to help me get my degree. I am blessed to have you as my husband.

TABLE OF CONTENTS

LIST OF TABLES

LIST OF FIGURES

LIST OF ABBREVIATIONS

ATP ..... adenosine triphosphate

CF ..... cystic fibrosis

CFU ..... colony forming unit

DR ..... direct repeat

heme ..... ferriprotoporphyrin IX

HK ..... histidine kinase

Hrt ..... heme regulated transporter

Hss ..... heme sensor system

HTS ..... high-throughput screen

IP ..... intraperitoneal

Isd ..... iron-regulated surface determinant

KCN ..... potassium cyanide

MK ..... menaquinone

MS ..... mass spectrometry

NARSA ..... Network on Antimicrobial Resistance in *S. aureus*

NFDM ..... non-fat dry milk

OD_{600} ..... optical density at 600 nm

PBS ..... phosphate buffered saline

pmf ..... proton motive force

PMN ..... polymorphonuclear leukocytes

PPIX ..... protoporphyrin IX

RR ..... response regulator

SAR ..... structure-activity relationship

SCV ..... small colony variant

SNP ..... single nucleotide polymorphism

TBS ..... tris buffered saline

TCS ..... two-component system

VANTAGE ..... Vanderbilt Technologies for Advanced Genomics

VICB ..... Vanderbilt Institute for Chemical Biology

WT ..... wildtype

CHAPTER I

INTRODUCTION

Staphylococcus aureus and *Bacillus anthracis* are important human pathogens.

Staphylococcus aureus is a Gram positive commensal organism that inhabits the anterior nares of 30% of the population (27). While colonization of the nares is relatively harmless, once *S. aureus* crosses the host epithelium it is capable of infecting nearly any host tissue. The morbidity and mortality associated with *S. aureus* infections are high and treatment is often challenging as *S. aureus* is constantly developing resistance to antibiotics. The ubiquitous presence of *S. aureus* in the human population, its ability to infect nearly any human tissue, and the increasing incidence of hospital-acquired and community-acquired multi-drug resistant *S. aureus* (MRSA) infections are reasons for alarm and highlight the necessity for identifying novel therapeutic targets to combat this pathogen.

Bacillus anthracis and *S. aureus* both belong to the Bacillales order of the Firmicutes. Among many differences from *S. aureus*, *B. anthracis* forms spores and primarily causes disease in livestock. Infection of humans with *B. anthracis* spores by either ingestion or inhalation is often associated with septicemia. Once the spores enter the blood, they germinate to vegetative cells which divide rapidly and at the time of death may account for 30% of a human's blood weight (21). The resiliency of and the mortality associated with *B. anthracis* spores makes the bacterium a potential bioweapon, as evidenced by the 2001 attacks sent through the US postal service. As such, a great deal of biodefense research has focused on anthrax pathogenesis, which is important for developing vaccines and treatments to protect humans from this biological threat.

B. anthracis and *S. aureus* are both pathogens that pose a significant threat to public health. Infections by either of these bacteria consist of a significant blood-component suggesting that they have intimate interactions with host leukocytes and erythrocytes. Defining how these

pathogens adapt to the host environment, particularly the blood, is imperative for advancing the methods by which we treat these aggressive infections.

Iron is an essential nutrient for pathogens.

Iron is a transition element with a high redox potential. This makes it a valuable cofactor for enzymes involved in protecting bacteria from host defenses, DNA replication, and respiration. Since iron is intimately involved in basic physiological processes, almost all pathogens require iron to successfully infect their hosts (96). At physiological pH, however, ferric iron is highly insoluble. Coordinating iron within a tetrapyrrole ring as ferriprotoporphyrin IX (heme) solubilizes iron and enhances its catalytic ability by 5 to 10 orders of magnitude (9). This catalytic activity is harnessed by hemoproteins involved in oxygenation reactions, oxidative stress responses, electron transport, oxygen transport, oxygen sensing, and oxygen storage. Both *S. aureus* and *B. anthracis* have the machinery to synthesize endogenous heme from glutamyl-$tRNA^{Glu}$ (57). While endogenous heme biosynthesis allows pathogens to solubilize, store, and augment the utility of iron, exogenous iron is still required for heme biosynthesis. In the vertebrate host, a major source of iron is in the form of heme bound to host hemoglobin in erythrocytes in the blood, a site accessed by both *S. aureus* and *B. anthracis*. Little is known about the dynamics between endogenously synthesized and exogenously acquired heme during bacterial pathogenesis. Data presented in Chapter II increase our understanding of the mechanisms by which *S. aureus* regulates endogenous heme biosynthesis.

Heme is both an iron source and a toxic liability to bacteria.

Since heme is the most abundant iron source in the vertebrate host and a valuable nutrient, bacterial pathogens have many systems for acquiring host heme. Both *S. aureus* and *B. anthracis* utilize the *i*ron-regulated *s*urface *d*eterminant (Isd) system to acquire heme-iron during infection (67). Once heme enters the cytoplasm it is degraded by IsdG family heme oxygenases to

staphylobilin and free iron (68). In iron-replete conditions, however, heme is no longer degraded. Instead, it is trafficked to the cell membrane where it is most likely used as a cofactor in proteins involved in respiration (77). *S. aureus* and *B. anthracis* both dedicate significant efforts to acquiring heme however too much heme is toxic to the bacteria (48, 83). While much is known about the mechanisms of heme toxicity in eukaryotes, most are not applicable to bacteria (1). The mechanisms by which heme is toxic to bacteria seem to be distinct from those in humans, yet they remain ill-defined (1). Currently there exist two ideas for the mechanism of bacterial heme toxicity. One suggests that DNA damage by heme is a source of toxicity to the cell, while the other proposes that heme-menaquinone interactions generate a superoxide generating cycle that is detrimental to *S. aureus* (44, 93). While identifying the source of heme toxicity is of great interest, studies presented here focus primarily on the mechanisms by which *S. aureus* and *B. anthracis* sense and alleviate heme toxicity.

***S. aureus* and *B. anthracis* sense heme to alleviate its toxicity.**

Previous work revealed that pre-treating either *S. aureus* or *B. anthracis* with a sub-toxic concentration of heme protects both bacteria from heme toxicity (90). This protection is mediated by the two-component signaling (TCS) system, *h*eme *s*ensor *s*ystem (HssRS) (Figure 1). In the presence of heme the HssS histidine kinase (HK) is auto-phosphorylated at a conserved histidine residue (Figure 1A) (83, 85). HssS then transfers this phosphate to an aspartic acid on its cognate response regulator (RR) HssR (Figure 1B). This activates HssR and allows it to bind to a conserved direct repeat (DR) in the promoter region upstream of the *h*eme *r*egulated *t*ransporter (*hrtAB*) to initiate transcription (Figures 1C-D). HrtAB is an ABC transporter that alleviates heme toxicity by a yet-to-be determined mechanism, most likely heme efflux (Figure 1E) (42). While the signaling pathway responsible for protecting *S. aureus* and *B. anthracis* from heme toxicity has been well-characterized, the ligand of HssS remains elusive. This is not uncommon for a

TCS, as less than 20 ligand-sensor pairs have been assigned for the over 20,000 predicted TCSs (40).

Heme sensing is conserved across Gram positive pathogens.

Heme sensing systems are found in many bacteria and the *hss/hrt* system is evolutionarily conserved across many Gram positive bacteria. This includes several pathogens such as *Staphylococcus epidermidis, Bacillus cereus, Listeria monocytogenes, Listeria inocua,* and *Enterococcus faecalis* (12, 84). The *hss/hrt* systems are generally found in either pathogenic or saprophytic Gram positive bacteria. For example, *hss/hrt* systems are found in *B. anthracis, B. cereus,* and *B. thuringiensis,* but not *B. subtilis* and *B. licheniformis* (83). In fact, *B. subtilis* and *B. licheniformis* are both more sensitive to heme toxicity than any of the *Bacilli* that encode an *hss/hrt* system. These observations suggest that the *hss/hrt* system is maintained by bacteria that come in contact with host blood and that it might be used to signal to the bacteria that they have entered their host.

Aside from the initial identification and characterization of HssRS and HrtAB in *S. aureus* and *B. anthracis,* orthologous HrtAB systems have been most thoroughly described in *Lactococcus lactis* and *Streptococcus agalactiae* (18, 42, 61, 82, 83, 85, 90). Neither of these species synthesize their own heme and as such require exogenous heme to activate respiration (17, 98). Although the function of HrtAB in each of these species is analogous to HrtAB in *S. aureus* and *B. anthracis*, each species has its unique strategy for maintaining heme homeostasis.

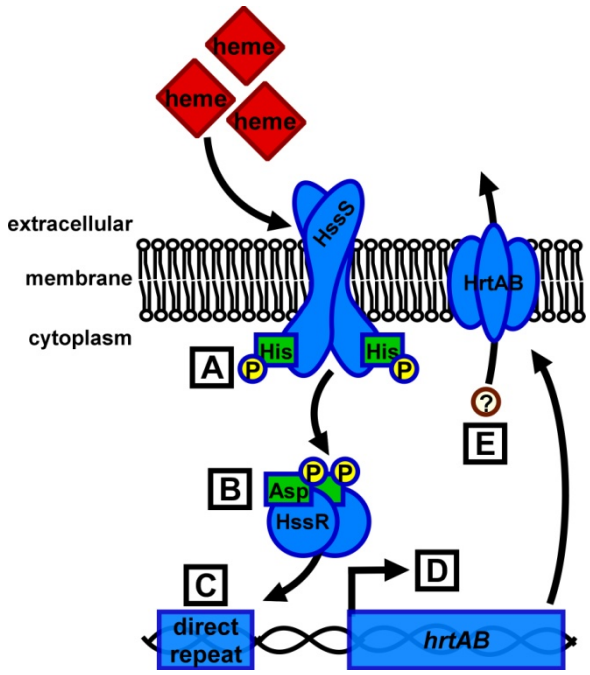

Figure 1. The HssRS two-component signaling system. ***A.*** In the presence of heme the HssS histidine kinase autophosphorylates at a conserved histidine residue located on the intracellular domain. ***B.*** The phosphate is transferred from HssS to a conserved aspartic acid on its cognate response regulator HssR. ***C.*** HssR is activated and binds to a conserved direct repeat DNA sequence in the promoter region of *hrtAB*. ***D.*** This increases expression of the *h*eme-*r*egulated *t*ransporter HrtAB. ***E.*** HrtAB alleviates heme toxicity by a yet-to-be-determined mechanism.

S. agalactiae encodes orthologous HssRS and HrtAB systems (18). *S. agalactiae* HssRS is stimulated by heme and results in high expression of *hrtAB* in the concentration range of 1 to 10 μM heme (18). Distinct from *S. aureus* and *B. anthracis*, *S. agalactiae* also encodes two other dual heme and protoporphyrin IX (PPIX) efflux pumps, *pefAB* and *pefCD* (18). These two efflux pumps are repressed by the MarR-superfamily repressor, PefR, at concentrations of less than 0.3 μM heme and 1 μM PPIX (18). The observation that *pefAB* and *pefCD* are activated at low heme and PPIX concentrations, while *hrtAB* is activated at higher heme concentrations suggests that the *pef* transporters are utilized to fine tune intracellular heme and PPIX levels while *hrtAB* is employed to protect *S. agalactiae* from heme toxicity in heme-rich environments (18). The differential activity of two heme-regulated transport systems highlights the delicate lifestyle *S. agalactiae* strives to maintain in order to cope with the heme paradox (1).

L. lactis also encodes an orthologous *hrtBA* (*ygfBA*) that, when mutated, results in increased sensitivity to heme toxicity (61). However, a corresponding HssRS TCS has not been identified in this species. Instead, *L. lactis* encodes a unique TetR-family transcriptional regulator, *hrtR* (*ygfC*), adjacent to *hrtBA* (42). HrtR binds heme, which alleviates HrtR repression of the *hrtRBA* operon promoter and increases expression of HrtR and HrtAB at heme concentrations ranging from 1 to 5 μM (42). Notably HrtR is also responsive to GaPPIX, but not most other metalloporphyrins (42). In *L. lactis* Δ*hrtRBA*, over-expression of *hrtBA* results in reduced accumulation of heme, suggesting that HrtAB is a heme efflux pump in *L. lactis* (42). Currently, these results have not been confirmed in any other *hrtAB* encoding bacterial species.

These studies of heme homeostasis in other Gram positive bacteria highlight the unique strategies bacteria employ in order to balance the energetic benefits of heme with its toxicity. This underscores the importance of maintaining appropriate intracellular levels of heme in diverse environments.

The ability to resist heme toxicity is important in pathogenesis.

TCSs are the primary way that bacteria adapt to environmental changes. Since heme is a host molecule it is likely that HssRS is activated during infection. This hypothesis is supported by the observation that the *hrt* promoter is transcriptionally active during *B. anthracis* infection (83). Furthermore the importance of HssRS heme sensing during bacterial pathogenesis is highlighted by the observation that BALB/c mice infected with *S. aureus* Δ*hssR* have significantly increased bacterial burdens in the livers (90). Taken together, these results support that HssRS mediated protection against heme toxicity during infection maintains the bacteria in a less virulent state. As such, small molecule activators of HssRS may be viable therapeutics for treating patients with aggressive *S. aureus* or *B. anthracis* infections.

A chemical genetics approach for studying bacterial signal transduction.

TCS signaling in response to host stresses is a critical aspect of bacterial adaptation to the host and other environmental changes. Years of probing TCS activity and function using classical genetic and biochemical techniques have provided insights into their biology. The scientific community has now identified a small fraction of the ligand-sensor pairs and come to understand some mechanisms by which TCS signaling purity is maintained; yet there are hints that bacterial signaling transduction may be more complex than previously thought. In order to further the field's understanding of bacterial signaling networks, new strategies need to be employed. A chemical genetics approach has been applied to HssRS and TCS biology here.

Chemical genetics is similar to classical genetics, but instead of using molecular techniques to study gene function, small molecules are used instead. To illustrate this more clearly, consider the example of identifying the genes required for protein secretion in *S. aureus*. In forward genetics, a genome would be randomly mutagenized to create a library of mutants and then that library would be screened for loss of protein secretion. Identifying the mutagenized gene that results in that loss of protein secretion ascribes a role of that gene in the production of protein

secretion. However, what if the genes required for protein secretion are essential? Or, what if multiple genes need to be disrupted to affect protein secretion? When combined with chemical genetics, some of these limitations may be overcome. Continuing with the example from above, the chemical genetics approach would screen a library of small molecules for effecting loss of protein secretion in bacteria. By characterizing the activity of the small molecules at a cellular level, other aspects of protein secretion may be elucidated.

A chemical genetics approach was undertaken to expand the current understanding of heme homeostasis and signaling networks in *S. aureus* and *B. anthracis* and to complement previous studies probing bacterial heme sensing by more classical approaches. The work described here has developed two small molecule activators of HssRS into tools for studying bacterial physiology and signal transduction and defines their potential use in perturbing bacterial pathogenesis.

CHAPTER II

MECHANISM OF HssRS ACTIVATION BY SMALL MOLECULE VU0038882

Introduction

Staphylococcus aureus is a commensal organism that primarily colonizes the anterior nares, as well as the skin (30). Upon breaching the epithelium of its host, *S. aureus* has the potential to infect virtually any tissue. This adaptability reflects the capacity of *S. aureus* to sense a variety of environmental signals and integrate them into its metabolic program enabling growth in diverse host niches.

Upon entering the iron-poor environment of the vertebrate host, the cellular program to import ferriprotoporphyrin IX (heme) from host hemoglobin into the cell is activated in order to satisfy cellular iron and heme requirements (51). *S. aureus* may also synthesize heme endogenously through the coordinated effort of enzymes encoded by the *hemAXCDBL, hemEHY,* and *hemN* operons, although this process requires that iron and other building blocks be available to the bacteria (33). The ability to exogenously acquire and endogenously synthesize heme allows *S. aureus* to satisfy cellular iron and heme requirements in diverse environments. This strategy is typical for most bacterial pathogens and reflects the integral role of heme in metabolism and physiology; however, the distinct contributions of endogenous and exogenous heme to the cellular physiology of bacteria are unknown.

Heme is a co-factor required for respiration. Furthermore, *S. aureus* respiration requires that the bacteria either synthesize or assimilate the electron carrier menaquinone (MK) and that a terminal electron acceptor be available. During respiration, reducing equivalents derived from the oxidation of carbon sources are donated to MK. The shuttling of electrons by MK through the electron transport chain generates a proton motive force (pmf) across the cytoplasmic membrane.

The energy stored in the pmf powers ATP synthesis and nutrient import. When heme, MK, or terminal electron acceptors are absent, *S. aureus* captures energy through fermentation. Fermentation employs substrate-level phosphorylation, which produces acid end products, to generate ATP and maintain the redox balance of the cell. Figure 2 outlines central metabolism in *S. aureus.*

Without heme, central metabolic pathways and enzymes cannot function; however, excess heme is toxic due to its redox cycling properties (93). Prior exposure of *S. aureus* to subinhibitory concentrations of heme increases heme tolerance (90). This adaptation is due to the heme-induced increase in expression of HrtAB, an efflux pump that protects the bacteria from heme toxicity. The increased expression of *hrtAB* is mediated by the *h*eme *s*ensor *s*ystem (Hss) two-component system (TCS). While the signaling pathway of HssRS has been previously described, the mechanism of activation remains to be determined. Defining the mechanisms by which HssRS is activated would reveal the signals that alert *S. aureus* to adapt to its host and inform the rational design of new therapeutic strategies that could subvert *S. aureus* energy homeostasis during infection.

In this study, the mechanism of HssS stimulation was probed by identifying small molecule activators of HssS. The most potent compound, VU0038882 (‘882), activates HssRS by inducing endogenous heme biosynthesis in *S. aureus* and leads to increased intracellular heme levels. A transposon screen for ‘882-insensitive mutants revealed that perturbations in central metabolism influence heme homeostasis. These studies have provided new insights into heme homeostasis and HssRS activation in *S. aureus* and highlight the utility of ‘882 as a powerful probe of bacterial physiology.

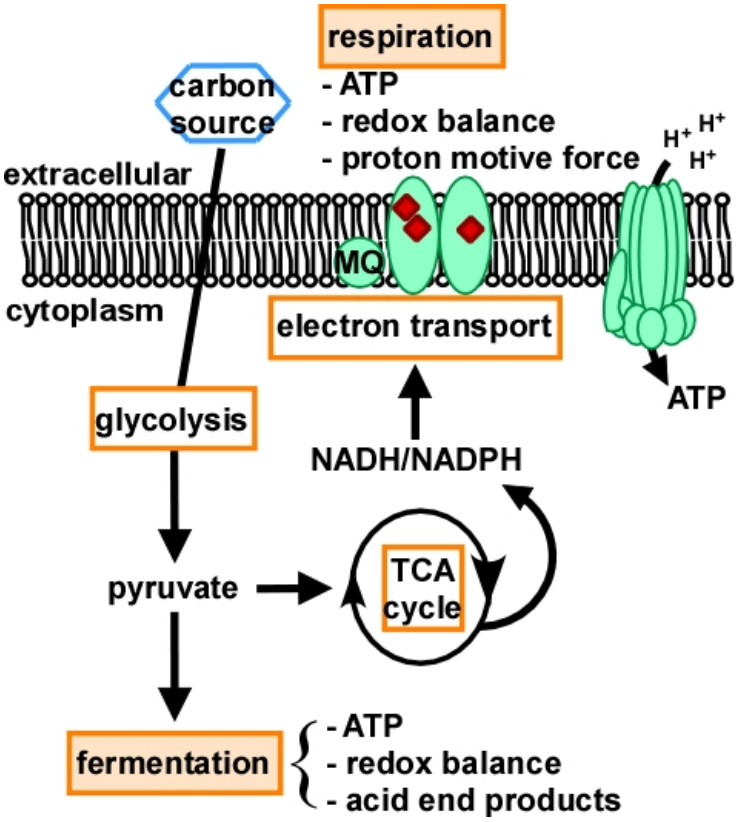

Figure 2. A schematic of central metabolism in *S. aureus*. Carbon sources such as glucose are brought into the cell and converted to pyruvate. During fermentation pyruvate is metabolized to acid end products such as lactate, ethanol, and acetate. The conversion of pyruvate to acid end products produces ATP and maintains the redox balance of the cell by regenerating NAD+. During respiration, pyruvate is shuttled into the TCA cycle. The conversion of pyruvate in the TCA cycle produces some ATP and many reducing equivalents in the form of NADH. The electrons from NADH are abstracted and shuttled through the electron transport chain by the electron carrier menaquinone. This transfer of electrons extrudes protons and generates a proton motive force (pmf). The pmf is harnessed by ATP synthase to produce more ATP for the cell. The cytochromes involved in electron transport require heme and menaquinone in order to successful shuttle electrons. Without heme or menaquinone, respiration does not occur.

Methods

Bacterial strains and growth conditions - *Staphylococcus aureus* strains Newman, Δ*hssR,* Δ*hssS*, Δ*hssRS*, Δ*menB* and Δ*isdG* have been described previously (16, 51, 83, 90, 93). *S. aureus hemB::ermC* (Δ*hemB*) has been described previously and was transduced into Newman using bacteriophage Φ-85 (51, 92). The Δ*pfk*A deletion construct (pBT2-ΔpfkA) was made by cloning the flanking regions of the *S. aureus pfkA* gene (primers: pfkA-5.1A, pfkA-5.1B, pfkA-3.1A, pfkA-3.1B) into the *S. aureus*/*E. coli* shuttle vector pBT2ts (53). This construct was then used to make an in-frame deletion of the *pfkA* gene in the wildtype *S. aureus* Newman background as previously described using TSB media without dextrose supplemented with 1% sodium pyruvate (23). *Corynebacterium diphtheriae* strain HCL2 and *Staphylococcus haemolyticus* strain NRS9 were used.

All *S. aureus* strains were grown on tryptic soy agar (TSA) containing 10 μg/ml chloramphenicol when appropriate and grown at 37°C for 20-30 h. All overnights were grown in 5 ml of tryptic soy broth (TSB) at 37°C with shaking at 180 rpm unless otherwise noted. Unless stated otherwise, vehicle treatment refers to a volume of DMSO comparable to the volume added containing the described compound (‘882).

Small molecule library screen with luciferase reporter - An overnight of Newman p*hrt.lux* was sub-cultured into 500 ml in a 1.5 L flask. The cells were grown for 1.5 h to an OD_{600} between 0.60–0.65. Seventy-five μl of culture were transferred into each well of a 384 well, flat-bottom plate containing synthetic compounds that resulted in a final concentration of 6.7 μM. DMSO and heme were used as negative and positive controls, respectively. The plates were incubated for 3 h. Luminescence values were measured either using a Synergy HT Multi-Mode Microplate Reader (Biotek, Inc.) or TopCount NXT™ Microplate Scintillation and Luminescence Counter (PerkinElmer, Inc.). A compound was considered a hit if the raw luminescence value exceeded the luminescence of cells grown in the presence of 81.25 nM heme.

XylE reporter assays - XylE assays were performed as described previously with modifications in growth conditions (90). For the Δ*hemB* experiments, overnights were sub-cultured 1:50 into 0.5 ml of media for 4 h. For all other reporter assays, the bacteria were grown for 9 h and diluted 1:100 into 0.5 ml of media for 15 h.

Chemical libraries - The synthetic compounds were obtained from the Vanderbilt Institute of Chemical Biology (VICB) collection, which is a high-diversity, synthetic small-molecule library consisting of approximately 160,000 compounds. Select compounds were repurchased from either ChemBridge or ChemDiv.

Growth curve analyses - Overnight cultures of Newman were diluted 1:100 into 100 µl of media. Bacterial cells were incubated and the OD_{600} was measured at the specified time points. For all staphylococcal adaptations, cultures were inoculated in 0.5 ml of TSB for 1 h at 37°C, 180 rpm and sub-cultured 1:100 in 100 ul of media containing the indicated additive. Cultures were pre-adapted overnight and analyzed as described above for a typical growth curve.

C. diphtheriae was inoculated into TSB containing vehicle, 5 µM heme, or 50 µM '882 and grown for 22-24 h. Cultures were diluted 1:50 into 5 ml of media containing 15 µM heme and grown with shaking at 180 rpm and 37°C. CFUs were enumerated on TSA.

Transposon library generation and screen - A transposon library was generated using Tn*917* (8). The pTV1 transposition vector was transformed into *S. aureus* Newman and selected for on TSA containing erythromycin (10 µg/ml) and chloramphenicol (10 µg/ml). Tn*917* transposition was induced on TSA-erythromycin (10 µg/ml) at 43°C for 24 h and mutants were screened for chloramphenicol sensitivity and erythromycin resistance in TSB at 37°C. Transposon mutants were arrayed in 96 well plates and stored at -80°C.

Mutants were revived in 150 µl of TSB and grown for 7 h before being sub-cultured 1 µl into 100 µl of 40 µM '882 in TSB and incubated overnight. Cultures were diluted 1:100 into 100 µl of TSB containing 20 µM heme. Bacterial cells were incubated and the OD_{600} was measured at 5 h and 7 h. Mutants with an OD_{600} more than 2 standard deviations below the plate average were

isolated for single colonies on TSA-erythromycin (10 μg/ml) and confirmed in a second adaptation in triplicate.

Transposon integration site identification - Transposon mutants were isolated on TSA-erythromycin (10 μg/ml) and grown overnight in TSB-erythromycin (10 μg/ml). Genomic DNA was isolated from 4 ml of the overnight using a Wizard Genomic purification kit (Promega). Genomic DNA (2 μg) was digested with DraI at 37°C overnight. DraI was heat inactivated and 200 μg of the digested DNA ligated at room temperature for 2 h. Ligated DNA (20 ng) was PCR amplified using DLS479 and DLS480 (53). PCR products were treated with exonuclease I (NEB) and SAP (Promega) according to the manufacturer's instructions. PCR-amplified DNA was column purified using a PCR Purification Kit (Qiagen) and sequenced using DLS493 or DLS494 (53). The sequence flanking the *tn917* inverted repeat was used to interrogate the *S. aureus* Newman genome sequence to determine the *tn917* integration site. Some integration sites were identified using previously published methods (2).

Metabolite detection - An overnight of Newman was diluted 1:100 in 125 ml of TSB containing either vehicle or 40 μM '882. Each hour, 5 ml of culture were sampled and pelleted by centrifugation at 3,200 x *g*. The pH of the supernatant was measured using a SevenEasy pH meter (Mettler Toledo). Glucose and lactate concentrations were quantified according to the manual (r-Biopharm) with the assays scaled to a final volume of 300 μl.

For the characterization of Δ*pfkA*, cultures were grown overnight at 37°C, in TSB+P (1% sodium pyruvate), with shaking at 250 rpm. Cultures were diluted to an OD_{660} of 0.05 in 8 ml of TSB+P and incubated at 37°C with shaking at 250 rpm (18x150 mm culture tube). Each hour, 350 μl of culture were sampled and analyzed for absorbance (OD_{660}). Two-hundred μl were pelleted at 16,000 x *g* for 1 min and the supernatants frozen at -20°C. Samples were thawed on ice. The pH was measured using Sigma pH Tests Strips (P-3536) and glucose levels were quantified using the R-Biopharm D-Glucose Kit (10 716 251 035).

Pyridine hemochromogen heme quantification assay - Bacteria were grown for 8 h. The cultures were diluted 1:100 and grown aerobically for 15-17 h. Pellets were washed in 0.5 ml of 20 mM K_2HPO_4/KH_2PO_4 (pH 7.6) and resuspended in 0.5 ml of 20 mM K_2HPO_4/KH_2PO_4 (pH 7.6) containing 30 μg of lysostaphin and incubated at 37°C for 20 min. Each sample was lysed by sonication and the protein concentration determined using a Pierce BCA Protein Assay Kit according to the manual (Thermo Scientific). Heme was extracted by adding an equal volume of 0.4 M NaOH and 40% pyridine and quantified as previously described using an extinction coefficient of 324 $mM^{-1}cm^{-1}$ (71).

Heme quantification by LC-MS - *S. aureus* was grown in 5 ml of TSB for 8 h and sub-cultured 1:250 into 300 ml of TSB containing DMSO or 40 μM '882. Cells were grown at 37°C, 200 rpm for 15 h and CFUs were enumerated. Cells were pelleted at 10,500 x *g* for 15 min and the pellets were washed in 30 ml of 20 mM potassium phosphate (pH 7.6). Cells were pelleted at 3,200 x *g* for 20 min and the pellets were resuspended in 40 ml of TSM (100 mM Tris-HCl pH 7, 500 mM sucrose, 10 mM $MgCl_2$) containing 25 μg/ml lysostaphin. Cells walls were digested at 37°C for 20 min and the samples were pelleted at 10,500xg for 15 min. The protoplast pellets were flash frozen in liquid N_2, and maintained at -80°C. Protoplast pellets were weighed and thawed in 7 ml of 0.1 M potassium phosphate buffer, pH 7. WT and '882-treated protoplast samples were sonicated (3 s on, 2 s rest, 50% amplitude, Branson 4c-15) on ice: four 5 min rounds, 5 min rest. The samples were then centrifuged for 50 min at 6,400 x *g*. The cleared lysates were syringe filtered (0.45 μm, Millipore) and diluted as needed to allow the measured extracted ion chromatogram (EIC) peak area to fit on the standard curve.

Porphyrin standards were purchased from Frontier Scientific Inc. (Logan, UT). Methanol, water, acetonitrile, DMSO, and formic acid solvents were all HPLC or Trace Metal grade and were purchased from Fisher Scientific. Samples were stored in Supelco slit top 2 mL vials prior to and during analysis (Fisher Scientific). These were stored at -20 ºC when not in use and kept at 5 ºC while in the autosampler tray immediately prior to analysis.

uHPLC separations were carried out on a Dionex Ultimate 3000 uHPLC system using a BDS Hypersil C18 column (150 x 2.1 mm) with a 2.4 μM particle size (Thermo-Scientific; cat # 28102-152130). Separations were performed at 2-4 kPa. Mass detection and analyte quantification were carried out using a microTOF-Q11 electrospray ionization time-of-flight quadrupole mass spectrometer equipped with a heated-electrospray ion source (Bruker).

Separations were achieved by linear gradient elution transitioning from 100% Solvent A (aqueous) to 100% Solvent B (organic) over 20 min, followed by a 3 min run of 100% Solvent B and then a return to 100% Solvent A in a final 3 min washing. A flow rate of 0.4 ml/min with a column temperature of 50 °C was determined to be optimal for separation using the above method. Solvent A: ultrapure water with 0.1 % formic acid; Solvent B: MeOH with 0.1 % formic acid. UV spectra were measured over 390-420 nm using the HyStar software package.

The uHPLC was coupled to an electrospray mass analyzer operating in positive ion mode. The spectrometer used a capillary voltage of 4,500 V and capillary temperature of 180°C. The nebulizing gas was set at 6.0 L/min. The software used for data analysis was Bruker Compass Data Analysis. The microTOF-Q11 instrument is capable of resolving ±0.001 amu mass differences. Due to the use of such high resolution, metabolites can be monitored via detection of their exact mass (heme parent ion mass: 616.1794 amu). The amounts of metabolites are quantified via integration of the corresponding extracted ion chromatogram (EIC) peak and comparison of the peak area to standard curves generated for known concentrations of pure hemin and internal standard (0.1 – 7 μM) measured at the same time as the analytes. Standard curves were generated in both potassium phosphate buffer. An internal standard (2-vinyl-4-hydroxymethyl-deuteroporphyrin IX) was added to each sample to a final concentration of 0.05 μM in order to compensate for run to run variability and instrument drift, neither of which proved to perturb the data substantially.

Intracellular heme quantification assay using IsdG - S. aureus Δ*isdG* and Δ*hemB* bearing a plasmid constitutively expressing IsdG (p*lgt.isdG*) were grown overnight (66). Based on

stationary phase culture density, Δ*isdG* and Δ*hemB* pellets were resuspended with 500 µl and 50 µl of lysostaphin in TSM buffer (6 µg/ml lysostaphin), respectively. Samples were incubated at 37°C for 25 min and pelleted by centrifugation at 16,300 x *g*. Δ*isdG* and Δ*hemB* were resuspended in 250 µl and 200 µl, respectively, of 100 µM PMSF in SoluLyse (Genlantis). Samples were lysed by sonication, normalized by BCA (ThermoScientific), and IsdG quantities were assessed as described previously (66). Band density was quantified using the Odyssey System software (LI-COR) and arbitrary units were converted to protein concentration based on an IsdG standard.

Statistical analysis - Where indicated, Student's *t*-tests were calculated using either Excel 2007 or GraphPad Prism 5. Tests of skewness, kurtosis, and D'Agostino and Pearson omnibus normality test were calculated using GraphPad Prism 5. When sample sizes were too small to apply standard tests for normality, samples were considered to be normally distributed if their skewness and kurtosis fell approximately within ±1 and ±3, respectively. Results were considered significant if the *p*-value was less than or equal to 0.05.

Results

A high-throughput screen identifies activators of HssRS. In order to identify small molecule activators of HssRS, a high-throughput screen (HTS) using luminescence as a reporter of HssRS activity was performed. The *hrtAB* promoter was cloned into the pXen-1 vector, which contains a *luxABCDE* operon that produces blue-green light when expressed (Figure 3A). This construct was transformed into wildtype *S. aureus* and the resulting strain was used to screen approximately 160,000 small molecules in the Vanderbilt Institute for Chemical Biology's compound library. This primary screen resulted in the identification of 250 positive hits. Based on luminescence values, the top 110 hits were subjected to a secondary screen using a *xylE* reporter assay to eliminate compounds that generate non-specific luminescence (90). Hits that passed this secondary screen were further tested in a tertiary screen for their ability to adapt *S. aureus* to

heme toxicity by growth curve analyses (90). Of all the compounds screened, ‘882 was the most potent activator of *hrtAB* expression. ‘882 activates the *hrtAB* promoter in a dose-responsive manner requiring HssRS and pre-adapts *S. aureus* for heme toxicity (Figure 3B and C). These properties were observed for both commercially purchased and independently synthesized preparations of ‘882 (Figure 3D). These results establish ‘882 as a small molecule activator of the HssRS-dependent heme stress response.

‘882 stimulates heme biosynthesis to activate HssRS. To determine the mechanism by which ‘882 activates HssRS, the residues required for HssS activation by ‘882 were compared to the residues required for HssS heme sensing. It was previously determined that residues R94A, T125A, and F165A reduce HssS heme sensing to different degrees. The impact of these mutations on HssS activation by ‘882 mirrored that observed upon heme exposure (Fig. 4A). This result indicates that heme and ‘882 trigger HssS signaling through similar residues despite being structurally distinct.

This observation suggests that ‘882 stimulates HssRS through a mechanism similar to that of heme. A potential explanation is that ‘882 is a small molecule activator of endogenous heme synthesis. To test this model, the p*hrt.xylE* reporter plasmid was transformed into the heme auxotroph *hemB::ermC* (Δ*hemB*) and HssRS activation was evaluated upon ‘882 exposure (92). In contrast to wildtype *S. aureus,* ‘882 does not activate HssRS in Δ*hemB* (Figure 4B). The loss of ‘882-mediated activation of HssRS in Δ*hemB* is not due to the slower growth rate of this strain as XylE activity from a constitutively expressed *xylE* (p*lgt.xylE*) is only modestly decreased (Figure 4B). Furthermore, exogenous heme activates HssRS in Δ*hemB*, indicating that Δ*hemB* HssRS is still able to sense heme (Figure 4C).

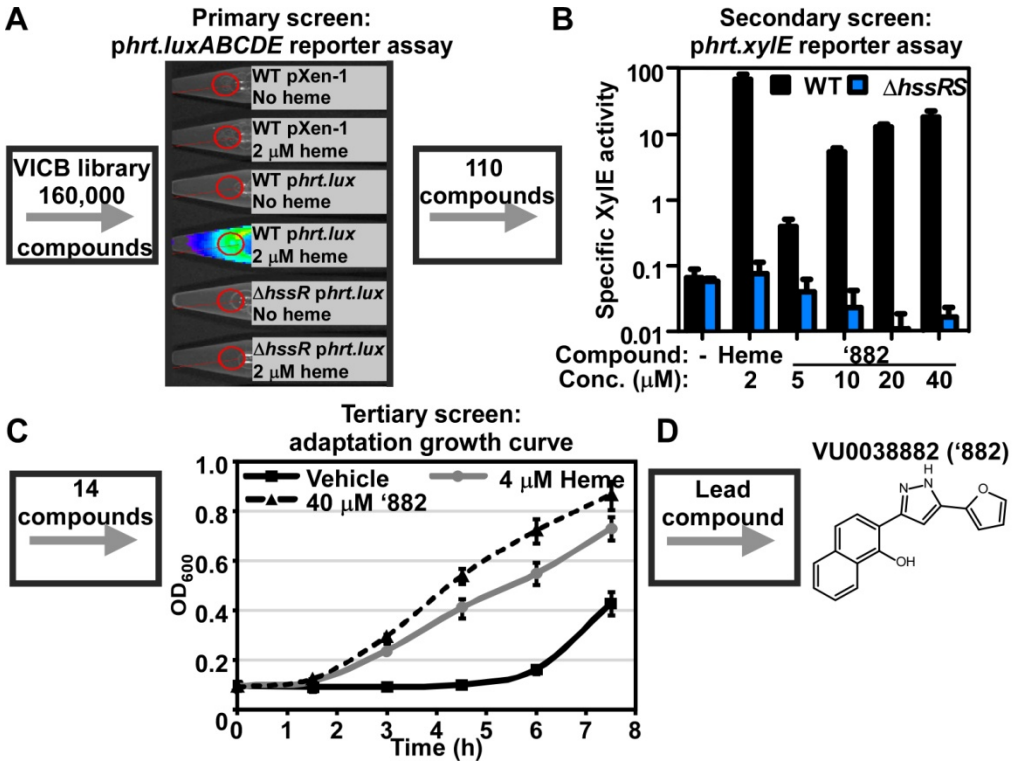

Figure 3. A high-throughput screen identifies small molecule activators of HssRS. *A.* 160,000 compounds from the Vanderbilt Institute for Chemical Biology small molecule library were screened using a *luxABCDE* reporter gene fused to the *hrtAB* promoter (p*hrt.lux*). Luminescence of *S. aureus* wildtype (WT) and Δ*hssR* carrying either promoterless *luxABCDE* (pXen1) or p*hrt.lux*. ***B.*** A secondary screen consisting of a XylE reporter assay verified the activity of the top 110 hits from the primary screen, including '882. Triplicate cultures of *S. aureus* WT and Δ*hssR* transformed with the *hrtAB* promoter-*xylE* fusion-containing plasmid (p*hrt.xylE*) were grown in the presence of the indicated additive and XylE activity was measured. ***C.*** '882 was confirmed as the top hit in a tertiary screen that measured the ability of the compound to pre-adapt *S. aureus* for growth in 20 μM heme. Triplicate cultures of WT *S. aureus* were grown overnight in medium containing the indicated additive and sub-cultured into medium containing 20 μM heme. Growth was monitored by measuring the optical density at 600 nm (OD_{600}) over time. ***D.*** The structure of lead compound VU0038882 ('882). (*B* and *C*) Error bars represent one standard deviation from the mean. The high-throughput screen was performed by DLS and OA.

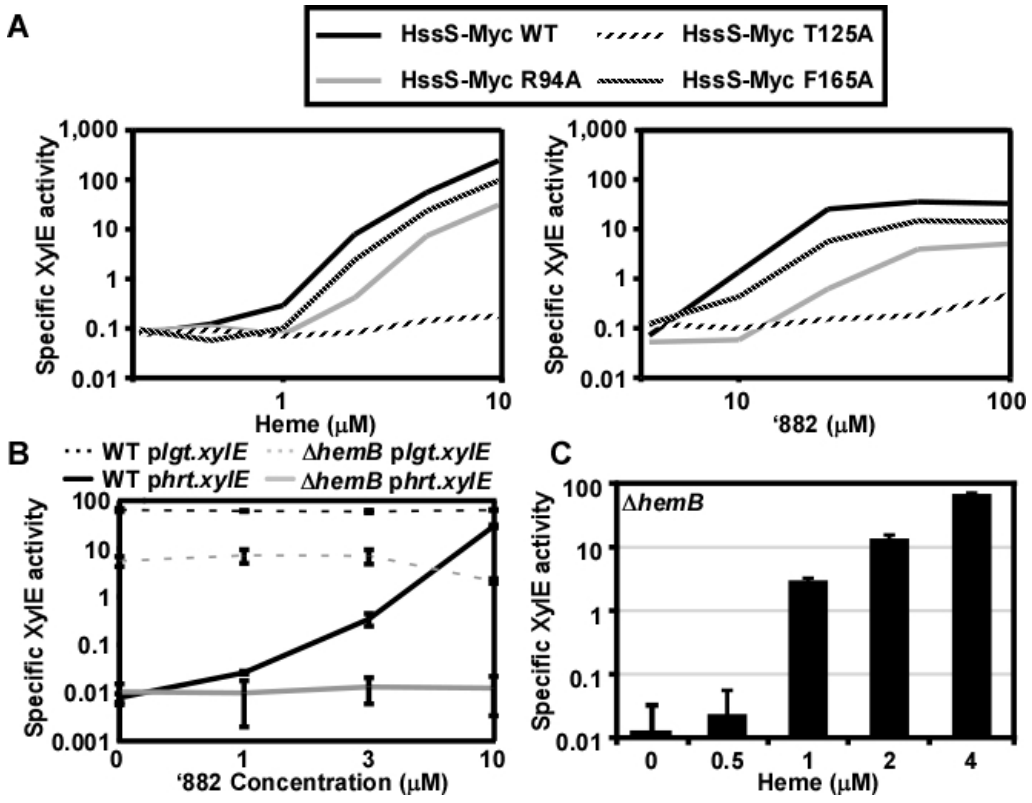

Figure 4. HssRS activation by '882 requires HssS residues required for heme sensing and endogenous heme biosynthesis. ***A.*** *S. aureus* Δ*hssS* was transformed with plasmids containing the *xylE* reporter gene fused to the *hrtAB* promoter and encoding Myc-tagged wildtype HssS (HssS-Myc) or HssS-Myc mutated at the indicated extracytoplasmic domain residue (R94A, T125A, or F165A). The resulting strains were grown in the presence of the indicated concentration of heme (left) or '882 (right) and XylE activity was quantified. Triplicate experiments were performed and averaged. ***B.*** *S. aureus* wildtype (WT, black lines) and the heme auxotroph *hemB*::*ermC* (Δ*hemB*, gray lines) were transformed with plasmids constitutively expressing XylE (p*lgt.xylE*, dashed lines) or with *xylE* under the control of the *hrtAB* promoter (p*hrt.xylE*, solid lines). Triplicate cultures of these strains were grown in the presence of '882 and XylE activity was measured. ***C.*** Triplicate cultures of Δ*hemB* carrying p*hrt.xylE* were grown in medium containing the indicated concentration of heme and XylE reporter activity was measured. (*B* and *C*) Error bars correspond to one standard deviation from the mean. Experiments in *A* and *B* were performed by DLS.

These observations are consistent with a model whereby ‘882 exposure leads to an increase in intracellular heme and subsequent HssS activation. In support of this model, intracellular heme levels increase in a dose-responsive manner in bacteria treated with ‘882 (Figures 5A and B). Moreover, ‘882 exposure leads to a darkening of *S. aureus* pellets indicative of massive heme accumulation in these cells (Figure 5A, inset). The activation of HssS by ‘882 is not due to enzymatic degradation of heme as ‘882 still activates HssS in a strain of *S. aureus* lacking all heme oxygenases (Figure 5C) (66).

To determine if the endogenous heme produced as a result of ‘882 exposure is available for use in cellular processes, cytoplasmic heme availability was measured by quantifying intracellular levels of the cytoplasmic heme oxygenase IsdG. In the absence of exogenous heme, IsdG is rapidly degraded; however, heme binding stabilizes IsdG and reduces its proteolytic degradation (66). Therefore, the abundance of IsdG reflects the cytoplasmic levels of heme. Following ‘882 treatment, the intracellular abundance of IsdG increased in a dose-dependent manner (Figures 5D and E). IsdG is not stabilized when *S. aureus* Δ*hemB* is grown in the presence of ‘882, demonstrating that stabilization of IsdG requires endogenous heme (Figures 5D and E). Moreover, IsdG abundance increases in Δ*hemB* exposed to exogenous heme, indicating that heme-dependent stabilization of IsdG is not generally disrupted in this strain (Figures 5D and E). Taken together, these experiments reveal that ‘882 exposure increases cytoplasmic heme availability.

To test whether other bacterial heme sensing proteins monitor endogenous heme, the ability of the *Corynebacterium diphtheriae* ChrAS and *Staphylococcus haemolyticus* HssRS TCSs to sense ‘882 by adaptation growth curve was examined (73, 85, 90). Due to the slow growth and low optical density achieved by *C. diphtheriae,* enumerating CFUs, a more sensitive measure of growth, was used to assess the adaptation of this pathogen. Pre-treatment of both species with either heme or ‘882 improved survival in heme as compared to non-adapted cultures (Figures 6A and B). These data suggest that ‘882 may stimulate heme biosynthesis in multiple

Gram positive bacteria and support the hypothesis that the ability to respond to both endogenous and exogenous heme is a conserved function of bacterial heme sensor systems.

‘882 diminishes fermentative activity of *S. aureus*. To define the mechanism by which ‘882 manipulates heme biosynthesis, a *S. aureus* transposon library was screened for mutants unable to sense ‘882 or heme by growth curve adaptation (90, 99). Of the approximately 7,000 mutants screened, only one strain was completely unable to be pre-adapted for heme toxicity by ‘882; this strain contained a transposon in the *hemL* gene involved in heme biosynthesis. Forty-four additional mutants were found to have a defect in ‘882 sensing and of those, 17 were also deficient in heme sensing (Table 1). A number of genes required for sensing heme and/or ‘882 are involved in central metabolic pathways including a predicted α-D-1,4-glucosidase (*malA*), the catabolite control protein (*ccpA*), respiratory response TCS (*srrAB*), branched-chain amino acid amino transferase (*ilvE*), bifunctional pyrimidine regulator/uracil phosphoribosyltransferase (*pryR*), and pyridoxal 5'-phosphate synthase glutamine amidotransferase subunit (*pdxT*) (19, 52, 80). Consistent with these observations, bacteria treated with ‘882 had reduced glycolytic activity as indicated by slower acidification of the medium that correlated with delayed consumption of D-glucose and reduced production of L- and D-lactate (Figure 7). These observations suggest that as ‘882 induces endogenous heme biosynthesis, it also reduces the glycolytic or fermentative capacity of *S. aureus*. These results support a model whereby the metabolic state of *S. aureus* and heme homeostasis are functionally interconnected.

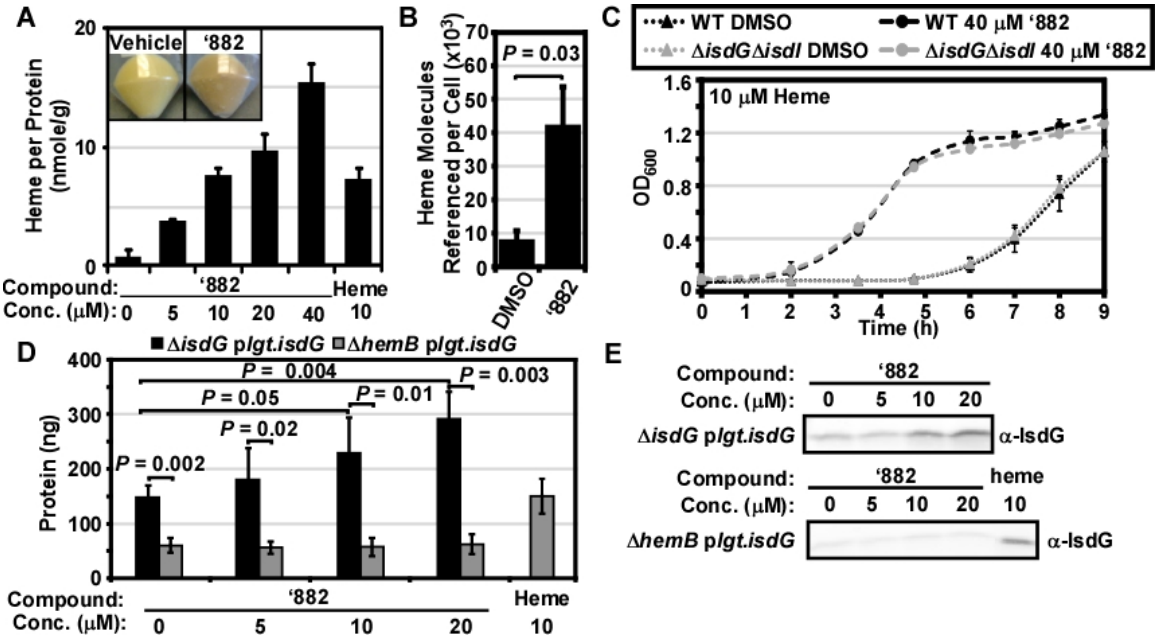

Figure 5. '882 treatment stimulates endogenous heme biosynthesis. ***A.*** Heme levels in triplicate cultures of *S. aureus* treated with the indicated additive were quantified using the pyridine hemochromogen assay and normalized to the concentration of protein in the whole cell lysates. *Inset*: Pellets from a culture grown with 40 μM '882 are red-brown when compared to vehicle treated *S. aureus*. ***B.*** Exact-mass mass spectrometric analysis was used in conjunction with UPLC to detect and quantify heme in protoplasts from cells treated with 40 μM '882 or vehicle grown in triplicate. Measured heme molecules were referenced to estimated CFUs per pellet, factoring in dilutions. Dead or lysed cells would also contribute to the measurement. Hence the measured numbers are considered upper estimates. Samples measured in duplicate or triplicate injections had typical errors of <5% between analytical replicates. Significance was calculated using a two-tailed Student's *t*-test. ***C.*** Triplicate cultures of Δ*isdG*Δ*isdI S. aureus* were grown overnight in medium containing the indicated additive and sub-cultured into medium containing 10 μM heme. Growth was monitored by measuring the optical density at 600 nm (OD_{600}) over time. Error bars represent one standard deviation from the mean. ***D.*** IsdG stabilization was used as a reporter for intracellular heme levels. *S. aureus* Δ*isdG* (black bars) and Δ*hemB* (gray bars) were transformed with plasmids that constitutively express IsdG (p*lgt.isdG*). These strains were grown in the presence of the indicated additive. Whole cell lysates, along with an IsdG standard, were blotted with anti-IsdG polyclonal antisera. Intracellular levels of IsdG were quantified using densitometry. Shown is the average of at least four replicates. Statistics were calculated using a two-tailed, Student's *t*-test. ***E.*** Representative blots of the Δ*isdG* (top) and Δ*hemB* (bottom) data shown in *D.* In all instances error bars represent one standard deviation from the mean. Data in *B* was generated by SS.

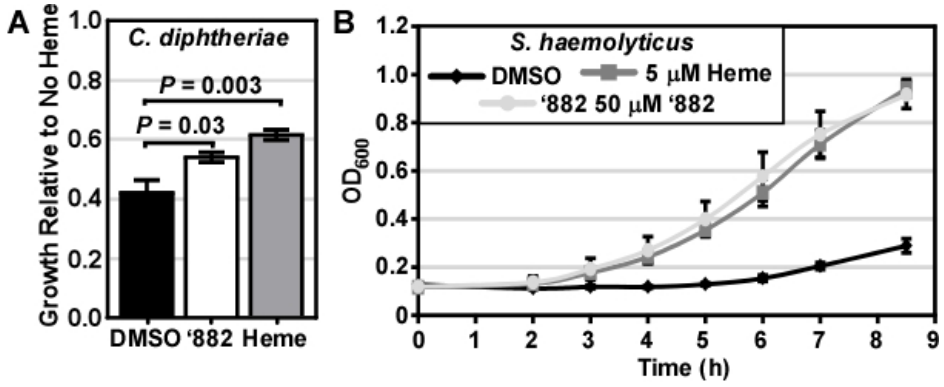

Figure 6. '882 pre-adapts other Gram positive bacteria for heme toxicity. *A.* Adaptation by heme and '882 in *Corynebacterium diphtheriae* was tested by growth analyses. Triplicate cultures were grown overnight in medium containing vehicle, 5 μM heme or 50 μM '882 and subcultured into medium containing 15 μM heme. The CFUs were enumerated 2.5 h after inoculation and normalized to cultures unexposed to heme. Shown is the average of five replicates; error bars represent standard error of the mean and significance was determined by a two-tailed Student's *t*-test. ***B.*** Adaptation by heme and '882 in *Staphylococcus haemolyticus* was tested by growth analyses. Triplicate cultures were grown overnight in medium containing the indicated additive and subcultured into medium containing 30 μM heme. Growth was monitored by measuring the optical density at 600 nm (OD_{600}) over time. Error bars represent one standard deviation from the mean.

Table 1: Transposon mutants less sensitive to '882				
Tranposon ID	***Integration site***	***Newman***	***Gene name***	***Gene description***
Co-factors				
11e11*,[1]	555437-8	NWMN_0482	*pdxT*	pyridoxal 5'-phosphate biosynthesis
21D1	1728844-5	NWMN_1561	*hemL*	glutamate-1-semialdehyde aminotransferase
Carbohydrates				
6E11	755114-5	NWMN_0672		aldo/keto reductase family protein
33F2, (66E5, 68B5, 68E8)[2], 67E11	1583073-4, 1584195-6, 1584189-90	NWMN_1414	*malA*	α-D-1,4-glucosidase
Cell wall				
52A8	1443696-7	NWMN_1310	*alr2*	alanine racemase 2
51C3	1444887-8	NWMN_1311	*lysA*	diaminopimelate decarboxylase
50 G5	1513348-9	NWMN_1349	*ald*	alanine dehydrogenase
Amino acids & proteins				
(24B2, 27D3, 24H6)*	595672-3	NWMN_0516	*ilvE*	branched-chain-amino-acid aminotransferase
75D6	1610144-5	NWMN_1439	*gcvPB*	glycine cleavage system P protein, subunit 2
6F8	1678876-7	NWMN_1513		peptidase U32 family protein
DNA & RNA				
8D8	1614867-8	NWMN_1446		competence protein ComGC-like protein
6H6	1659859-60	NWMN_1490		DNA internalization-related competence protein ComEC/Rec2
4E5, 5B10, 14D7, 18G5, 51G4*	1628735-36, 1629189-90,1629015-6, 1629152-3, 1628880-1	NWMN_1461		ATP dependent RNA helicase DEAD/DEAH box family protein
76C11	1660941-2	NWMN_1491		competence protein ComEB required for DNA binding and uptake
17B7*	1681514-5	NWMN_1517		conserved hypothetical protein
2F2*	2296289-90	NWMN_rRNA15		23S rRNA
Transporters				
11B6, 12F8*	982508-9, 982803-4	NWMN_0886		Hypothetical protein; transporter; next to murGE
(66C5, 69D11)	1670973-4	NWMN_1505		hypothetical protein contains NRAMP domain

Table 1 cont'd: Transposon mutants less sensitive to '882				
Tranposon ID	***Integration site***	***Newman***	***Gene name***	***Gene description***
Regulators				
63C6	736803-4	NWMN_0655		MarR family protein
48F5*	756768-9	NWMN_0674	*saeS*	*S. aureus* accessory element histidine kinase
44C2*	1213708-9	NWMN_1109	*pryR*	pyrimidine operon regulatory protein,
10D6*	1569662-3	NWMN_1399	*srrB*	staph respiratory response histidine kinase
32G6*	1461723-4	NWMN_1328		response regulator
31H6*	1813162-3	NWMN_1629	*ccpA*	catabolite control protein A
Phage				
33G8	1124401-2	NWMN_1026		conserved hypothetical protein; identical to ORF040 of Bacteriophage 53
66F2	1990835-6	NWMN_1776		conserved hypothetical protein
Hypothetical and intergenic				
69E5	780077-8	NWMN_0695/0696	intergenic	Hypothetical protein (similar to MDR transporter) and di-/tripeptide ABC transporter
9F8*	846026-7	NWMN_0751	promoter	hypothetical protein
49G8	1060937-8	NWMN_0955/0956	intergenic	conserved hypothetical proteins
50F8	1624756-7	NWMN_1457/*sodA*	intergenic	Zn specific metalloregulatory protein and superoxide dismutase Mn/Fe family protein
8G6	1668046-7	NWMN_1502/1503	intergenic	hypothetical protein and enterotoxin family protein
77D12	1670682-3	NWMN_1504	promoter	hypothetical protein
46B9	1690951-2	NWMN_1524		aminotransferase, class V
52F2	1755385-6	NWMN_1584	promoter	hypothetical protein
2F9	1931846-7	NWMN_1732		hypothetical protein
52B8	2137622-3	NWMN_1930		hypothetical protein
52G4	2270169-70	NWMN_2051/ 52	intergenic	lytic regulatory protein and truncated resolvase
32C7*	2384526-7	NWMN_2161		conserved hypothetical protein

[1]An asterisk denotes mutants that are less sensitive to both heme and '882.
[2]Mutants grouped in parentheses reflect identical integration sites.

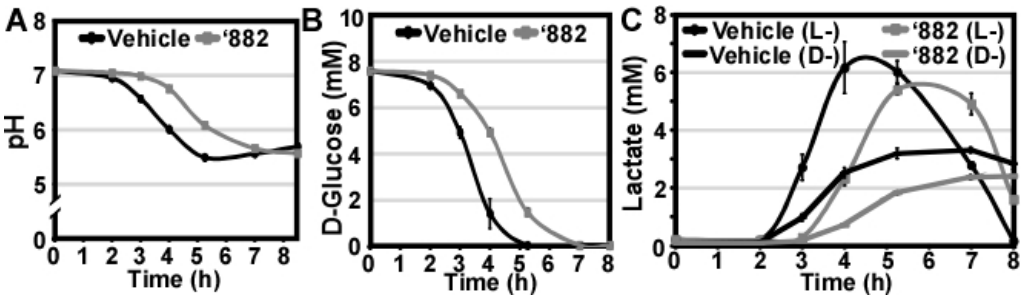

Figure 7. '882 diminishes fermentative activity. *S. aureus* was grown in triplicate under aerobic conditions in the presence of vehicle (black lines) or 40 μM '882 (gray lines). At the indicated time intervals, culture supernatants were sampled and the ***A.*** pH, ***B.*** D-glucose, and ***C.*** D- and L-lactate were quantified. Error bars represent one standard deviation from the mean.

The metabolic state of the cell impacts heme biosynthesis. To test whether heme biosynthesis interfaces with central metabolism, the effect of 2-deoxyglucose (2dG) on heme biosynthesis was assessed. The glucose analogue 2dG primarily inhibits the phosphoglucoisomerase reaction, the second step in glycolysis (97). Treatment of *S. aureus* with 2dG reduces endogenous heme levels and antagonizes ‘882 activity (Figure 8A). Deletion of 6-phosphofructokinase (*pfkA*), the third enzyme in glycolysis, results in a loss of glucose uptake and decreased acid end product secretion in *S. aureus* (Figures 8B and C). In agreement with the effect of 2dG on heme biosynthesis, both basal and ‘882-induced heme biosynthesis are suppressed in Δ*pfkA* (Figure 8D). These data implicate a product of glycolysis in coordinating heme biosynthesis, strengthening the observed link between the regulation of heme biosynthesis and central metabolism.

Discussion

Here, we describe an HTS that identified small molecule activators of the *S. aureus* heme sensor system HssRS. The most potent hit, ‘882, increases endogenous heme levels and activates HssRS through the heme biosynthesis pathway. This effect appears to be due to a perturbation of the metabolic state of *S. aureus* as transposon insertions targeting genes involved in metabolism contribute to the ability of the bacteria to sense ‘882. This hypothesis is supported by the observations that ‘882 reduces fermentative processes and that inhibiting upper glycolysis suppresses endogenous heme biosynthesis. Finally, we have shown that ‘882 activates heme sensing systems in other Gram positive pathogens as it pre-adapts *C. diphtheriae* and *S. haemolyticus* for heme toxicity.

Employing ‘882 as a probe has revealed that HssRS responds to both exogenous and endogenous heme accumulation. It was previously thought that HssS was stimulated by heme in the extracellular environment. Data presented here reverses this model as increased levels of endogenous heme activate HssS. This indicates that the ligand sensing domain of HssS is most likely intracellular or membrane localized.

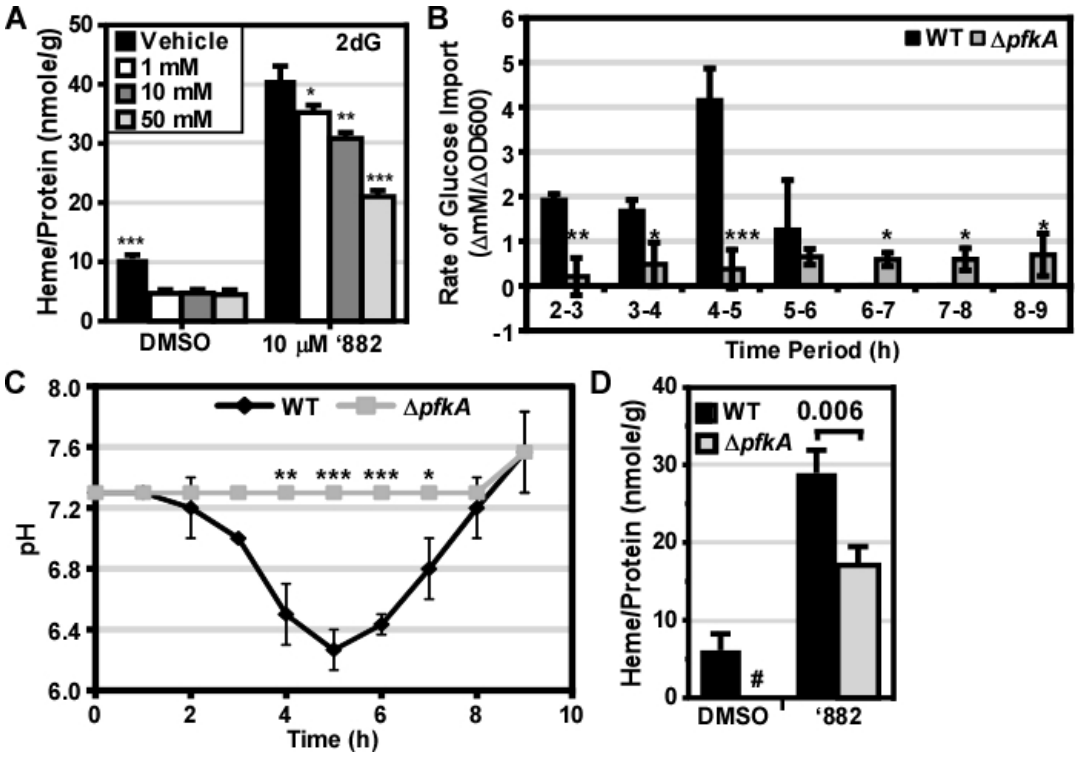

Figure 8. Glycolytic activity regulates heme biosynthesis. *S. aureus* was grown in triplicate in the presence of vehicle or 10 μM '882. Heme levels were quantified using the pyridine hemochromogen assay and normalized to the concentration of protein in the whole cell lysates. ***A***. Cultures were treated with the indicated dose of 2-deoxyglucose (2dG). (***B***-***C***). Wildtype (WT) and Δ*pfkA* Newman cultures were sampled during growth and the absorbance at 660 nm measured. ***B***. Glucose levels in supernatants were quantified and used to calculate the rate of glucose import [Δglucose (mM/hr)/Δabsorbance (OD_{660}/hr)]. ***C***. The pH of the supernatants was measured. (*B* and *C*) Data collected in three independent experiments are shown. Error bars represent twice the standard error of the mean (n = 3). ***D.*** Wildtype (WT) and Δ*pfkA* Newman were cultured in TSB+1% pyruvate. # indicates the signal was below the limit of detection. (*A* and *D*) Error bars represent the standard error of the mean from three independent experiments. Statistical significance was determined using an unpaired Student's *t*-test. * = $p \leq 0.05$, ** = $p \leq 0.001$, *** = $p \leq 0.0001$ Results shown in *B* and *C* were performed by NPV.

The discovery that *S. aureus* monitors intracellular heme status through HssRS suggests that other bacterial heme sensing systems may also sense intracellular heme. Already HrtR, which functions alone as a transcriptional repressor of *hrtRBA* in *L. lactis*, has been shown to monitor intracellular levels of heme, but no other TCS HK has been proposed to monitor intracellular heme (42). Since ‘882 also adapts *C. diphtheriae* and *S. haemolyticus* for heme toxicity and both of these species have heme-responsive TCSs, these data suggest that ‘882 also stimulates heme biosynthesis in these bacteria and is sensed by their corresponding HKs (73). Furthermore, the fact that ‘882 is sensed by *C. diphtheriae* and *S. haemolyticus* indicates that the target of ‘882 is present in multiple pathogens, establishing this molecule as a powerful probe for studying intracellular heme metabolism.

The utility of ‘882 as a probe is further supported by the observation that IsdG binds endogenously synthesized heme following stimulation with ‘882. There are two families of heme-degrading oxygenases, the Isd-family and the HO-family which, in addition to liberating iron from the protoporphyrin ring of heme, also produce staphylobilin and biliverdin, respectively. The HO-family heme oxygenase *hemO* from *P. aeruginosa* has previously been shown to bind endogenous heme (3). Thus, with data presented here, both families of heme-degrading oxygenases have now been shown to target endogenous heme (3). These data implicate a potential role for bacterial heme oxygenases in endogenous heme turnover, a result that is likely generalizable to all bacterial heme oxygenases (3). In bacteria, heme oxygenases are currently thought to primarily function as a mechanism by which exogenous heme may be used as an iron source, although a couple of heme oxygenases, specifically, *B. anthracis* IsdG and *Neisseria gonorrhoeae* HemO, have also been implicated in alleviating heme toxicity (75, 100).

The turnover of endogenous heme by bacterial heme oxygenases highlights several intriguing hypotheses. To begin with, it points to the possibility that endogenous heme and iron homeostasis may be regulated by bacterial heme oxygenases (51, 66). Furthermore, it begs the question of whether there is a physiological function of the heme degradation products

staphylobilin and biliverdin. The synthesis of heme requires energy, cellular building blocks and reducing equivalents; degrading heme simply to release iron and maintain heme homeostasis seems to be energetically inefficient. The functions of the heme oxygenase products (biliverdin and staphylobilin) in bacteria remain unclear. In cyanobacteria, algae, and plants, the heme degradation product biliverdin is a precursor for light-harvesting phytobilin pigments (20). A reaction specific to mammals is the conversion of biliverdin to the potent antioxidant bilirubin (47, 88). It is possible that bacterial biliverdin and staphylobilin are excreted as waste products or further metabolized to be used as a carbon and nitrogen sources. The energetically economical nature of bacteria, however, suggests that it is unlikely that biliverdin and staphylobilin are simply refuse. In the context of iron and heme homeostasis, it is possible that biliverdin and staphylobilin might function as signaling molecules or somehow provide protection from heme toxicity. In order to study these exciting ideas, ‘882 may be used as a probe to dissect the impact of endogenous heme metabolism by bacterial heme oxygenases on the regulation of heme uptake and biosynthesis, which may reveal a physiological function of heme degradation products.

Heme biosynthesis is typically regulated by cellular iron or heme levels, although there is some evidence that it is tied to central metabolism (14, 22). The perturbation of heme homeostasis and central metabolism by ‘882 suggests that the two cellular processes are coordinated in *S. aureus*. Strengthening this hypothesis, both chemical and genetic inhibition of the upper steps in glycolysis result in suppressed basal and ‘882-induced heme levels. These data suggest that an intact glycolytic pathway is required for ‘882-dependent activation of heme biosynthesis, further supporting a functional interconnection between central metabolism and heme biosynthesis in *S. aureus*. Since inhibiting upper glycolysis suppresses endogenous heme biosynthesis and repressing fermentation stimulates endogenous heme biosynthesis, this suggests that a metabolic signal between upper glycolysis and fermentation coordinates heme biosynthesis. The opposing effects on heme homeostasis observed upon targeting upper glycolysis and fermentation suggest that when upper glycolysis is inhibited, a metabolic signal is depleted versus

when fermentation is repressed, a metabolic signal accumulates. In this way heme biosynthesis could be functionally tied to the energetic flux of the cell. An integration of heme homeostasis with central metabolism is consistent with the fact that heme and iron are critical co-factors for many enzymes involved in energy homeostasis. Further studies employing ‘882 could dissect the interplay between heme and central metabolism in both *S. aureus* and other pathogens.

In summary, we have identified a small molecule that diminishes fermentative processes in *S. aureus,* stimulates endogenous heme biosynthesis and activates HssRS. This molecule has proven to be valuable as a probe of bacterial heme homeostasis. Tools for stimulating endogenous heme biosynthesis are limited and these probes, which stimulate heme biosynthesis across genera, will provide insight into conserved mechanisms of heme regulation. The effect of ‘882 on suppressing fermentative processes does suggest that ‘882 may have therapeutic efficacy in environments where *S. aureus* is forced to rely on fermentation. The potential utility of ‘882 as a new therapeutic strategy is addressed in the next chapter.

CHAPTER III

THERAPEUTIC POTENTIAL OF '882 FOR THE TREATMENT OF PERSISTENT INFECTIONS

Introduction

Small colony variants (SCVs) of *S. aureus* are spontaneous, slow-growing mutants associated with persistent and recurrent *S. aureus* infections that are recalcitrant to antibiotic therapy (63). Their slow growth is often due to lesions that eliminate respiration, such as inactivation of MK or heme biosynthesis. SCVs are not exclusive to *S. aureus* as they have been isolated in other pathogens, including *Escherichia coli, Neisseria gonorrhoeae, Pseudomonas aeruginosa,* and *Salmonella enterica* serovar Typhimurium (6, 63).

The two prototypical disease states associated with *S. aureus* SCVs are cystic fibrosis (CF) and osteomyelitis. Both diseases typically involve prolonged infection and antibiotic treatment. In CF, *S. aureus* is usually isolated from complex microbial infections that primarily include *P. aeruginosa. P. aeruginosa* secretes several antibacterial compounds including pyocyanin, which inhibit bacterial respiration. Since SCVs do not have a functional respiration branch for energy production, they can resist assaults from *P. aeruginosa,* the host immune response, and antibiotic treatment. One study analyzed the sputa from 72 CF patients and found that 70% are chronically colonized with *S. aureus* and, of those samples, 46% contained SCVs (35). The deep-tissue infections associated with *S. aureus* osteomyelitis require prolonged antibiotic treatment as the blood flow is restricted to the site of infection. Therefore, analogous to CF, osteomyelitis tends to select for SCV persister populations. This is evidenced by the identification of *S. aureus* SCVs in approximately 29% of patients with *S. aureus* osteomyelitis (91). In this study, *S. aureus* SCVs were only isolated from the patients who had previously

received gentamicin bead therapy at the site of infection; these patients were prone to recurrent osteomyelitis.

SCVs are intrinsically resistant to antibiotics and host defenses primarily because their respiratory branch is inactive. The loss of respiration results in a low $\Delta\psi$ across the membrane (39). Both aminoglycosides, such as kanamycin and gentamicin, as well as antibacterial cationic peptides require $\Delta\psi$ to cross the bacterial envelope. Therefore SCVs are intrinsically resistant to aminoglycosides and some host defense peptides. Furthermore, the slow growth of SCVs also results in reduced cell wall production, which makes the bacteria less susceptible to cell wall targeting antibiotics such as β-lactams (64).

The host-pathogen interaction is complex and it is likely the metabolic flexibility of *S. aureus* which enables this microbe to be a successful pathogen. Abscesses, which are purulent lesions containing bacteria and neutrophils surrounded by a pseudocapsule, are a hallmark of *S. aureus* infections (11). Upon encountering *S. aureus*, the neutrophil releases a toxic milieu of chemicals to kill the invading pathogen. One component of this toxic milieu is nitric oxide (NO·), which inactivates iron-containing proteins critical for respiration (69). When *S. aureus* relies on fermentation, NO· no longer has a negative effect on growth (69). Therefore it is likely that fermentation is critical to staphylococcal pathogenesis since abscesses are thought to be anaerobic environments and *S. aureus* can persist in that niche (59).

In Chapter II it was determined that ‘882 suppresses fermentative processes such as glucose uptake and acid end product excretion. This suggests that ‘882 may be toxic to fermenting *S. aureus,* including clinically relevant SCVs. In the following chapter this hypothesis is tested and the potential utility of a small molecule inhibitor of fermentative growth is elaborated.

Methods

Bacterial strains and growth conditions- *Staphylococcus aureus* strains Newman, Δ*hssRS*, Δ*menB,* and Δ*isdG* have been described previously (16, 51, 83, 90, 93). *S. aureus hemB::ermC* (Δ*hemB*) has been described previously and was transduced into Newman using bacteriophage Φ-85 (51, 92). *Corynebacterium diphtheriae* strain HCL2 was used.

All *S. aureus* strains were grown on tryptic soy agar (TSA) containing 10 µg/ml chloramphenicol when appropriate and grown at 37°C for 20-30 h. All overnights were grown in 5 ml of tryptic soy broth (TSB) at 37°C with shaking at 180 rpm unless otherwise noted. All aerobic growth conditions were at 37°C with shaking at 180 rpm in TSB unless otherwise stated.

Anaerobic growth was obtained by growing cultures in 5 ml of TSB in aeration tubes at 37°C with shaking at 180 rpm for 15 h. Cultures were diluted to a theoretical OD_{600} of 0.0001 and 200 µl were added to 5 µl of additive in a 96 well plate. Cultures were placed in an anaerobic jar and incubated at 37°C for 18 h.

Unless stated otherwise, vehicle treatment refers to a volume of DMSO comparable to the volume added containing the described compound (‘882 or ‘373).

XylE reporter assays - XylE assays were performed as described previously with modifications in growth conditions (90). The bacteria were grown for 9 h and diluted 1:100 into 0.5 ml of media for 15 h.

Growth curve analyses - Overnight cultures of Newman were diluted 1:100 into 100 µl of media. Bacterial cells were incubated and the OD_{600} was measured at the specified time points. For all staphylococcal adaptations, cultures were inoculated in 0.5 ml of TSB for 1 h at 37°C, 180 rpm and sub-cultured 1:100 in 100 ul of media containing the indicated additive. Cultures were pre-adapted overnight and analyzed as described above for a typical growth curve.

Gentamicin resistance assay - An overnight of Newman grown on a Cel-Gro Tissue Culture Rotator (Lab-Line) was sub-cultured 1:100 into 5 ml of TSB containing the indicated additive

(gentamicin, 10 μg/ml; ‘882, 20 μM) and growth on the rotator was continued for 24 h. CFUs were enumerated on TSA and TSA containing 5 μg/ml gentamicin.

Neutrophil killing assay - All mice were maintained in compliance with Vanderbilt’s Institutional Animal Care and Use Committee regulations. Polymorphonuclear leukocytes (PMNs) were elicited using casein and harvested from 13-16 week old male C57BL/6 mice (Jackson Labs) as previously described (36). Bacteria were prepared and assayed as previously described with modifications (36). An overnight of Newman grown on a Cel-Gro Tissue Culture Rotator (Lab-Line) was sub-cultured 1:100 and grown in the rotator to mid-log. Following growth, the bacteria were resuspended to an OD_{600} of 0.4 in phosphate buffered saline (PBS) and 1 ml of culture was pelleted. The pellet was incubated in 50% normal mouse serum, 50% RPMI/H (10 mM HEPES in RPMI), 10 μM $MnCl_2$ and either vehicle or 40 μM ‘882 for 30 min. The pellet was resuspended in 1 ml RPMI/H with 20 μM $MnCl_2$ and 2X vehicle or ‘882.

NO· growth curve - 1 ml of an overnight of Newman grown at 37°C, 250 rpm was washed with PNG (PN media with 0.5% glucose) (60). The cultures were diluted to an OD_{660} of 0.01 in PNG and 200 μl were aliquoted into a 96 well plate. The plate was incubated at 37°C with shaking (14 min 30 sec 1 mm Orbital, 30 sec 1 mm Linear) on a Tecan Infinite F200Pro. When the cultures reached an OD_{660} of 0.15, NO· was added with a final concentration of 10 mM NOC-12 and 1 mM DEANO.

C. diphtheriae growth curve - *C. diphtheriae* was grown aerobically in brain heart infusion (BHI) medium for 20 h at 37°C, 180 rpm. The cultures were back-diluted in BHI to a theoretical OD_{600} of 0.0001 and 150 μl of bacterial culture were added to 5 μl of ‘882 stock. Cultures were grown at 37°C, 180 rpm for 18 h and the OD_{600} measured.

Systemic murine model of infection - All mice were maintained in compliance with Vanderbilt’s Institutional Animal Care and Use Committee regulations. Seven week old BALB/c (Jackson Laboratory) female mice were infected retro-orbitally with $2x10^7$ CFU of Newman as described previously (77). ‘373 was prepared in 10% Tween 80 and brought to a neutral pH with 0.1 M

sodium hydroxide. Intraperitoneal (IP) treatments were given 2 h before infection and every subsequent 24 h until the mice were euthanized with CO_2 96 h post-infection. Liver abscesses and CFUs were enumerated.

Imaging MALDI-MS/MS - Livers from mice infected and treated as described above were harvested 24 h post infection (1 h after the 2nd treatment) and flash frozen on hexane and dry ice. Ten μm sections were prepared using a cryostat and thaw-mounted directly to a gold-coated stainless steel MALDI target plate (Applied Biosystems). 30 mg/ml of 2,5-dihydroxybenzoic acid (DHB) was prepared in 1:1 acetonitrile:water with 0.1% trifluoroacetic acid. Matrix was applied using a thin layer chromatography glass reagent sprayer (Kontes Glass Company).

Mass spectra were acquired in positive-ion MS/MS mode using a MALDI LTQ XL linear ion trap mass spectrometer (Thermo Scientific) equipped with 337-nm nitrogen laser operating at 60 Hz. Two in-line neutral density filters were used. Protonated ‘373 molecules (*m/z* 255.2*)* were isolated and fragmented with Helium gas serving as the trapping and collisional gas. Ion density images were extracted from the raw data using ImageQuest version 1.0.1 (ThermoScientific).

‘373 Quantitation via HPLC - Levels of ‘373 in liver tissue analyzed via Imaging MALDI-MS/MS (IMS) were quantified using HPLC-MS/MS. Tissues were homogenized in 1:1 acetonitrile:methanol manually using a pestle and a Model 100 Sonic Dismembrator (Fisher Scientific). Homogenate was diluted to a final concentration of 20 mg/ml, and cellular debris was removed by centrifugation at 3,000 rpm for 5 min. Infected, untreated control liver was homogenized to serve as a blank and to prepare calibration standards.

Deferasirox (AK Scientific, INC.) was used as an internal standard and was spiked at a concentration of 100 pg/ml into the supernatant solution of all samples analyzed. A calibration series of ‘373 was spiked into control tissue supernatant at concentrations of 0, 7, 50, 100, 150, and 200 ng/mL.

Separations were performed on a 1260 Infinity HPLC system (Agilent Technologies) with a 6430 Triple Quadrupole Mass Spectrometer (Agilent Technologies) using a ZORBAX

Rapid Resolution High Definition SB-C18 column (2.1mm id × 50 mm, 1.8μm). Analytes were eluted over 15 min using the following gradient: initial flow 50% Solvent A (0.1% formic acid in water) and 50% Solvent B (0.1% formic acid in 1:1 acetonitrile:methanol) for 30 seconds, ramped to 80% Solvent B over 10 min, held for an additional min, ramped back to 50% Solvent B over 3 min, and held for an additional min.

Optimal parameters for transitions were determined using Mass Hunter optimizer version B.04.01 (B4114). Four transitions were monitored for both the target of interest and the internal standard. For '373, a precursor [M+H]+ of 255 was monitored at a retention time of 4.7 min for transitions to 122 for quantitation and 65, 102, and 190 as qualifiers. For Deferasirox, a precursor [M+H]+ of 374 was monitored at a retention time of 5.0 min for transitions to 120 for quantitation and 65, 108, and 182 as qualifiers. Data were analyzed using Mass Hunter workstation software Quantitative Analysis version B.04.00/build 4.0.225.19. Calibration curves were generated as response ratios of '373 relative to the internal standard and had an R^2 value of 0.996.

Statistical analysis - Where indicated, Student's *t*-tests were calculated using either Excel 2007 or GraphPad Prism 5. Tests of skewness, kurtosis, and D'Agostino and Pearson omnibus normality test were calculated using GraphPad Prism 5. When sample sizes were too small to apply standard tests for normality, samples were considered to be normally distributed if their skewness and kurtosis fell approximately within ±1 and ±3, respectively. Results were considered significant if the *p*-value was less than or equal to 0.05.

Results

'882 is bacteriostatic to fermenting *S. aureus.* The '882-dependent suppression of substrate level phosphorylation in aerobic cultures suggests that the compound may inhibit fermentative growth. Indeed, when *S. aureus* was grown anaerobically in the presence of '882, growth was dramatically reduced (Figure 9A). In addition, a strain bearing a lesion in the MK biosynthesis

gene *menB* (Δ*menB*), which cannot respire and solely ferments to produce energy, is more susceptible to ‘882 toxicity than wildtype (Figure 9A). ‘882 is bacteriostatic to Δ*menB* both aerobically and anaerobically (Figure 9B). Moreover, when ‘882 is combined with the respiratory poison potassium cyanide (KCN), *S. aureus* growth is inhibited, even under aerobic conditions (Figure 9C). Taken together, these data indicate that ‘882 inhibits *S. aureus* fermentative growth and that respiration is protective against ‘882 toxicity. Notably, ‘882 inhibits the growth of *C. diphtheriae*, supporting the conserved activity of ‘882 in heme sensing organisms (Figure 9D). Furthermore, Δ*hemB*, an SCV deficient in heme biosynthesis, is also sensitive to ‘882, indicating that heme accumulation is not the source of toxicity, but rather a result of ‘882 perturbing *S. aureus* metabolism (Figure 9A).

‘882 prevents the evolution of antibiotic resistance. *S. aureus* SCVs are obligate fermenters that emerge in response to aminoglycoside treatment (63). The sensitivity of fermenting *S. aureus* to ‘882 lead to the hypothesis that this compound could prevent the outgrowth of antibiotic resistant SCVs in the presence of aminoglycosides. To test this, *S. aureus* was grown in the presence of vehicle, gentamicin, ‘882, or a combination of gentamicin and ‘882, and the evolution of gentamicin resistance was monitored. Bacteria treated with gentamicin alone became resistant to gentamicin, whereas ‘882 treatment alone did not affect the number of viable or gentamicin-resistant bacteria (Figure 8). Combining ‘882 with gentamicin resulted in a 5-log reduction in bacterial viability and eliminated all detectable gentamicin-resistant colonies (Figure 10). This suggests that targeting fermentation can be used as an adjunctive therapy with antibiotics that are active against respiring *S. aureus* to improve antibacterial action and reduce the emergence of antibiotic resistance.

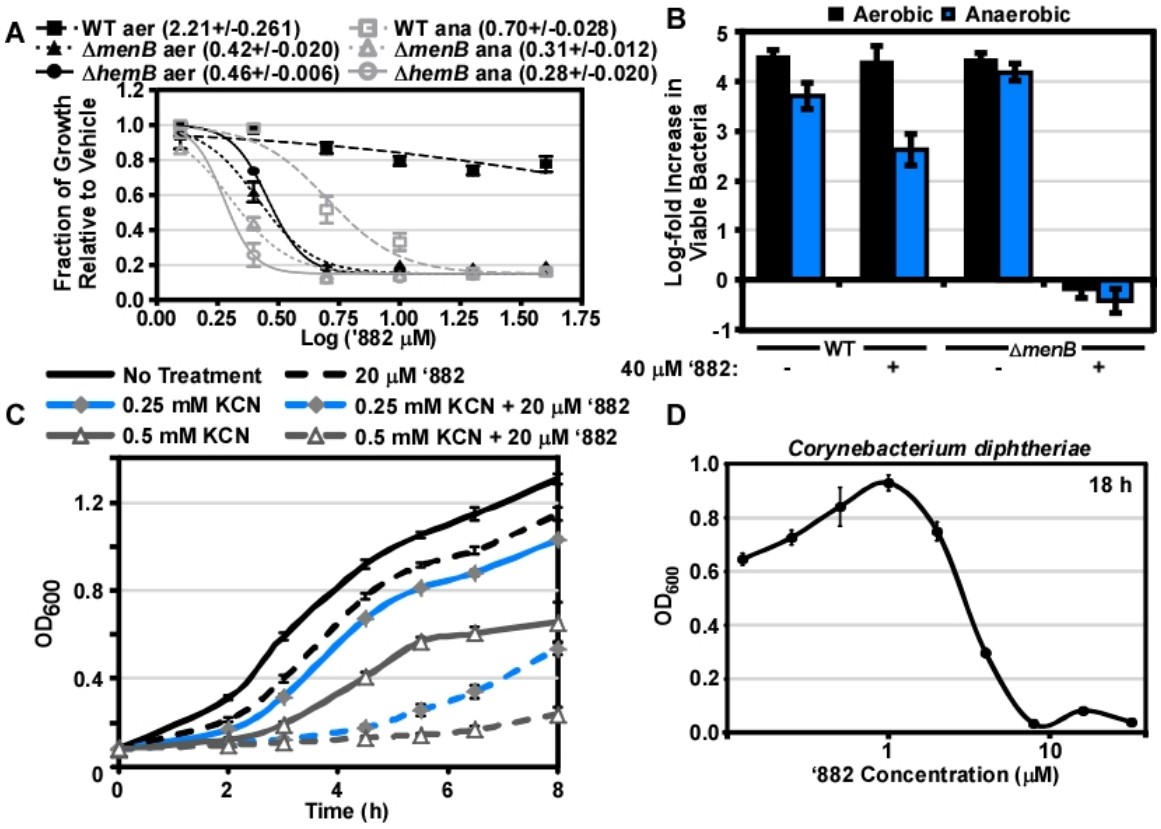

Figure 9. '882 inhibits fermenting *S. aureus*. *A*. *S. aureus* wildtype (WT, dashed lines), the menaquinone auxotroph (Δ*menB*, dotted lines), and the heme auxotroph *hemB*::*ermC* (Δ*hemB*, solid lines) were grown in triplicate under aerobic (aer, black lines) and anaerobic (ana, gray lines) conditions in the presence of the indicated log of the concentration of '882 (μM). After 18 h the absorbance at 600 nm (OD_{600}) was measured and normalized to vehicle (DMSO) treated bacteria. Curves were fit by nonlinear regression analysis and absolute $logIC_{50}$ values were calculated in Prism with the top set at 1.0 and the bottom set at 0.15. $LogIC_{50}$ values are indicated in parentheses in the figure key +/- standard error of the mean. All $logIC_{50}$ values were statistically different from WT aerobic $logIC_{50}$ when analyzed by one-way ANOVA with a Dunnett post test ($p<0.001$). Error bars represent the standard error of the mean. ***B.*** CFUs from *A* were enumerated at the beginning and end of the time course for bacteria treated with vehicle and 40 μM '882. The fold increase over the input of bacteria was determined. ***C.*** Triplicate cultures of *S. aureus* were grown in the presence of vehicle (DMSO), 1 mM potassium cyanide (KCN), 40 μM '882, or a combination of 1 mM KCN and 40 μM '882. Growth was monitored by measuring the OD_{600} at the indicated time points. ***D.*** Triplicate cultures of *C. diphtheriae* were grown in the presence of the indicated concentration of '882. Growth was measured by OD_{600} at 18 h. Shown is the average of three independent experiments. Error bars in panels *B-D* represent one standard deviation from the mean.

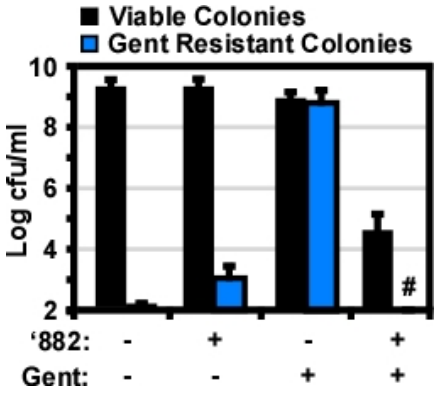

Figure 10. Co-treatment of *S. aureus* with '882 and gentamicin prevents the outgrowth of antibiotic resistant isolates. Triplicate cultures of *S. aureus* were grown in the presence of the indicated additive. After 24 h, CFUs were enumerated on TSA containing 5 μg/ml gentamicin and plain TSA with a limit of detection of 100 CFUs/ml (minimum y-value); # indicates colonies were not identified above the limit of detection. Shown is the average of three independent experiments. Error bars represent one standard deviation from the mean.

‘882 enhances innate immune function. Neutrophils are the first immune cells to respond to the site of a *S. aureus* infection (13). As part of the innate defense program, they secrete noxious chemicals to kill invading pathogens; this includes NO·, which inactivates respiration (13, 69). In agreement with the observation that ‘882 is particularly toxic to fermenting *S. aureus,* simultaneous exposure of *S. aureus* to ‘882 and NO· is more antibacterial than treatment with either molecule alone (Figure 11A). Additionally, ‘882 improves neutrophil-dependent killing of *S. aureus* but does not overtly affect neutrophil viability (Figure 11B). These results support the notion that ‘882 may have therapeutic efficacy against bacterial invaders by augmenting the killing activity of neutrophils.

A derivative of ‘882 reduces *S. aureus* pathogenesis *in vivo.* Abscesses are a hallmark of *S. aureus* infections (11). It is likely that fermentation is critical to staphylococcal pathogenesis since abscesses are thought to be anaerobic environments (59). Testing this hypothesis is challenging as *S. aureus* fermentation is branched and is accomplished by multiple parallel-acting enzymes, so genetic inactivation of fermentation is impractical. The toxic effect of ‘882 toward fermenting *S. aureus* provides an opportunity to gain initial insights into the role of fermentation in pathogenesis. However, ‘882 has a metabolically labile furan group which may form protein adducts and deplete glutathione *in vivo* (7). Thus, the furan was replaced with a 2-fluorophenyl group to create a more biologically stable derivative, VU0420373 (‘373) (Figure 12A). ‘373 activates HssRS as evidenced by its ability to increase the expression of the *xylE* reporter gene and pre-adapt *S. aureus* for heme toxicity (Figures 12B and C). In addition, ‘373 inhibits the growth of *S. aureus* Δ*menB,* although to a lesser extent than ‘882 (Figure 12D).

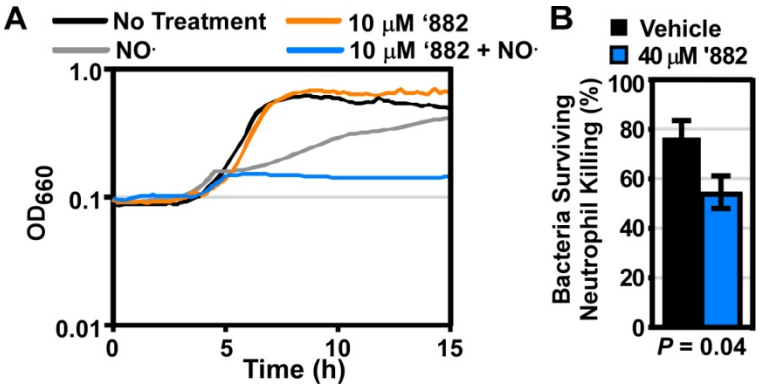

Figure 11. '882 enhances *S. aureus* susceptibility to neutrophil killing mechanisms. *A.* *S. aureus* was grown in the presence or absence of 10 μM '882. When the cultures reached an optical density at 660 nm (OD_{660}) of 0.15, nitric oxide (NO·) was added to the indicated cultures with a final concentration of 10 mM NOC-12 and 1 mM DEANO. ***B.*** *S. aureus* was grown in the presence of vehicle (DMSO) or 40 μM '882 and coated in serum. Murine PMNs were elicited with casein and harvested from the peritoneum. The ability of neutrophils to kill *S. aureus* in the presence of '882 was assessed by comparing CFUs recovered from neutrophil-exposed *S. aureus* to those recovered from identical conditions lacking neutrophils. The mean of at least six independent experiments performed in triplicate are represented by the data; error bars represent standard error of the mean and significance was determined by a two-tailed Student's *t*-test. Data presented in *A* were performed by NPV and in *B* were performed with the assistance of TKF.

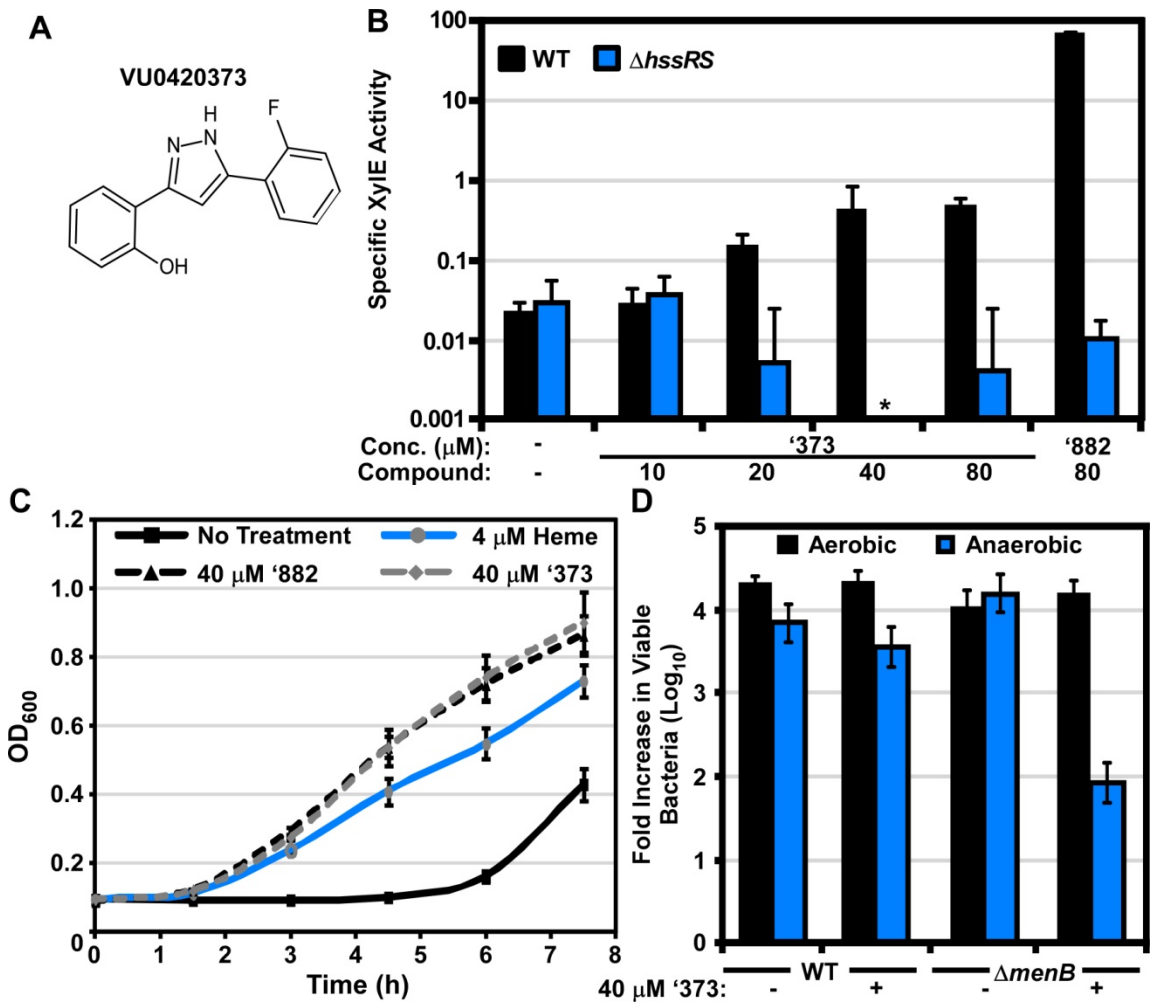

Figure 12. '373 exhibits effects similar to '882. ***A.*** Shown is the structure of derivative VU0420373 ('373). ***B.*** Triplicate cultures of *S. aureus* wildtype (WT) and Δ*hssRS* transformed with a plasmid containing the *xylE* reporter gene fused to the *hrtAB* promoter (p*hrt.xylE*) were grown in medium containing the indicated additive. Following growth to stationary phase, XylE activity was measured and normalized to lysate protein concentrations. An asterisk denotes the value was below the limit of detection. ***C.*** Triplicate cultures of *S. aureus* were grown overnight in medium containing the indicated additive. Cultures were back-diluted into medium containing 20 μM heme. The absorbance at 600 nm (OD_{600}) was taken at the indicated times after inoculation. ***D.*** *S. aureus* WT and the menaquinone auxotroph (Δ*menB*) were grown in triplicate under aerobic and anaerobic conditions in the presence of vehicle (DMSO) or 40 μM '373. CFUs were enumerated at the beginning and end of the time course. Based on these values, the fold increase over the input of bacteria was determined. (*B-D*) Error bars represent one standard deviation from the mean. '882 SAR and '373 synthesis was performed by BFD.

Intraperitoneal administration of ‘373 to mice intravenously infected with *S. aureus* resulted in a significant 1-log decrease in CFUs recovered from the livers of ‘373-treated animals as compared to vehicle (Figure 13A). Notably, ‘373-treatment reduced tissue pathology associated with infection as demonstrated by a significant reduction in the number of liver abscesses (Figure 13B). This liver-specific reduction in bacterial burden and inflammation correlates with an accumulation of ‘373 in the livers of treated animals as shown by Imaging Mass Spectrometry (IMS) (Figures 13C-F) (49). To quantify the tissue level of ‘373, portions of the livers were excised and '373 concentrations were determined by HPLC-MS (Figure 13E). A linear relationship between tissue level and dose of ‘373 administered was observed. Average spectral intensity extrapolated from IMS data of '373 reflected a dose-response relationship similar to that observed by HPLC-MS, confirming the suitability of IMS for monitoring tissue levels of '373 (Figure 13F). Both the HPLC-MS and IMS data support the notion that the therapeutic effect of ‘373 is due to the interaction of the compound with *S. aureus* as it is found at the site where bacterial growth is restricted. Although the therapeutic benefits of ‘373 could be due to alternative activities of this molecule, these results provide evidence that targeting fermentation in a facultative anaerobe may be a viable therapeutic strategy.

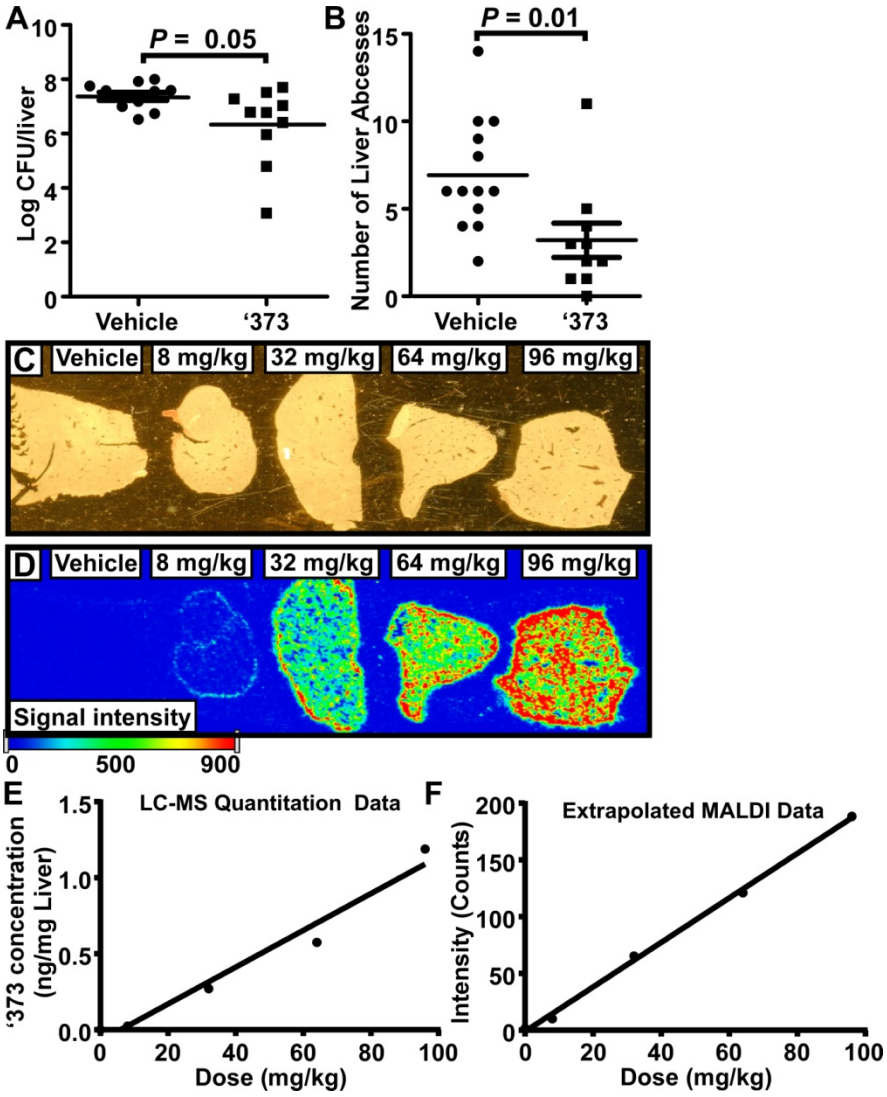

Figure 13. '373 reduces *S. aureus* pathogenesis *in vivo*. Mice infected retroorbitally with *S. aureus* were treated intraperitoneally with vehicle (10% Tween 80) or '373. After 96 h mice were sacrificed and ***A.*** CFUs and ***B.*** surface abscesses were enumerated from the livers. Each marker represents an individual mouse. Data were collected from three independent experiments resulting in $n = 13$ for vehicle and $n = 12$ for '373-treated mice once the highest and lowest values were removed from each group. The horizontal line indicates the mean and the error bars represent the standard error of the mean. Statistical significance was determined by a two-tailed Student's *t*-test. ***C.*** Livers from mice treated with the indicated dose of '373 were harvested 24 h post-infection (1 h after the 2nd treatment), sectioned, and mounted on MALDI target plates. ***D.*** Tissue sections were imaged by MALDI-MS/MS for accumulation of a fragment of '373 by MALDI-MS/MS (*m/z* 255.2→134). Spectra were acquired at 10 microscans per step. 5 laser shots were acquired per pixel and pixels were obtained every 100 µm. ***E.*** Quantitative data from liver extract showing an increase in ng of '373 per mg liver tissue commensurate to dose. ***F.*** Average spectral intensity extrapolated from MALDI IMS data (*D*) for each liver showing a similar dose-response relationship as observed by HPLC-MS in *E*. Data presented in panels *C-F* were collected by JMH.

Discussion

The observation that ‘882 suppresses fermentation suggested that ‘882 would be toxic to fermenting *S. aureus*. This proved true as ‘882 is bacteriostatic to fermenting staphylococci and *C. diphtheriae*. The potential therapeutic utility of targeting fermenting *S. aureus* was verified as ‘882 treatment augments innate immune function and prevents outgrowth of antibiotic resistant colonies *in vitro*, and ‘373 treatment reduces *S. aureus* liver colonization and associated inflammation *in vivo.*

The activity of ‘882 against fermenting bacteria has broad therapeutic potential. ‘882 is bacteriostatic to SCVs, which often emerge during recurrent and persistent *S. aureus* infections (63). This may be generalizable across other infectious diseases such as *N. gonorrhoeae, E. coli, P. aeruginosa*, and *S.* Typhimurium which can also spawn SCVs (6, 63). In addition to being used as a treatment for persistent infections, derivatives of ‘882 could have utility in combinatorial-therapy with antibiotics that target respiring bacteria. As a proof of principle, co-treating *S. aureus* with gentamicin and ‘882 *in vitro* reduces bacterial viability and the outgrowth of antibiotic resistant populations. If gentamicin is used to treat *S. aureus* infections, it is typically used in combination with other primary antibiotic agents or conjugated to beads and used as the primary antibiotic agent at the site of osteomyelitis infections. SCVs often arise during the prolonged antibiotic regimen required for treatment of osteomyelitis. Therefore, it is possible that an ‘882-gentamicin dual therapy could be used to improve therapy for osteomyelitis by preventing the generation of SCVs during infection. If ‘882 proves synergistic with other primary anti-staphylococcal agents such as β-lactams and vancomycin, it is possible that ‘882 could be used more broadly as an adjuvant to expand the antibiotic armamentarium that is effective against *S. aureus* infections.

The majority of bacterial pathogens use some combination of fermentation and respiration to produce ATP, suggesting that both are important for colonization and persistence (34). Resisting neutrophil assaults requires *S. aureus* to rely on fermentation. Adding ‘882 to *ex*

vivo neutrophil-*S. aureus* mixtures resulted in improved neutrophil killing, suggesting that ‘882 could augment host defense. *In vivo,* the importance of *S. aureus* fermentative pathways during infection is demonstrated by the fact that ‘373 reduces abscess formation and *S. aureus* growth in the livers of systemically infected mice. The observed effects of ‘373 on *S. aureus* pathogenesis support the notion that the abscess is an anaerobic environment and that bacterial fermentation is required for efficient colonization (59). Furthermore, the modest effect ‘373 has on *S. aureus* pathogenesis *in vivo,* despite its diminished bacteriostatic activity *in vitro*, highlights the promise of more potent, biologically compatible derivatives of ‘882 as novel therapeutics.

In summary, a small molecule has been identified that diminishes fermentative processes, stimulates endogenous heme biosynthesis and activates the HssRS heme sensor. This molecule has two-fold utility as both a probe of bacterial physiology and an unconventional therapeutic. The utility of targeting fermenting bacteria is exemplified by the fact that this compound prevents the emergence of antibiotic resistance, enhances phagocyte killing, and reduces *S. aureus* pathogenesis. Compound ‘882 is a powerful tool not only for studying bacterial heme biosynthesis and central metabolism but also establishes targeting of fermentation as a viable antibacterial strategy. Further studies confirming the mechanisms by which ‘882-derived compounds reduce *S. aureus* pathogenesis and associated inflammation *in vivo* will lay the groundwork for improved strategies for treating recalcitrant infections.

CHAPTER IV

A CHEMICAL GENETICS APPROACH FOR DISSECTING THE MECHANISM OF '882-MEDIATED ANTIMICROBIAL ACTIVITY

Introduction

Compound '882 is toxic to fermenting *S. aureus*. This has therapeutic utility in either mono- or dual-therapy regimens. Understanding the source of '882 toxicity in fermenting *S. aureus* will not only elucidate basic mechanisms of *S. aureus* energy homeostasis, but may also identify a cellular target that is sufficient for ablating fermentative growth. Identifying the cellular target of '882 will enable the activity of '882 to be more rapidly improved through structure-activity relationship (SAR) studies. It may also serve as a platform that would support the identification of alternative strategies for targeting fermenting *S. aureus*.

While there are several approaches to target identification, chemical genetics approaches undertaken by other groups have successfully identified small molecule targets by isolating suppressor mutants (29, 94). If spontaneously '882-resistant strains can be identified then their genomes can be sequenced to identify genetic lesions that support '882 resistance.

Here, strains spontaneously resistant to '882 toxicity were isolated and characterized. All suppressor mutants were found to have deficits in SaeRS function. SaeRS is one of the 16 known TCSs in *S. aureus*. SaeRS is activated by iron and human neutrophil peptides, suppressed by heme, and regulates the secretion of exoproteins and other virulence factors (24, 72). The *sae* operon consists of *saeP, saeQ, saeR,* and *saeS*. SaeRS functions as a prototypical TCS and SaeP and SaeQ enhance SaeS phosphatase activity toward SaeR (32). SaeRS is constitutively expressed from the P3 promoter but the P1 promoter drives the expression of all 4 *sae* ORFs; SaeR recognizes P1, therefore SaeRS is autoregulatory (24). *S. aureus* strain Newman SaeS

carries an L18P mutation that increases basal SaeS activation and results in hyperactivity of SaeRS in strain Newman compared to other *S. aureus* isolates (24, 70). It is this hyperactive SaeS that is required for ‘882 toxicity in *S. aureus*. Transcriptional studies of genes regulated by SaeRS have provided potential leads to the cellular target of ‘882. These studies employing ‘882 suppressor mutants have revealed that the SaeRS TCS is required for ‘882 toxicity. Identifying the regulatory targets of SaeRS that are the source of ‘882 toxicity will reveal genes essential for fermentation, provide guidance for SAR studies, and potentially reveal how energy metabolism and heme homeostasis are coordinated.

Methods

Bacterial strains and growth conditions- Staphylococcus aureus strains Newman wildtype, Δ*saeRS*, and *saeS*P18L have been described previously (16, 46). The USA300 type *S. aureus* clinical isolate LAC cured of erythromycin-resistance (AH1263) was described previously (5).

All *S. aureus* strains were grown on tryptic soy agar (TSA) at 37°C for 20-30 h. All overnights were grown in 5 ml of tryptic soy broth (TSB) in aerobic tubes at 37°C with shaking at 180 rpm unless otherwise noted. Anaerobic growth was obtained by growing cultures in 5 ml of TSB in aeration tubes at 37°C with shaking at 180 rpm for 15 h. Cultures were diluted to a theoretical OD_{600} of 0.0001 and 200 µl were added to 5 µl of additive in a 96 well plate. Cultures were placed in an anaerobic jar and incubated at 37°C for 18 h.

Unless stated otherwise, vehicle treatment refers to a volume of DMSO comparable to the volume added containing the described compound (‘882).

Isolation of ‘882 suppressor strains – Triplicate cultures of *S. aureus* strain Newman were grown for 15 h at 37°C, 180 rpm in 5 ml of TSB in aeration tubes. The OD_{600} of the cultures was measured and then the cultures were back-diluted in TSB to a theoretical OD_{600} of 0.0001. 100 ul of the dilute cultures were inoculated onto TSA containing 20 and 40 µM ‘882 and grown under anaerobic conditions for 36 h. Each suppressor colony was isolated on TSA and confirmed to be

resistant to ‘882 on TSA plates under anaerobic conditions. Each isolate was also tested for catalase activity using H_2O_2 and Gram-stained. All isolates were catalase positive, Gram positive cocci.

Whole genome sequencing of ‘882 suppressor strains – Genomic DNA from Newman wildtype and the five ‘882 suppressor strains 20A, 40A, 20-1, 20-6, and 20-11 was purified and resuspended to a final concentration of 5 µg in 30 µl of sterile dH_2O. It was submitted to the Vanderbilt Technologies for Advanced Genomics (VANTAGE) core. Shotgun sequencing was performed on an Illumina MiSeq and genomes were assembled using *S. aureus* Mu50 as a reference strain and single nucleotide polymorphisms (SNPs) were reported by VANTAGE. The validity of each SNP was determined by comparing the suppressor genomes to the assembled Newman genome using the Integrative Genomics Viewer available from the Broad Institute.

All SNPs were confirmed by Sanger sequencing. Overlapping regions of approximately 1,000 bp were amplified by PCR from the genomes of the suppressor strains using the high-fidelity DNA polymerase Pfu Turbo (Stratagene). PCR products were checked for amplification on an agarose gel and column purified using the Qiagen PCR purification kit. DNA was sequenced by GenHunter and SNPs confirmed using DNASTAR LaserGene8 SeqBuilder and MegAlign programs.

Hemolysis profiles – Hemolytic profiles of each of the suppressor strains were assessed by patching each of the suppressor isolates from TSA to a sheep blood agar plate (BAP). BAP were incubated at 37°C for 24-48 h and inspected for zones of clearing.

Exoprotein profile – Each strain was inoculated from TSA into 15 ml of TSB in a 50 ml conical tube and grown for 16 h. Cultures were pelleted at 5,900 x *g* for 5 min and the supernatants were transferred to a clean tube to be stored at -80°C. Samples were later thawed at room temperature and syringe filtered through a 0.45 µm membrane. Supernatants were concentrated over a 3 kDa column for 60 min at 3,200 x *g*. Samples were mixed 1:1 with 2X SDS-PAGE loading dye and

boiled. 25 µl of each sample was resolved on a 15% SDS-PAGE gel. Proteins were visualized using a Coomassie stain.

anti-SaeQ western blots – Each strain was grown in 5ml of TSB for 15 h under either aerobic or anaerobic conditions at 37°C. Anaerobic cultures were sub-cultured 1:50 into 10 ml of TSB containing 4 µM '882 or an equivalent volume of DMSO and maintained under anaerobiosis. Aerobic cultures were sub-cultured 1:100 into 5 ml of TSB containing 40 µM '882 or an equivalent volume of DMSO and maintained under aerobiosis. All sub-cultures were grown at 37°C for 8 h and then pelleted at 3,200 x *g* for 10 min. The supernatants were removed and the pellets preserved at -80°C.

Pellets were subsequently thawed at room temperature and then maintained on ice. Each pellet was resuspended in TSM (100 mM Tris-HCl pH 7, 500 mM sucrose, 10 mM $MgCl_2$) with 3 µl/ml lysostaphin. To compensate for differences in cell density, the aerobic samples were resuspended in 500 µl and the anaerobic samples were resuspended in 175 µl. The cell walls were removed by incubating all samples at 37°C for 25 min and then centrifugation at 16,100 x *g* for 10 min at 4°C. The supernatants were removed and the pellets resuspended in 250 µl of SoluLyse Reagent for Bacteria (Genlantis) supplemented with 100 µM phenylmethanesulfonylfluoride (PMSF). Each sample was sonicated at 100% for 10 s using a Branson 4c-15 sonicator and normalized based on total protein concentration as determined by BCA assay (Pierce). Samples were diluted to a final concentration of 3 µg/µl in SDS-PAGE loading buffer, boiled, and 20 µl were resolved on a 15% SDS-PAGE gel. Gels were transferred to nitrocellulose membrane for 1 h at 1000 mA and then blocked overnight at 4°C in 10% non-fat dry milk (NFDM) in tris buffered saline (TBS: 50 mM Tris-HCl pH 7.5 and 150 mM NaCl).

Membranes were probed with 1:2,500 anti-SaeQ antibody for 1 h at room temperature in 10% NFDM in TBS-T (TBS containing vol/vol 0.01% Tween-20). Membranes were then washed 3 times in TBS-T. An Alexa fluor 660 goat anti-rabbit IgG (Life technologies) was diluted 1:6,000 in TBS-T and used as a secondary antibody. Membranes were probed with the secondary

antibody for 1 h and then washed 3 times in TBS-T. Western blots were scanned on an Odyssey Infrared imaging system (LI-COR).

RNA preparation and microarray analysis – Strains were cultured anaerobically overnight in 5 ml TSB at 37°C. Samples were sub-cultured 1:100 into 10 ml of TSB and maintained at 37°C under anaerobiosis. At mid-log (5 h after sub-culture), either 10 µl of DMSO or 25 mM '882 (final concentration 25 µM) was spiked into the cultures. Cultures were incubated 10 min at 37°C and then mixed with an equal volume of ice cold 1:1 acetone:ethanol and stored at -80°C. All samples ranged within 2-6x10^8 CFU/ml. Replicates were collected on separate days.

Samples were thawed on ice and then pelleted at 10,000 x *g* for 10 min at 4°C. The pellets were dried on ice and then resuspended in 500 µl of TE (10 mM Tris-HCl, 1 mM EDTA, pH 7.6). Samples were transferred to an RNase/DNase free tube containing Lysing Matrix B (MP). Cells were lysed on a FastPrep-24 bead beater for 20 s at setting 5.0, iced for 5 min, and then disrupted again for 40 s at setting 4.5. Samples were centrifuged at 16,100 x *g* for 15 min at 4°C. The upper phase was transferred to a clean 1.5 ml tube and mixed with 350 µl of RLT for every 100 µl of sample resulting in a final volume of approximately 1.5 ml. Samples were centrifuged for 15 s at 8,000 x *g* and the supernatant transferred to a clean tube. 250 µl of ethanol was added for every 100 µl of sample.

RNA was bound to a Qiagen RNeasy mini column by centrifugation for 15 s at 8,000 x *g*. Each column was washed with 350 µl of RW1 buffer and the flow-through discarded. DNA was removed by adding 10 µl DNase I to 70 µl RDD buffer (Qiagen) and incubated on the column for 20 min at 37°C. Each column was incubated with 350 µl RW1 for 5 min, centrifuged and the flow-through discarded. 500 µl of RPE was added to each column then the samples were centrifuged and the flow-through discarded; this was performed twice. The column was transferred to a clean 1.5 ml tube and the RNA eluted with 40 µl of RNase-free water.

Transcriptional changes were analyzed by microarray analysis in the Dunman laboratory at the University of Rochester as described previously (4). Two replicates were prepared

independently for each condition. Genes with at least a 2-fold change expression, a *P*-value ≤ 0.05 as determined by a Student's *t* test, and levels detectable above background based on Affymetrix algorithms were considered to be differentially regulated.

Results

'882-resistant colonies are isolated under anaerobiosis. One strategy employed to identify the cellular target that mediates '882 toxicity was the isolation of strains spontaneously resistant to '882. If spontaneously '882-resistant strains could be isolated, their genomes could be sequenced to identify genetic lesions that support '882 resistance. To select for '882-resistant isolates *S. aureus* strain Newman was grown on TSA plates containing 20 and 40 μM '882. The plates were grown under anaerobiosis for 36 hours and 15 colonies were identified. Each colony was isolated on plain TSA grown aerobically and then patched on plain TSA, 10 and 20 μM '882 anaerobically. Nine of the 15 colonies remained resistant to '882 on solid agar under anaerobiosis. All nine isolates are catalase positive and appear to be *S. aureus* by Gram stain. These data reveal that *S. aureus* generates resistance to '882 in anaerobic conditions with a frequency of approximately 1 in 10^{-7} CFUs.

The genetic stability and heritability of the '882 resistance was tested by sequentially passing each strain four times at 37°C. After passaging, the nine strains were assessed for '882 resistance in liquid media under anaerobiosis. All passaged strains were resistant to '882 (Figure 14).

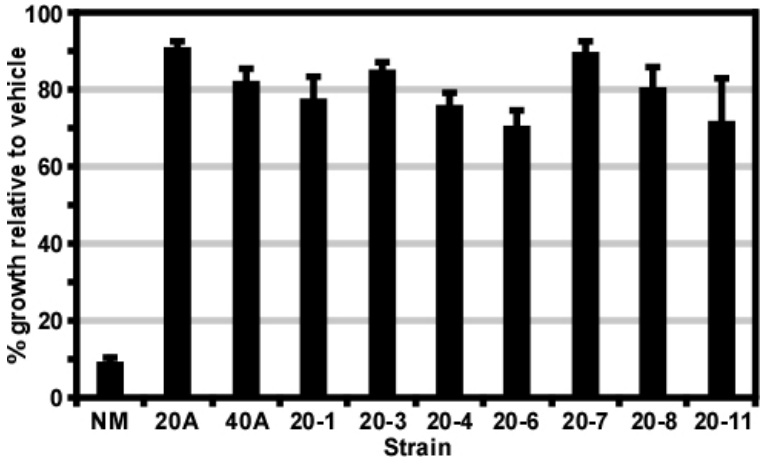

Figure 14. ‘882-resistance is heritable and stable. Wildtype *S. aureus* Newman (NM) and 9 strains isolated on toxic concentrations of ‘882. The first two digits of each name indicate the μM concentration of ‘882 from which the colony was isolated. All strains were grown in triplicate, aerobically overnight, and back-diluted to a theoretical optical density at 600 nm (OD_{600}) of 0.0001 in TSB. In a 96 well plate, 200 μl of each diluted culture was added to a stock of ‘882, so that the final concentration was 40 μM, or an equivalent volume of DMSO (vehicle). The plate was grown in an anaerobic jar and the OD_{600} was recorded after 18 h of growth. Growth was analyzed relative to cultures grown with vehicle alone. Shown are data representative of three independent experiments. Error bars represent one standard deviation from the mean.

‘882-resistant isolates have genetic lesions in the *sae* operon. Since the ‘882 resistance of all nine isolates is heritable and stable, the identities of the genetic mutations that provide‘882 resistance were pursued. The genomes of five isolates (20A, 40A, 20-1, 20-6, and 20-11) along with the parental Newman strain were sequenced at the VANTAGE core. Shotgun sequencing was performed on an Illumina MiSeq and genomes were assembled using *S. aureus* Mu50 as a reference strain. Each strain only had non-synonymous mutations in the *sae* operon (Figure 15).

The obsevation that mutations were only found in the *sae* operon suggested that the four remaining unsequenced strains (20-3, 20-4, 20-7, and 20-8) may also have lesions in the *sae* operon. To test this hypothesis, the *sae* locus of each strain was amplified by PCR and analyzed by Sanger sequencing. Mutations in the *sae* locus were also identified in 20-3 and 20-8 (Figure 15). In total, six unique lesions in the *sae* operon were identified. Isolates 20A and 40A both had a point mutation 15 base pairs (bp) 5’ to the *saeR* translation start site. This could either affect *saeR* expression or mutate SaeQ (G146D). Isolate 20-3 also had a single point mutation, which occurs in the TATA box of promoter 1 (P1). Only one isolate, 20-8, had a nucleotide duplication. In this strain, 15 bp in the receiver domain of SaeR was duplicated. The three remaining isolates 20-1, 20-6 and 20-11 all had deletions. Two deletions occurred in the receiver domain of SaeR as isolates 20-1 and 20-6 each have unique 9 and 15 bp deletions, respectively. Strain 20-11 has 198 bp of the DNA binding domain of SaeR deleted. Intriguingly, all mutations either maintained the same number of bp in the *sae* operon or affected the size by a multiple of three. That is, no frame shift mutations occurred. The significance of this observation remains to be understood. Nonetheless, the clustering of mutations in one regulatory locus of *S. aureus* Newman suggests that the activity of SaePQRS is altered in ‘882-resistant strains and impacts ‘882 susceptibility.

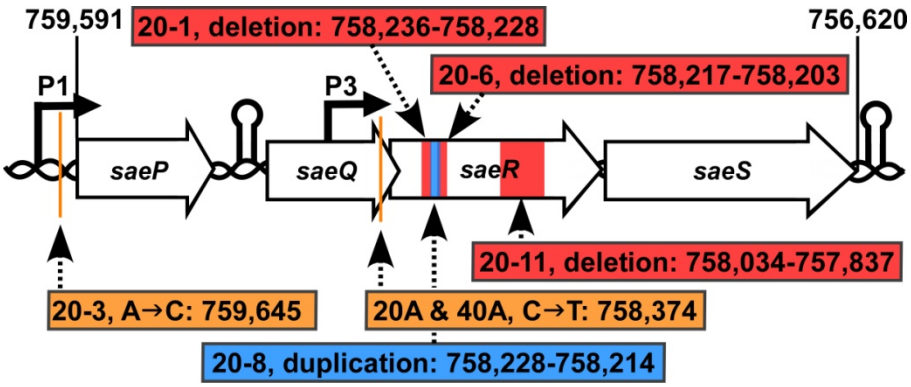

Figure 15. Genetic lesions present in '882-resistant isolates. The *sae* locus of nine spontaneously '882-resistant isolates were sequenced by Sanger sequencing to confirm and identify any mutations in the locus. A schematic of the *sae* locus is depicted above with the two promoters (P1 and P3) marked with a bent arrow and the two terminators marked with a hairpin. Three isolates: 20-3, 20A, and 40A (orange) had a point mutation. Three isolates: 20-1, 20-6, and 20-11 (red) had deletions. And one isolate, 20-8, had a 15 base pair duplication. The number following the colon denotes the base pair location in the Newman genome affected by the mutation.

SaePQRS is functionally inactivated in ‘882-resistant mutants. SaePQRS was first identified as a *S. aureus* TCS that regulates the secretion of exoproteins and toxins (25, 26). To examine the activity of SaePQRS in ‘882-resistance the hemolytic activity and exoprotein profiles of each isolate were visualized (Figures 16A and B). All ‘882-resistant isolates, including those strains which have no identifiable genetic lesions in the *sae* operon, had decreased hemolysis and visibly reduced exoprotein abundance. These data suggest that SaePQRS is inactivated in all ‘882-resistant strains.

Since SaePQRS is an autoregulated TCS, inactivating any component of the TCS should result in reduced protein abundance of all components of the TCS. In order to determine if SaeRS is active in the ‘882-resistant strains, the abundance of SaeQ in each isolate was determined by western blot. SaeQ was completely absent in all ‘882-resistant isolates, indicating that each strain had a loss of SaePQRS function (Figure 16C). The loss of SaePQRS activity in ‘882-resistant strains suggests that an active SaePQRS is required for ‘882 toxicity.

Newman SaeS is necessary for ‘882 toxicity. The observation that all spontaneous ‘882-resistant strains phenocopied the isogenic *saeRS* deletion strain (Δ*saeRS*) pointed to the hypothesis that a functionally active SaePQRS signaling system is required for ‘882 to be toxic under anaerobic growth conditions. To test this hypothesis, the sensitivity of an isogenic *saeRS* deletion strain (Δ*saeRS*) to ‘882 was assessed by anaerobic growth analyses and in fact Δ*saeRS* is resistant to ‘882 (Figure 17). The necessity of SaeRS signaling for ‘882-induced heme accumulation and HssRS activation was also assessed. ‘882 still induces heme accumulation and HssRS activation even in the absence of SaeRS (data not shown). These data agree with the observation that ‘882 is toxic even in the heme biosynthesis deletion strain *hemB::ermC* and strengthen the model that heme is not the cause of ‘882-induced anaerobic growth inhibition.

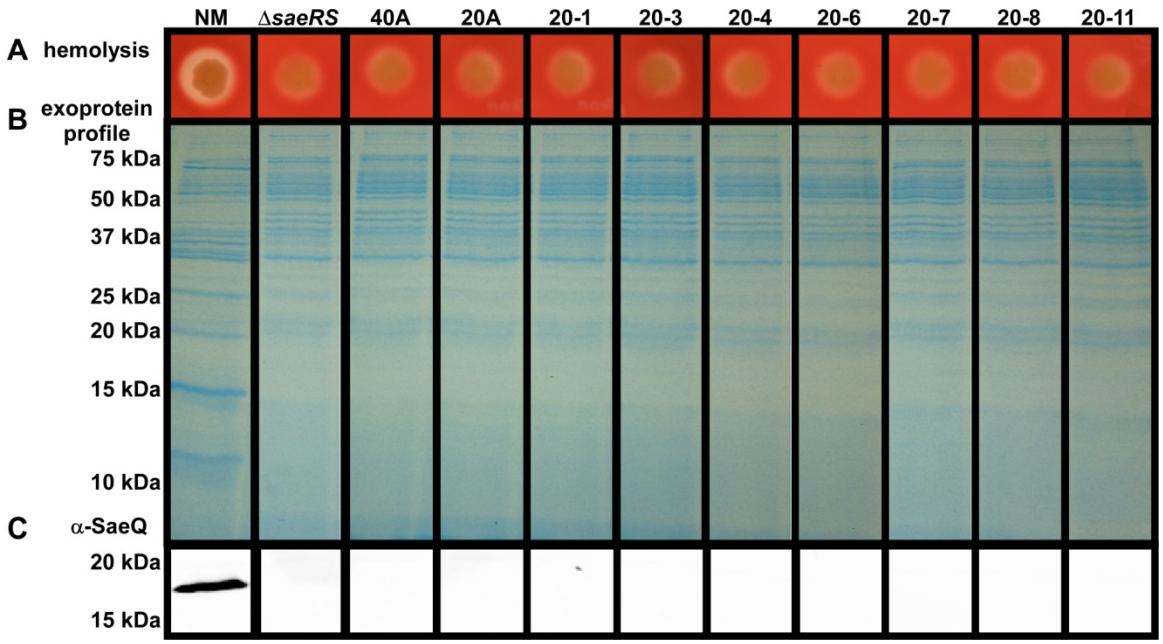

Figure 16. '882-resistant isolates have a loss in SaePQRS activity. *S. aureus* strain Newman, Newman Δ*saeRS*, and 9 isogenic strains resistant to anaerobic '882 toxicity were screened for SaePQRS function. ***A.*** Each strain was spotted onto a sheep blood agar plate and incubated at 37°C for 24 h. ***B.*** All strains were grown overnight in TSB and their supernatants concentrated over a 3 kD spin column. Concentrated supernatants were separated on a 15% SDS-PAGE gel and visualized using Coomassie dye. ***C.*** Whole cell lysates from aerobic cultures were blotted with anti-SaeQ antisera.

While determining the toxicity of ‘882 toward other staphylococcal species it was noted that ‘882 is not toxic to the prevalent community acquired, methicillin-resistant *S. aureus* (CA-MRSA) strain USA300 LAC (Figure 17). Newman SaeS has a single nucleotide point (SNP) mutation that switches the amino acid residue at position 18. In most strains, including USA300, residue 18 is leucine but in Newman it is proline (24). This mutation results in a hyperactive SaeS. Noting that ‘882 is not toxic to USA300 and USA300 does not have the SaeS mutation guided the hypothesis that the hyperactive SaeS activity in Newman is necessary for ‘882 toxicity. To test this hypothesis, Newman SaeS was isogenically converted from proline at residue 18 to a leucine (46). This SaeS-repaired strain is not sensitive to ‘882 toxicity under anaerobiosis (Figure 17). Together, these data indicate that a hyperactive SaeS is required for anaerobic ‘882 toxicity.

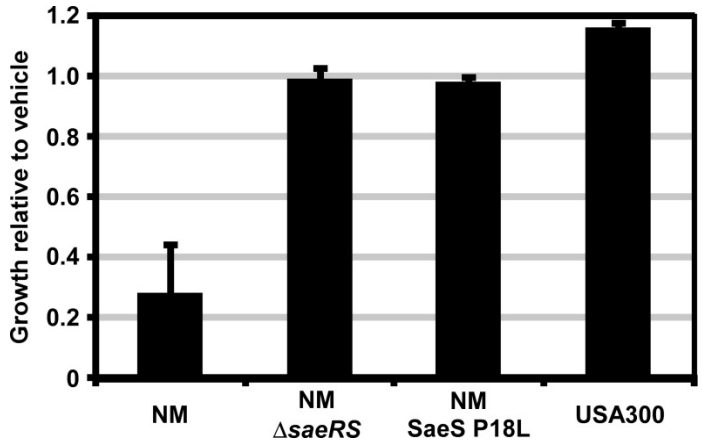

Figure 17. Newman SaeS is necessary for '882 toxicity. Newman (NM) wildtype, Δ*saeRS*, and SaeS P18L (CYL111481), along with USA300 were analyzed for sensitivity to '882. Each strain was analyzed in triplicate. Overnights were diluted to a theoretical optical density at 600 nm (OD_{600}) of 0.0001. Each culture was grown in the presence of vehicle (an equal volume of DMSO) and 10 μM '882. Cultures were grown at 37°C in an anaerobic jar for 18 h. At the end of the time course the cultures were resuspended and OD_{600} was recorded. Each '882 treated culture was normalized to the vehicle controls. Error bars correspond to one standard deviation from the mean.

‘882 and oxygen impact SaeQ abundance. The necessity of Newman SaeS for ‘882 toxicity points to the hypothesis that the source of ‘882 toxicity is either SaePQRS or an Sae-regulated target. If ‘882 is targeting an Sae-regulated product specifically under anaerobiosis, this suggests that oxygen may impact Sae activity. To determine the effect of ‘882 and oxygen on SaePQRS activity, SaeQ levels were probed by western blot in both Newman and USA300.

In the presence of vehicle alone, growth in an anaerobic environment reduced SaeQ abundance in both Newman and USA300. In USA300, however, SaeQ was undetectable, while Newman retained a low level of SaeQ (Figure 18). This is in agreement with the report that Newman SaePQRS is hyperactive. What is particularly intriguing is that ‘882 treatment increases SaeQ abundance under both aerobic and anaerobic conditions in Newman, but suppresses SaeQ levels aerobically and does not affect the already absent SaeQ anaerobically in USA300 (Figure 18). These data suggest that aberrant activation of SaePQRS under anaerobiosis by ‘882 is toxic to the bacteria. This leads to two primary hypotheses for the cause of ‘882 toxicity. First, SaePQRS over-expression alone under anaerobiosis is stressful to *S. aureus*. Or second, the effect of ‘882 treatment on an Sae-regulated target is the source of toxicity. The latter hypothesis is supported by several observations. First, SaeRS regulates many cellular target including genes involved in energy homeostasis. Second, SaeRS is a TCS specific to staphylococci, yet ‘882 is toxic to non-staphylococcal species (Figure 7). And finally, SaeQ is modestly expressed at basal levels in Newman without overt detriment to anaerobic growth suggesting that SaeRS expression under anaerobiosis alone is not sufficient to inhibit anaerobic growth.

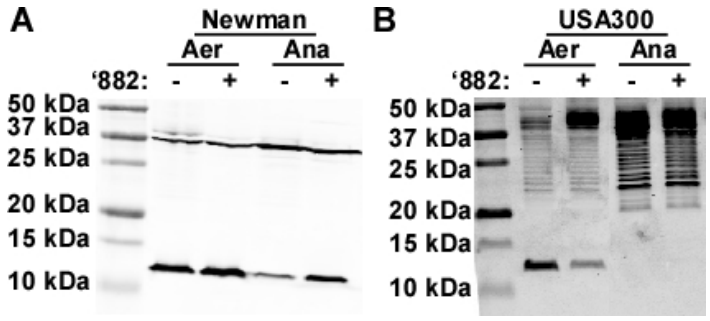

Figure 18. Oxygen and '882 impact SaeQ abundance. ***A.*** Newman and ***B.*** USA300 LAC were grown under aerobic and anaerobic conditions for 8 h. Media was supplemented with either vehicle (DMSO) or '882 (4 μM-anaerobic and 40 μM-aerobic). Whole cell lysates were normalized to protein content and resolved on a 15% SDS-PAGE gel. Proteins were transferred to a nitrocellulose membrane and probed with anti-SaeQ antibody.

Genes differentially regulated by SaePQRS under anaerobiosis. As it seems most likely that an Sae-regulated target contributes to anaerobic ‘882 toxicity, identifying the genes differentially regulated by SaePQRS under anaerobiosis could reveal the source of ‘882 toxicity. To detect genes regulated by SaePQRS *S. aureus* Newman wildtype and Δ*saeRS* were grown anaerobically to mid-log phase. The samples were pulsed with either vehicle (DMSO) or 10 μM ‘882 for 10 min. The RNA from these samples was isolated and differential gene expression was analyzed by microarray.

SaeRS is a major regulatory system in *S. aureus* so it is not surprising that many genes were differentially regulated in the *saeRS* mutant. The positive regulation of many virulence factors, exoproteins and proteases by SaeRS has been well described and were reproduced in our microarray (Table 2) (43). The most striking gene clusters regulated by SaeRS were those involved in amino acid metabolism (Table 2). Operons involved in cysteine, methionine, aspartate, lysine, leucine, isoleucine, valine, glutamate, and histidine metabolism are all positively regulated by SaeRS. Transporters of oligopeptides and amino acids are also positively regulated by SaeRS. Gene clusters involved in protein synthesis, mevalonate and THF synthesis are repressed by SaeRS activity. It is also interesting to note that SaeRS function impacts several genes involved in energy homeostasis including two fermentation products: acetoin and lactate.

By microarray analysis a total of 81 transcripts were observed to be positively regulated by SaeRS. Of these transcripts, 70 are annotated as coding transcripts and 64 are available in the Network on Antimicrobial Resistance in *S. aureus* (NARSA) defined transposon library. Many positively regulated gene targets are in shared operons and therefore of the 64 transposon mutants available in the NARSA library, 35 are in independent operons. Furthermore, 30 transcripts are negatively regulated by SaeRS and 25 of these are annotated to coding transcripts. Of these 25 genes, 13 are available in the NARSA library and 11 are independent operons. If the exotoxins, proteases and other virulence factors are assumed to not be the source of ‘882 toxicity, then there

are 36 operons already disrupted in the NARSA defined mutant library that may be the source of ‘882 toxicity.

To begin to dissect the factors regulated by SaeRS that may be the source of ‘882 toxicity, transposon insertion mutants in these 36 operons of interest will be transduced from the NARSA library (USA300 background) into *S. aureus* strain Newman. Each transductant will then be assessed for sensitivity to ‘882 under anaerobiosis. If anaerobic toxicity is due to ‘882 interacting with a gene positively regulated by SaeRS then the deletion of the target would be predicted to result in ‘882-resistance. Alternatively, if ‘882 is causing toxicity through a gene repressed by SaeRS then the deletion would be expected to be unable to grow under anaerobic conditions.

In order to begin investigating the potential role of each operon in ‘882 toxicity, seven of these operons have been transduced into *S. aureus* strain Newman, these include *ilvD, oppB, hom, asd, NWMN_2616, pknB,* and *budA1.* As a negative control the toxin *hlgC* was also transduced into Newman. Each gene was confirmed to be disrupted by sequencing and then the sensitivity of each strain to ‘882 under anaerobic conditions was assessed. None of these eight operons affect anaerobic sensitivity to ‘882; although *pknB* has a modest growth defect under anaerobiosis. It is possible that this serine/threonine kinase may contribute to *S. aureus* sensitivity to ‘882 or anaerobic growth in general. The data collected on these eight transposon mutants rule out acetoin synthesis, oligopeptide transport, branched chain amino acids, aspartate and lysine metabolism as the source of ‘882 toxicity. The involvement of the remaining 29 operons remains to be assessed.

Table 2: Transcripts regulated by SaeRS under anaerobiosis and ‘882 treatment				
Newman	***USA300***	***Fold change***	***Gene name***	***Gene description***
Protein synthesis				
NWMN_1175	SAUSA300_1158	-2.48	-	conserved hypothetical protein
NWMN_1497	SAUSA300_1554	-3.24	-	conserved hypothetical protein TIGR00253, RNA binding protein
NWMN_1957	SAUSA300_2002	-2.12	*rimJ*	ribosomal-protein-alanine acetyltransferase, putative
NWMN_2022	SAUSA300_2072	-2.21	*prfA*	peptide chain release factor 1
NWMN_2146	SAUSA300_2198	-2.15	*rpsC/rplF*	ribosomal protein L6
NWMN_2147	SAUSA300_2199	-2.12	*rplV*	ribosomal protein L22
NWMN_2150	SAUSA300_2202	-2.65	*rplW*	ribosomal protein L23
Nucleic Acid				
NWMN_0249	SAUSA300_0307	-3.24	-	acid phosphatase5-nucleotidase, lipoprotein e(P4) family
Co-factor Synthesis				
NWMN_0553	SAUSA300_0572	-2.10	*mvk/mvaK1*	mevalonate kinase
NWMN_0554	SAUSA300_0573	-2.37	*mvaD*	mevalonate diphosphate decarboxylase
NWMN_0926	SAUSA300_0959	-2.03	*fmt*	Synthesizes THF and F-met-tRNA
Cell signaling				
NWMN_0484	SAUSA300_0700/0701	-2.11	*ctsR*	conserved hypothetical protein: transcription repressor of class III stress genes homologue
NWMN_1130	SAUSA300_1113	-2.08	*pknB*	serine/threonine-protein kinase
NWMN_1852	SAUSA300_1895	-2.13	-	nitric-oxide synthase, oxygenase subunit
Energy Production				
NWMN_0071	SAUSA300_0129	3.60	-	acetoin reductase
NWMN_0171	SAUSA300_0229	5.05	-	propionate CoA-transferase, putative
NWMN_1616	SAUSA300_1669	2.13	-	aminotransferase, class V
NWMN_1617	SAUSA300_1670	2.16	*serA*	D-3-phosphoglycerate dehydrogenase
NWMN_2110	SAUSA300_2165	-5.67	*budA1*	alpha-acetolactate decarboxylase; converts pyruvate to acetoin
NWMN_2111	SAUSA300_2166	-4.16	*budB*	acetolactate synthase, catabolic
NWMN_2499	SAUSA300_2537	4.61	*ldh*	L-lactate dehydrogenase 2

Table 2 cont'd: Transcripts regulated by SaeRS under anaerobiosis and '882 treatment				
Newman	***USA300***	***Fold change***	***Gene name***	***Gene description***
Amino acid metabolism				
Cys/Met				
NWMN_0011	SAUSA300_0012	2.60	-	homoserine O-acetyltransferase, putative
NWMN_0348	SAUSA300_0357	2.82	*metE*	5-methyl-tetrahydropteroyltriglutamate-homocysteine methyltransferase (metE)
NWMN_0351	SAUSA300_0360	2.08	-	trans-sulfuration enzyme family protein
NWMN_0426	SAUSA300_0435	3.28	-	ABC transporter, ATP-binding protein; predicted to transport methionine
NWMN_0427	SAUSA300_0436	3.19	-	ABC transporter, permease protein
NWMN_0428	SAUSA300_0437	3.04	-	ABC transporter, substrate-binding protein
NWMN_2021	SAUSA300_2071	-2.13	-	SAM-dependent modification methylase, HemK family
Asp				
NWMN_1239	SAUSA300_1224	2.05	*thrA*	aspartate kinase
NWMN_1241	SAUSA300_1226	2.39	*hom*	homoserine dehydrogenase
NWMN_1242	SAUSA300_1227	2.71	*thrC*	threonine synthase
NWMN_1243	SAUSA300_1228	2.89	*thrB*	homoserine kinase
Lys				
NWMN_1305	SAUSA300_1286	2.18	*asd*	aspartate-semialdehyde dehydrogenase
NWMN_1306	SAUSA300_1287	2.39	*dapA*	dihydrodipicolinate synthase
NWMN_1307	SAUSA300_1288	2.65	*dapB*	dihydrodipicolinate reductase
NWMN_1308	SAUSA300_1289	2.74	*dapD*	2,3,4,5-tetrahydropyridine-2,6-dicarboxylate N-succinyltransferase
Val, Leu, Ile				
NWMN_1960	SAUSA300_2005	4.45	*ilvD*	dihydroxy-acid dehydratase
NWMN_1961	SAUSA300_2006	4.48	*ilvB*	acetolactate synthase, large subunit, biosynthetic type
NWMN_1963	SAUSA300_2008	4.94	*ilvC*	ketol-acid reductoisomerase
NWMN_1964	SAUSA300_2009	4.64	*leuA*	2-isopropylmalate synthase
NWMN_1965	SAUSA300_2010	4.85	*leuB*	3-isopropylmalate dehydrogenase
NWMN_1966	SAUSA300_2011	4.27	*leuC*	3-isopropylmalate dehydratase, large subunit
NWMN_1967	SAUSA300_2012	3.97	*leuD*	3-isopropylmalate dehydratase, small subunit
NWMN_1968	SAUSA300_2013	2.56	*ilvA2*	threonine dehydratase

Table 2 cont'd: Transcripts regulated by SaeRS under anaerobiosis and '882 treatment				
Newman	***USA300***	***Fold change***	***Gene name***	***Gene description***
Glu				
NWMN_0145	SAUSA300_0202	2.33	-	peptide ABC transporter, permease protein
NWMN_0147	SAUSA300_0204	2.29	*ggt*	gamma-glutamyltranspeptidase; releases cysteine from glutathione
NWMN_0436	SAUSA300_0445	2.42	*gltB*	glutamate synthase, large subunit
NWMN_0437	SAUSA300_0446	2.72	*gltD*	glutamate synthase, small subunit
His				
NWMN_0692	SAUSA300_0708	2.68	*hisC*	histidinol-phosphate aminotransferase
Cell Envelope				
NWMN_0193	SAUSA300_0253	-2.59	*scdA*	cell wall synthesis
NWMN_1145	SAUSA300_1128	-2.01	-	cell division protein FtsY, putative; FtsY recognizes signal peptide for secretion
NWMN_1342	SAUSA300_1324	-2.92	-	membrane protein, putative
NWMN_1309	SAUSA300_1291	2.95	*hipO*	peptidase, M20/M25/M40 family
NWMN_1310	SAUSA300_1292	3.09	*alr2*	alanine racemase family protein, pyridoxal 5'phosphate dependent
Transport				
NWMN_0856	SAUSA300_0887	2.43	*oppB*	oligopeptide ABC transporter, permease protein
NWMN_0857	SAUSA300_0888	2.27	*oppC*	oligopeptide ABC transporter, permease protein
NWMN_0858	SAUSA300_0889	2.47	*oppD*	oligopeptide ABC transporter, ATP-binding protein
NWMN_0859	SAUSA300_0890	2.86	*oppF*	oligopeptide ABC transporter, ATP-binding protein
NWMN_0860	SAUSA300_0891	2.69	*oppA*	oligopeptide ABC transporter, oligopeptide-binding protein
NWMN_2303	SAUSA300_2349	-2.27	-	formate/nitrite transporter family protein
NWMN_2500	SAUSA300_2538	2.32	-	amino acid permease
NWMN_2581	SAUSA300_2616	2.75	-	cobalt transport family protein
NWMN_2582	SAUSA300_2617	3.67	-	ABC transporter, ATP-binding protein
NWMN_2584	SAUSA300_2619	3.61	-	conserved hypothetical protein

Table 2 cont'd: Transcripts regulated by SaeRS under anaerobiosis and '882 treatment				
Newman	***USA300***	***Fold change***	***Gene name***	***Gene description***
Virulence factors and exoproteins				
NWMN_0362	SAUSA300_0370	68.74	-	staphylococcal enterotoxin, putative
NWMN_0388	SAUSA300_0395	12.85	*ssl1nm*	exotoxin 3, putative
NWMN_0389	SAUSA300_0396	23.62	*ssl2nm/set7*	exotoxin 1, putative
NWMN_0390	SAUSA300_0397	7.81	*ssl3nm*	exotoxin 8
NWMN_0392	SAUSA300_0399	5.48	*ssl5nm*	exotoxin 3
NWMN_0393	SAUSA300_0400	5.81	*ssl6nm*	exotoxin
NWMN_0395	SAUSA300_0402	21.35	*ssl8nm*	exotoxin 12
NWMN_0396	SAUSA300_0403	29.33	*ssl9nm*	exotoxin 5, putative
NWMN_0397	SAUSA300_0404	14.54	*ssl10*	exotoxin 4, putative
NWMN_0758	SAUSA300_0774	53.71	*empbp/ssp*	secretory extracellular matrix and plasma binding protein
NWMN_1067	SAUSA300_1053	60.29	-	hypothetical protein, formyl peptide receptor-like 1 inhibitory protein
NWMN_1246	SAUSA300_1232	2.25	*katA*	Catalase
NWMN_1075	SAUSA300_1059	14.62	-	exotoxin 1, putative
NWMN_1076	SAUSA300_1060	22.31	-	exotoxin 4, putative
NWMN_1077	SAUSA300_1061	69.11	-	exotoxin 3, putative
NWMN_1872	SAUSA300_1917	137.5	*map*	map protein, authentic frameshift
NWMN_1926	SAUSA300_1973	64.33	*hlb*	phospholipase C
NWMN_2318	SAUSA300_2365	94.07	*hlgA*	gamma-hemolysin, component A
NWMN_2320	SAUSA300_2367	135.74	*hlgC*	gamma hemolysin, component C
NWMN_2321	SAUSA300_2368	47.03	*hlgB*	gamma hemolysin, component B
Hypothetical				
NWMN_0150	SAUSA300_0207	2.45	-	M23/M37 peptidase domain protein
NWMN_0206	SAUSA300_0266	-2.5	-	hypothetical protein
NWMN_0402	SAUSA300_0409	114.43	-	hypothetical protein
NWMN_0896	SAUSA300_0929	2.1	-	hypothetical protein
NWMN_2370	SAUSA300_2417	2.39	-	transporter, putative
NWMN_2579	SAUSA300_2614	2.06	-	hypothetical protein
NWMN_2608	SAUSA300_2642	-2.71	-	conserved hypothetical protein

Discussion

This chemical genetics approach to understanding the mechanism of ‘882 toxicity has begun to reveal a source of anaerobic toxicity for *S. aureus*. The successful isolation of nine ‘882-resistant strains, each strain null for SaeRS activity, has led to the conclusion that the SaeRS TCS is required for ‘882-induced anaerobic toxicity, but not heme biosynthesis and HssRS activation. Furthermore, it was noted that USA300 LAC was resistant to ‘882 toxicity, while Newman was sensitive. Converting Newman SaeS proline 18 to leucine, which is present in USA300 LAC SaeS, provided resistance to ‘882 indicating that the hyperactivity of Newman SaeS is required for ‘882 toxicity. Finally, it was determined that ‘882 activates SaeRS expression in Newman and represses SaeRS expression in USA300 LAC. It is likely that the up-regulation of SaeRS in Newman by ‘882 is a source of stress during anaerobic growth.

The toxicity of ‘882 toward other bacterial species that do not encode SaeRS points to the hypothesis that a cellular factor impacted by SaeRS activity is the target of ‘882. To identify genes differentially regulated by SaeRS, microarray analysis was performed to identify transcriptional changes in Newman and Newman Δ*saeRS* under anaerobiosis. In total, 95 coding transcripts, which comprise 74 unique operons, were differentially regulated by SaeRS. The next step is to identify if any of these genes are involved in ‘882 toxicity. To begin to assess the contribution of each transcriptional target in anaerobic ‘882-toxicity, the 36 genes that are not predicted to be toxins but are available in the NARSA transposon library are being transduced into Newman to determine if they contribute to sensitivity to ‘882 toxicity or anaerobic growth. The first seven genes tested do not contribute to ‘882 toxicity. The remaining genes will be analyzed in the future.

It is possible that the target of ‘882 is an essential gene and is therefore not present in the NARSA transposon library. In fact, it is quite likely, as suppressor mutations have only been identified in the *saePQRS* locus. It is possible that the loss of *saePQRS* titrates the target of ‘882 to levels that still allow growth but prevent ‘882-induced toxicity. If this is the case, a strain of

Newman will be generated that contains two copies of the *saePQRS* operon. This strain can then be used to select for ‘882 suppressor strains. Isolating ‘882 resistance in this strain would require two mutations in two independent *sae* operons in order for the bacteria to become resistant to ‘882, which would have a much lower frequency of occurence. This may allow other suppressor mutants to be isolated that have mutations distinct from the *saePQRS* locus.

The requirement of Newman SaeRS for ‘882 toxicity is intriguing. The SaeRS TCS positively regulates hemolysins and has been reported to be repressed upon heme exposure and activated upon iron limitation, thus implicating SaeRS in contributing to iron and heme homeostasis; these observations were made in an *S. aureus* strain encoding SaeS Leu18 (72). Despite increasing intracellular levels of heme, ‘882 actually increases Newman SaeRS activity. As expected, ‘882 does repress SaeRS activity in USA300, which encodes SaeS Leu18. It is possible that the hyperactivity of the SaeS Pro18 encoded by Newman may override heme-induced repression of SaeRS signaling. It could be this inappropriate regulation of SaeRS in response to endogenous heme levels that results in ‘882 toxicity. Nonetheless, the inappropriate response of SaeRS to endogenous heme levels is unlikely to be the source of ‘882 toxicity as heme biosynthesis is not required for ‘882 toxicity (Figure 4B). That is, ‘882 is still toxic to anaerobic *S. aureus* without activating endogenous heme biosynthesis. These data suggest that it is neither heme nor the regulation of SaeRS by heme that is the source of ‘882 toxicity.

Nonetheless, HssRS and SaeRS are two heme responsive TCSs in *S. aureus*. HssRS seems to solely sense heme while SaeRS activity is also impacted by human neutrophil peptides, oxygen, and iron. It is possible that SaeRS and HssRS may have a complex signaling network that integrates information on the nutrient status of the cell and the external environment to coordinate the metabolic and virulence programs of the bacteria with these signals. Perhaps ‘882 twitches a thread in this complex web of energy homeostasis to exert its effects on heme biosynthesis and anaerobic growth.

Further work towards identifying the source of ‘882-induced anaerobic toxicity is critical. To further confirm that it is the hyperactivity of SaeS Pro18 that generates ‘882 toxicity, the Newman SaeRS has been cloned into the Δ*saePQRS* USA300 genome (5). This strain provides the opportunity to investigate the sufficiency of the Newman SaePQRS in conferring ‘882 sensitivity to USA300 LAC. Pinpointing the source of ‘882 toxicity in *S. aureus* may identify pathways that, when manipulated appropriately, limit *S. aureus* fermentative growth. Specifically targeting fermentative growth does have utility as there are circumstances in which *S. aureus* relies on fermentation to resist host defenses, antibiotics and successfully colonize its host (Chapter III). Therefore, identifying this ‘Achilles heel’ of *S. aureus* fermentation will allow for future work to improve ‘882 activity and develop new methods for targeting anaerobic growth.

CHAPTER V

PROBING A *BACILLUS ANTHRACIS* SIGNALING NETWORK WITH VU0120205

Introduction

Two-component signaling systems (TCSs) are the primary way bacteria sense and adapt to changes in their environment. TCSs are present in nearly all sequenced bacterial genomes; most species encode 20-30 TCSs, while others carry upwards of 200-300 putative TCSs (78). The classic bacterial TCS system is thought to function in a linear fashion, in that each HK has a defined input and that results in a specific output from the RR. The appreciation that interactions, both beneficial and detrimental, occur between TCSs has become more prevalent. This 'cross-talk' has been previously defined as the "communication between two pathways that, if eliminated, would leave intact two distinct, functioning pathways" (41). When cross-talk between two signaling systems benefits an organism this is referred to as 'cross-regulation' (41).

Bacillus anthracis is predicted to encode approximately 45 TCSs. In *B. anthracis,* all HKs and RRs share at least 20% identity with other encoded HKs and RRs. This conservation is manifested primarily in the domains involved in the phosphotransfer event of the signaling pathway. It is the input domains of HKs and the output domains of RRs that are more variable. This allows TCSs to sense a variety of environmental signals to enact an array of outputs, while the fundamental mechanisms of HK autophosphorylation and phosphotransfer to the RR remain central to the function of the system. The mechanisms by which a single HK maintains fidelity to its cognate RR in a bacterial cell expressing 20-300 other HK-RR pairs is a major question in TCS research.

The current understanding of how HK-RR signaling purity is maintained implicates molecular recognition, HK phosphatase activity, and substrate competition as the primary mechanisms for ensuring specificity (62). That is to say molecular recognition dictates that each

HK-RR pair has co-evolved amino acid residues that drive a strong preference for phosphotransfer from the HK to its cognate RR. This phenomenon is observable *in vitro* as most HKs have a strong kinetic preference for their cognate RR over other RRs encoded in the same genome (79). Furthermore, if a HK is a bi-functional kinase/phosphatase, its phosphatase activity is specific for its cognate RR (28). This buffers against non-specific phosphorylation of the cognate RR and limits the activation of the pathway (62). Specificity is further maintained by a high ratio of RR:HK, which would essentially allow the cognate RR to outcompete other RRs for binding to its cognate HK (8, 62). Specificity may also be influenced by the temporal expression and spatial localization of TCSs (41).

Much focus has been on the maintenance of specificity at the HK-RR level and the general conclusions have been that cross-talk between non-cognate HK-RR pairs is possible, but atypical. It may be more likely for cross-talk to occur at other points in the signal transduction pathway. At the transcriptional level, multiple RRs may influence overlapping sets of genes (41). Alternatively, a protein product regulated by a RR may itself be a transcriptional regulator or phosphatase that impinges on the regulatory outputs of other TCSs (41). Essentially it has become clear that bacterial signaling networks are not purely insulated linear systems that have a singular response to a particular input. Rather the complex interactions of TCSs at both the HK-RR and post-RR regulatory levels allow bacteria to integrate multiple signals to generate the appropriate biological response.

Bacillus anthracis is an environmental pathogen that inhabits various environments ranging from the soil to a myriad of mammalians hosts. To survive and persist in adverse environments, *B. anthracis* also possesses the ability to sporulate. Sporulation is a complex process regulated by a complex TCS-like phosphorelay system. During *B. subtilis* sporulation, at least five different HKs impinge upon a single response regulator (86). The complex phosphorelay pathways employed by the *Bacilli* during sporulation hint at the possibility that this

genus may be particularly adept at integrating environmental signals to initiate an appropriate response as well as insulating against unwanted cross-talk between signaling systems.

To further study the activation of the HssRS TCS, the activity of the *S. aureus* HssRS activators were screened for activation of the *hrt* promoter (p*hrt*) in *B. anthracis*. Since *B. anthracis* is closely related to *S. aureus,* it was hypothesized that small molecule activators of *S. aureus* HssRS may also activate *B. anthracis* HssRS. The top 14 hits from the HTS were assessed for XylE activity in *B. anthracis*, and some were found to increase p*hrt* activity. Compound VU0120205 (‘205) became of particular interest as it activates p*hrt* independent of HssRS. This resulted in the identification of a second TCS that cross-talks with HssRS. The new HK is called BAS1817 and its cognate RR is BAS1816. Data presented in this chapter characterize BAS1816-17 as a TCS and dissect the bi-directional mechanisms by which HssRS and BAS1816-17 influence each other. Finally, in an effort to understand the native function of BAS1816-17 other small molecule activators of this TCS are identified. In summary, this chapter uses chemical biology to probe a new *B. anthracis* signal transduction network to understand the integration of heme homeostasis with other environmental signals.

Methods

Bacterial strains and growth conditions – B. anthracis strain Sterne was used for all experiments (87). It was grown in BHI or LB. All plasmid construction was performed in *E. coli* DH5α or TOP10. To move plasmids from *E. coli* to *B. anthracis* they were first transformed into *E. coli* K1077 (37). Proteins were expressed in *E. coli* BL21DE3 pREL. Antibiotic concentrations used were ampicillin 100 μg/ml in *E. coli* (pET15b constructs), chloramphenicol 10 μg/ml in *B. anthracis* (XylE reporter assays) and 34 μg/ml in *E. coli* (protein expression) and kanamycin 20 μg/ml in *B. anthracis* and 40 μg/ml in *E. coli* (knockout generation).

Preparation of heme and other compound stocks – 10 mM heme stocks (Fluka) were prepared daily in 0.1 M NaOH. A 50 mM stock of ‘205 was prepared in DMSO and stored at -20°C. A 20

mM stock of NDGA was prepared in ethanol and stored at -20°C. Stocks of 250 μM vancomycin and 100 mM chlorpromazine were prepared in water and stored at -20°C. A 1 M stock of sodium phosphate monobasic was prepared in water, brought to a pH of 7, and stored at room temperature. A stock of 20 mg/ml of targocil was prepared in DMSO and stored in the dark at 4°C.

Genetic manipulation of B. anthracis – Electroporations and mutant generation were performed as previously described (83). Electroporations were also performed with the following modifications. DNA purified for K1077 *E. coli* was eluted in 10 mM Tris-HCl, pH 8.5 and this solution was used for electroporations. After the *B. anthracis* competent cells were prepared, the optical density at 600 nm (OD_{600}) was determined in phosphate buffered saline (PBS, 137 mM NaCl, 2.7 mM KCl, Na_2HPO_4 10 mM, KH_2PO_4 1.8 mM, pH 7.4). Cells were flash frozen in liquid nitrogen and thawed on ice for electroporations. For electroporation the competent cells were diluted in SMG (0.5 M D-sorbitol, 0.5 M D-mannitol, 10% glycerol) to a final OD_{600} of 8.0. To 50 μl of cells 0.5 – 5 μl of DNA was added (approximately 3 μg total). Cells were incubated with DNA in a pre-chilled 1 mM cuvette for 1 minute on ice and then electroporated using the conditions described previously (83). Cells were recovered in 1 ml BHI + 0.5 M D-sorbitol for 3 h at 30°C, 200 rpm in aeration tubes. All knockouts were generated without an antibiotic cassette. Instead, 1,000 bp (including 100 bp of the target gene) from the 5' and 3' flanking regions of the gene targeted for deletion were cloned into the pLM4 knockout vector to generate clean knockouts.

Generation of xylE reporter plasmids – The *BAS1814* promoter *xylE* reporter construct was generated in a pOS1 background (74). The *BAS1814* promoter-*xylE* fusions was generated by PCR-SOE (31) . This resulted in a seemless fusion between the *BAS1814* promoter and the *xylE* reporter gene. PCR-SOE DNA was digested with BamHI and EcoRI and ligated into pOS1. Mutagenesis of the *BAS1814* DR was carried out by inverse PCR-based mutagenesis. The selected mutations were incorporated on one primer and a second non-overlapping, non-

mutagenic primer was designed to amplify in the opposite direction. The primers were 5' phosphorylated by T4 polynucleotide kinase (NEB) and the parental plasmid amplified using the high-fidely DNA polymerase Pfu Turbo. The amplified DNA was blunt end ligated and transformed into *E. coli.* Mutagenized constructs were verified by DNA sequencing.

XylE assays – XylE assays were performed as described previously with the following exceptions (83). All cultures were grown overnight in 5 ml LB/chloramphenicol at 30°C, 180 rpm. Bacteria were sub-cultured into 4 ml LB/chloramphenicol and grown as indicated: either 1:100 sub-culture and growth for 6 h at 37°C, 180 rpm or 1:1,000 sub-culture and growth for 24 h at 37°C, 180 rpm.

Generation of protein purification constructs – BAS1816 was amplified from genomic DNA by Pfu Turbo using the 3rd ATG as the start site. Inverse PCR was used to insert a SacII site in the multiple cloning site (MCS). Briefly, two complementary, overlapping primers that amplify in the opposite direction were designed, which included the addition of the SacII site after the BamHI restriction. The PCR product was transformed into *E. coli* and successful incorporation of the SacII site was confirmed by sequencing. This inverse PCR generated pLOLA (pET15b.SacII) and resulted in the MCS changing from: CATATGCTCGAGGATCCGGCTGCT to CATATGCTCGAGGATCCGG**CCGCGG**CTGCT. The *BAS1816* PCR product was digested with SacII and BamHI-HF (NEB) and ligated into pLOLA. The intracellular domain (ICD) (bp 221 to the end) of *BAS1817* was amplified using Pfu Turbo and digested with SmaI. The vector pET15b was digested with XhoI and purified using the Qiagen gel purification kit. Blunt ends were generated on pET15b by treating the cut vector with DNA Polymerase I, Klenow fragment (NEB). The Klenow fragment was inactivated, the vector was column purified and blunt-end ligated to the digested *BAS1817* ICD. The mutation of BAS1816 D56N and BAS1817 ICD H137A were generated by inverse PCR as described above. All constructs result in the generation of N-terminal hexahistidine-tagged proteins and were transformed into BL21 DE3 pREL.

Protein purification – Protein purifications were carried out as described previously with the following modifications (82). All proteins were induced in 0.5 mM IPTG, cells were lysed for 5 min on an EmulsiFlex C3 (Avestin) at a peak PSI of 20,000 and the lysates were centrifuged at 20,000 x *g* for 1 h at 4°C. BAS1817 ICD and HssR ICD and their corresponding mutants were purified in TSB containing 10 mM imidazole and eluted in 75 mM imidazole in TBS. BAS1816 and HssR and their corresponding mutants were purified in TSB containing 1 mM EDTA, 10% glycerol, and 10 mM imidazole and eluted in 50 mM imidazole in TBS. BAS1816 was induced after 2 h of growth at 16°C in 0.5 mM IPTG and a second time 5 h later with an equal volume of IPTG to bring the final concentration to 1 mM.

Autophosphorylation and phosphotransfer assays – Autophosphorylation assays were performed as described previously with the following modifications (83). Ten µl autophosphorylation reactions were assembled with HssS and BAS1817 ICDs and their corresponding mutatnts were used at a final concentration of 5 µM (640 µg/ml). For HssS 10 µCi of [γ-^{32}P]-ATP was used and due to the high autophosphorylation of BAS1817, 5 µCi of [γ-^{32}P]-ATP was used. All reactions were incubated at 37°C for 30 min. To analyze the phosphotransfer of each HK to each RR, the HKs were autophosphorylated as described above in a 30 µl reaction volume. After the HKs autophosphorylated for 30 min, 10 µl were sampled into 2X SDS-PAGE loading buffer. To the remaining 20 µl, 3 µl of 100 µM RR was added for a final concentration of approximately 10 µM. HK-RR mixtures were incubated for 5 min and then 10 µl was sampled into 2X SDS-PAGE loading buffer. Samples were analyzed as described previously (83). To examine the preferential phosphotransfer of each HK for each RR, a 220 µl autophosphorylation reaction was run for each HK. Serial dilutions of each RR were prepared so that when 2 µl of the RR stock was added to 9.5 µl of phosphorylated HK, the final RR concentration was 20, 10, 5, 2.5, 1.25, 0.625, 0.31, 0.16, 0.08, and 0.04 µM. Each RR concentration was incubated with each phosphorylated HK for 30 sec, after which 10 µl of 2X SDS-PAGE buffer was added. The samples were stored on ice and analyzed as described previously (83).

Biolog Phenotypic Microarray Screen – Phenotypic Microarray plates (PM 1-20) and IF-0a GN/GP (1.2X) were purchased from Biolog. Preparation of PM inoculating fluids was adapted from the manufacturer's recommendations for *B. subtilis.* The following solutions were prepared: PM-A = 800 mM tricarballylic acid, pH 7.1; PM-B = 240 mM $MgCl_2$ and 120 mM $CaCl_2$; PM-C = 3 mM L-arginine and 6 mM L-glutamic acid; PM-D = 0.5 mM L-cystine pH 8.5 and 1 mM 5'-UMP; PM-E = 0.6% yeast extract; PM-F = 0.6% tween-80; PM-G = 300 mM D-glucose and 600 mM pyruvate. In all instances pH was adjusted with NaOH and all solutions were filter sterilized and stored at 4°C. 12X PM additive for PM-1,2 = 5 ml each of PM-B, PM-C, PM-E, PM-F, and 15 ml each of PM-D and sterile water. 12X PM additive for PM-3,6,7 = 5 ml each of PM-B, PM-E, PM-F, PM-G and 15 ml each of PM-A and PM-D. 12X PM additive for PM-4 = 5 ml each of PM-B, PM-C, PM-E, PM-F, PM-G and 15 ml of PM-A and 10 ml of sterile water. 12X PM additive for PM-5 = 5 ml each of PM-B and PM-G and 15 ml of PM-A and 25 ml of sterile water. 12X PM additive for PM-9-20 = 5 ml each of PM-B, PM-E, PM-F, PM-G and 30 ml of sterile water. The inoculating solution for each plate consisted of 20 ml of IF-0A GN/GP (1.2X), 2 ml of 12X PM additive (specific for each plate, described above), and 20 µl of 10 mg/ml chloramphenicol. *B. anthracis* p*14.xylE* was grown overnight on solid media and the colonies were inoculated into the inoculating solution to a final OD_{600} of approximately 0.6. The inoculating solution with the bacterial suspension was aliquoted 100 µl into each well of a 96 well PM plate. A single well was also inoculated with 1.67 µl of 50 mM '205 as a positive control; the well was selected based on chemical redundancy with other wells on the same plate to avoid masking a potential hit. Plates were covered with a Kim wipe to allow oxygen exchange and incubated at 37°C, 180 rpm. At 3 h and 5 h, wells with significant liquid loss were supplemented with 50 µl of sterile water. After 6-7 h, each PM plate was centrifuged at 3,200 x *g* for 10 min. The supernatant was removed by pipetting and the plate frozen at -80°C. To analyze the XylE activity, the PM plates were thawed and cells were lysed by the addition of 50 µl of 2 mg/ml lysozyme in 100 mM potassium phosphate buffer (pH 8.0), 10% (v/v) acetone. Cells were

incubated at 37°C for 30 min. To each well 25 µl of 100 mM potassium phosphate (pH 8.0), 0.2 mM pyrocatechol was added immediately before assaying XylE activity (85). Each PM plate was screened twice, using a different well for a '205 positive control each time.

Results

Compound VU0120205 ('205) activates the p*hrt* direct repeat independent of HssR.

Compound '205 was evaluated for HssRS activation in *B. anthracis* by quantifying the activation of the *hrt* promoter fused to the *xylE* reporter gene (p*hrt.xylE*). This compound has negligible activation of p*hrt* in wildtype *B. anthracis*; although, some activation could be masked by the high basal p*hrt* expression in *B. anthracis* (Figure 19A and B) (83). What is most notable about this compound is that the p*hrt* promoter was still activated upon '205 exposure by nearly 100-fold, while all activation of p*hrt* by heme was absent in Δ*hssR* (Figure 19A). The activation of p*hrt* by '205 was ablated when the four nucleotides required for HssR recognition in the direct repeat (DR) of the *hrt* promoter were mutated (Figure 19). These data suggest that there is at least one other regulator in *B. anthracis* that stimulates *hrt* expression through the *hrt* DR and that this regulator is activated by '205. This hypothesis is supported by the observation that there is a second DR in *B. anthracis* that is closely related to the DR in p*hrt* (12).

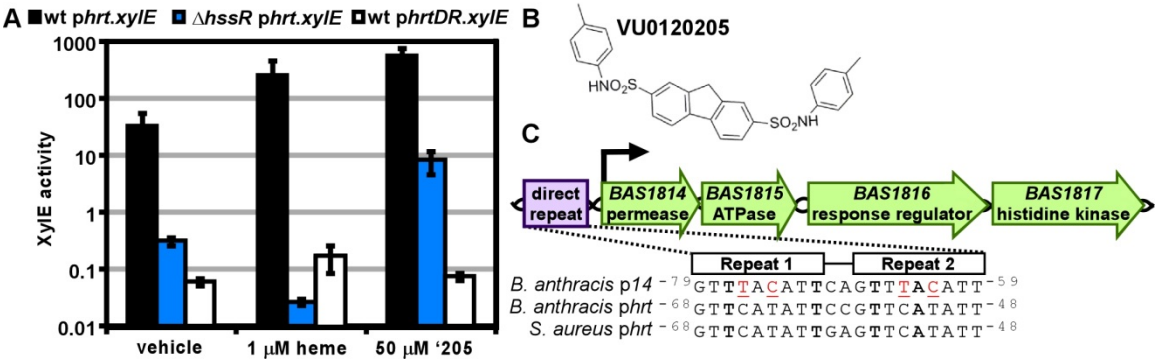

Figure 19. '205 activates the *B. anthracis hrt* promoter through two pathways that depend on the direct repeat. *A.* Wildtype (wt) and Δ*hssR B. anthracis* Sterne were transformed with the *hrt* promoter fused to the *xylE* reporter gene (p*hrt.xylE*). The direct repeat (DR) of the *hrt* promoter-*xylE* fusion was mutated (p*hrtDR.xylE*) and transformed into wt. Each strain was grown in triplicate in the presence of either vehicle (DMSO), 1 μM heme, or 50 μM '205 for 24 h. XylE activity in cell lysates was quantified. Shown are data representative of at least three replicates. Error bars represent one standard deviation from the mean. ***B.*** Structure of VU0120205 ***C***. Genomic locus (top) and DR (bottom) of BAS1814-17. In the inset is an alignment of the direct repeats found in the *hrt* promoter (p*hrt*) regions of *S. aureus* and *B. anthracis* and the *BAS1814* promoter (p*14*) region in *B. anthracis*. Highlighted in bold are nucleotides previously shown to be required for HssR recognition of the p*hrt* DR (83). Underlined in red are nucleotides that differ between p*14* and p*hrt*. Superscript numbers indicate the nucleotide distance from the start site. Each DR remains 18 base pairs from the predicted ribosome binding site.

This alternative DR retains the four nucleotides required for HssR binding, but differs from p*hrt* by four other nucleotides (Figure 19C) (83). This previously uncharacterized DR is located in the promoter region (p*14*) of the *BAS1814-17* operon. BAS1814 and BAS1815 are conserved in the *Bacilli* genus and are predicted to function together as an ABC transporter. BAS1816 and BAS1817 are a putative TCS in *B. anthracis* where BAS1817 is the histidine kinase (HK) and BAS1816 is the response regulator (RR) that is predicted to regulate p*14* (12). Furthermore, protein BLAST analysis of BAS1816 in *B. anthracis* identifies HssR as the most similar RR in *B. anthracis* with 87% coverage and 52.5% identity. A similar analysis of BAS1817 identifies HssS as the most similar HK in *B. anthracis* with 81.8% coverage and 40.7% identity. It is intriguing that HssRS is most closely related to the BAS1816-17 TCS in *B. anthracis* and that they share a very similar DR. These observations lead to the hypothesis that BAS1816-17 is a functional TCS that responds to ‘205 and regulates both p*14* and p*hrt*.

Compound ‘205 activation of p*14* and p*hrt* is mediated through BAS1816-17. To determine if BAS1816 and BAS1817 auto-regulate the *BAS1814-17* operon in response to ‘205 treatment, the *BAS1814* promoter was fused to the *xylE* reporter gene (p*14.xylE*) and transformed in wildtype, Δ*hssRS,* Δ*BAS1816-17,* and Δ*hssRS/BAS1816-17.* These strains were grown in the presence of vehicle (DMSO) or 50 μM ‘205 and then XylE activity was quantified. The *BAS1814* promoter (p*14*) is activated in the presence of ‘205 in a manner that requires BAS1816-17, not HssRS (Figure 20A). The four nucleotides in the p*14* DR, which are shown in bold in Figure 19C and were previously determined to be required for HssR activation of the *hrt* promoter were mutated on the p*14.xylE* reporter plasmid and transformed into wildtype *B. anthracis*. Mutation of these four nucleotides ablated ‘205 activation of p*14* (Figure 20A). Together these data reveal that ‘205 activates BAS1816-17, which auto-regulates the p*14* DR through four conserved nucleotides. These experiments were repeated using 2 μM heme as the activating compound instead of ‘205. Heme does not activate p*14* at this concentration (Figure 20B).

In Figure 19A it was observed that '205 activates p*hrt* independently of HssR but requiring the p*hrt* DR. To determine if this activation of the *hrt* promoter was due to BAS1816-17 activity, the p*hrt.xylE* reporter plasmid was transformed into Δ*BAS1816-17* and Δ*hssRS/BAS1816-17*. The high basal activation of p*hrt* masked any '205-induced activation of this promoter in Δ*BAS1816-17*; however, the '205-induced activation of p*hrt* in Δ*hssRS* was ablated in the quadruple Δ*hssRS/BAS1816-17* knock-out (Figure 20C). These data reveal that the '205-induced activation of p*hrt* is indeed mediated through BAS1816-17.

B. anthracis HssRS has already been well-characterized to activate p*hrt* in response to heme treatment. To determine if BAS1816-17 responds to heme and regulates the *hrt* promoter, the activation of p*hrt* in Δ*BAS1816-17* upon treatment with 1 μM heme was quantified and found to be similar to wildtype (Figure 20D). This indicates that BAS1816-17 does not activate the *hrt* promoter in response to heme.

In summary these experiments identify BAS1816-17 as a new TCS that is activated by compound '205. BAS1816-17 can activate both the p*hrt* and p*14* promoters. Reciprocally, HssRS is activated by heme and regulates p*hrt* (83). At the concentrations used in these experiments neither p*14* nor BAS1816-17 were responsive to heme. These two TCSs present a unique opportunity to study the mechanisms by which similar TCSs either integrate or maintain their signaling purity and may provide insight into how bacteria adapt to diverse environmental signals. Due to the similarity of the DRs and RRs of BAS1816-17 and HssRS, it is possible that an activated RR may be able to act at both DRs. Alternatively, cross-signaling may occur due to phosphorylation of a non-cognate RR by a HK. The role of RR-DR and HK-RR interactions in maintaining signaling purity will be investigated in subsequent data sections.

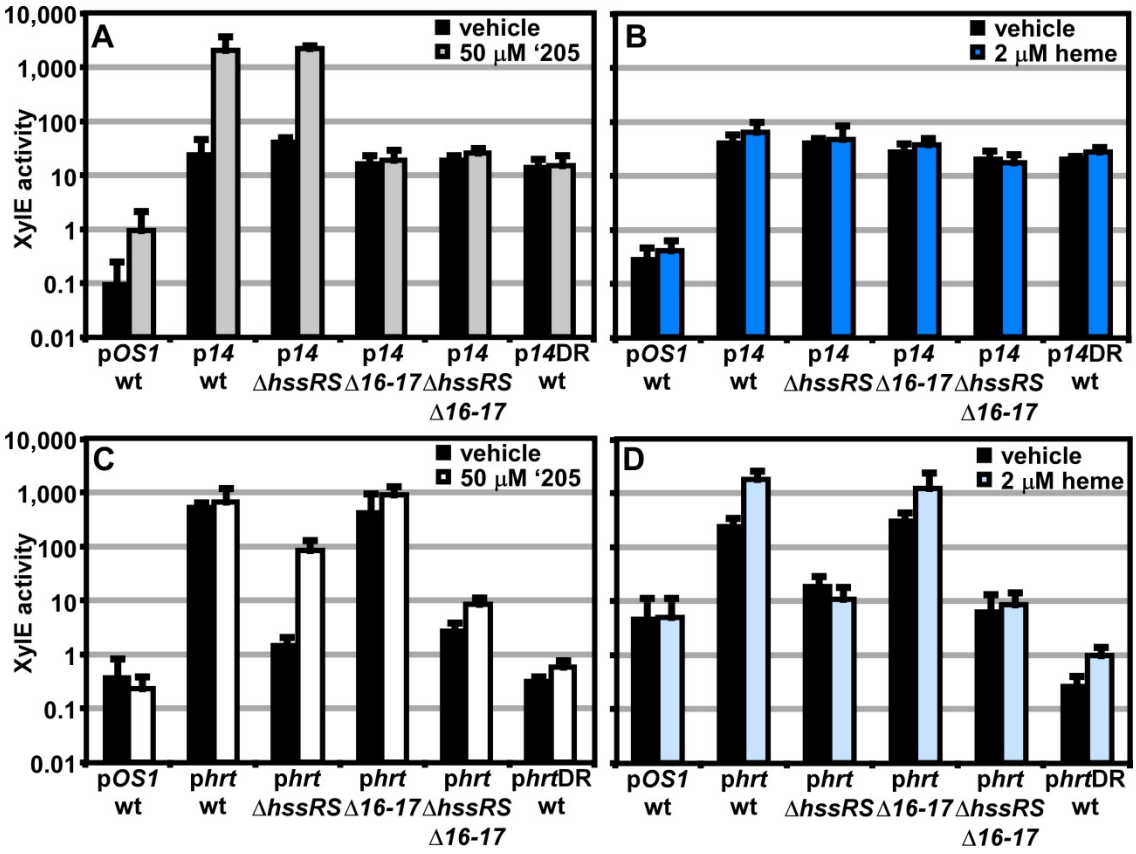

Figure 20. BAS1816-17 activates both the *BAS1814* and *hrt* promoters while HssRS activates just the *hrt* promoter. Wildtype (wt), Δ*hssRS*, Δ*BAS16-17* (Δ*16-17*), Δ*hssRS*/Δ*16-17* were transformed with the *BAS1814* promoter fused to the *xylE* reporter gene (p*14*) (***A*** and ***B***) and *hrt* promoter fused to the *xylE* reporter gene (p*hrt*) (***C*** and ***D***). Wt was also transformed with a promoterless *xylE* (p*OS1*) and the direct repeat of each promoter mutated (p*14DR* and p*hrtDR*). Each strain was grown in triplicate and exposed to either vehicle (DMSO) or 50 μM '0070 (*A* and *C*), or 2 μM heme (*B* and *D*) for 24 h. Cells were lysed and XylE activity was quantified. Shown are data averaged from at least two independent experiments performed with biological triplicates. Error bars represent one standard deviation from the mean. XylE assays were performed by LQO.

The direct repeat determines the response of each promoter region. The four nucleotides of the p*hrt* DR previously shown to be required for HssR-p*hrt* DR interactions are conserved in the p*14* DR. However, four other nucleotides of the DR discriminate the p*hrt* DR from the p*14* DR. This leads to the hypothesis that the four nucleotides unique to p*14* are sufficient to differentially regulate p*14* as compared to p*hrt.* To test this hypothesis, the four nucleotides unique to the p*14* DR were incorporated into the p*hrt.xylE* reporter construct to make p*hrt.14DR.xylE* and the four nucleotides unique to the p*hrt* DR were switched into the p*14.xylE* reporter construct to generate p*14.hrtDR.xylE*. These constructs were transformed into wildtype *B. anthracis* and then the strains were exposed to either heme or '205. The response of each promoter to heme and '205 was quantified by measuring the XylE activity in each strain.

As predicted, swapping the four unique nucleotides in each DR switches the responsiveness of each promoter to heme and '205 (Figure 21). Therefore these four unique nucleotides in the p*14* DR are sufficient to determine the response of the promoter to environmental stimuli. One exception to this result is the loss of the high basal activation of p*hrt* when the p*hrt* DR was placed in p*14*. This result, when considered in conjunction with previous observations that the high p*hrt* background is also lost upon *hssR* deletion and p*hrt* DR mutation (Figure 19A and 20C-D), suggests that the high basal activation of p*hrt* is due to the interaction of HssR with the p*hrt* DR in the context of p*hrt*.

It is important to note that since only wildtype *B. anthracis* was investigated in this experiment, the bacteria could be treated with a higher concentration of heme (5 μM). This concentration of heme activates p*14* and p*hrt.14DR* in wildtype *B. anthracis.* Since this strain has all TCSs intact the activation of p*14* by heme suggests that cross-talk from HssRS to BAS1816-17 does occur naturally.

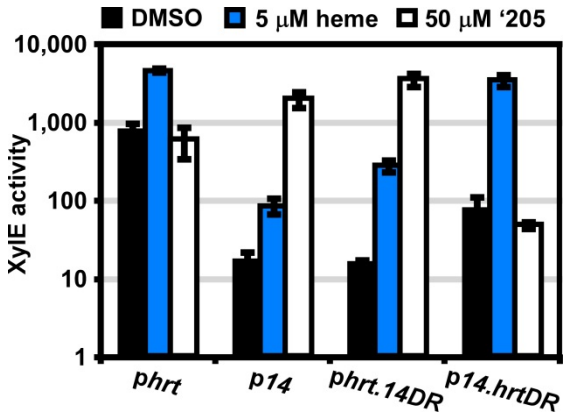

Figure 21. The direct repeat in each promoter determines specificity *in vivo*. Wildtype *B. anthracis* Sterne was transformed with the *hrt* promoter fused to the *xylE* reporter gene (p*hrt*) and the *BAS1814* promoter fused to the *xylE* reporter gene (p*14*). Furthermore, the direct repeat of each promoter was swapped into the other reporter plasmid (p*hrt.14DR* and p*14.hrtDR*) and transformed into wildtype *B. anthracis*. Each strain was grown in triplicate and exposed to either vehicle (DMSO), 5 μM heme, or 50 μM '0070 for 24 h. Cells were lysed and XylE activity was quantified. Data are averaged from at least 4 independent experiments. Error bars represent one standard deviation from the mean. Plasmids were generated by DLS.

Cross-talk at the response regulator-direct repeat level is limited. It is remarkable that four nucleotides allow for discrete regulation of two very similar DRs. Swapping the DRs between promoter regions, however, does not indicate whether each RR influences its cognate DR exclusively. To investigate if a RR impacts the recognition of its non-cognate DR, each RR was individually mutated and then promoter activation was analyzed in the mutant strains.

First the influence of BAS1816 on the p*hrt* DR was examined. The p*hrt.xylE* and p*14.hrtDR.xylE* reporter constructs were transformed into wildtype, Δ*hssR,* and Δ*hssR/1816* strains. BAS1816-17 was stimulated with 50 μM '205 and the vehicle DMSO was used as a negative control, see Figure 22A for a scheme of the experimental design. As expected, activation of p*hrt* was observed upon deletion of Δ*hssR* and was lost in Δ*hssR/1816* (Figure 22C). The elimination of the high basal activity of p*hrt* in p*14.hrtDR* revealed low levels of p*hrt* DR recognition in wildtype in addition to Δ*hssR*; nearly all activation was lost in Δ*hssR/1816* (Figure 22C). These data utilizing both reporter constructs suggest that BAS1816 can recognize the p*hrt* DR; however, the high basal activity of wildtype p*hrt* may limit BAS1816 influence on its non-cognate DR under native conditions.

Next the ability of HssR to regulate p*14* was probed. Using an analogous strategy, the p*14.xylE* and p*hrt.14DR.xylE* reporter constructs were transformed into wildtype, Δ*1816,* and Δ*hssR/1816*. HssRS was stimulated with 1 μM heme and the vehicle 0.1 M NaOH was used as a negative control, see Figure 22B for a scheme of the experimental design. Although there is only weak activation of the p*14* in wildtype *B. anthracis*, more robust p*14* activation has been observed in wildtype *B. anthracis* treated with 5 μM heme (Figure 21 and 22D). The weak activation of p*14.xylE* in wildtype is lost upon deletion of *BAS1816* and unchanged in Δ*hssR/1816* (n.b. the decrease in XylE activity in this strain upon heme treatment is most likely due to the heme sensitivity of Δ*hssR*) (Figure 22D). When the p*14* DR is placed in the context of p*hrt*, clear activation of p*hrt.14DR* is observed in Δ*BAS1816* and lost in Δ*hssR/1816*. This suggests that HssR may be able to recognize the p*14* DR, however, it requires some other factor

only found on p*hrt*. This could be either a *cis*-acting DNA sequence or *trans*-acting enhancer element.

In summary, these studies investigating the RR-DR interactions between two closely related TCSs suggest that BAS1816 may recognize both DRs, but other cellular factors may insulate this cross-talk at the RR-DR level. For example BAS1816 can recognize the p*hrt* DR only in the absence of HssR or when the DR is placed in the context of p*14* (Figure 22A). This suggests that when the p*hrt* DR is in the context of p*hrt,* both the presence of HssR and the increased activity of HssR at the p*hrt* DR limits cross-talk from BAS1816. Conversely, p*14* in wildtype *B. anthracis* is activated only at higher concentrations of heme (Figure 21). At non-toxic concentrations of heme, HssR does not seem to recognize the p*14* DR unless it is in the context of p*hrt* (Figure 22B), suggesting that other *cis*- or *trans*-acting factors enhance HssR activity specifically at p*hrt* and therefore limit HssR activation of the p*14* DR. These observations suggest that activation of p*14* at higher heme concentrations may be beneficial to the bacteria. It is possible that the putative ABC transporter BAS1814-15 may contribute to heme tolerance in *B. anthracis.*

BAS1816-17 is a two-component system that cross-phosphorylates with HssRS. To begin to explore the HK-RR interactions and to demonstrate that BAS1816-17 is a novel, functional TCS, the intracellular domain of BAS1817 and the full length BAS1816 were each N-terminally tagged with a hexa-histidine sequence, heterologously expressed in *E. coli* and purified over a Ni-NTA column. The full length BAS1816 as predicted based on the sequence annotated in the Sterne genome is highly insoluble when expressed. Within the first 81 nucleotides there are three predicted ATG translation start sites. When BAS1816 was aligned with homologs from other *Bacilli* it became apparent that the third ATG is most likely the true transcription start site. Expressing BAS1816 with the N-terminus beginning at the third predicted translation start site and therefore lacking the first predicted 26 amino acids resulted in pure, soluble RR.

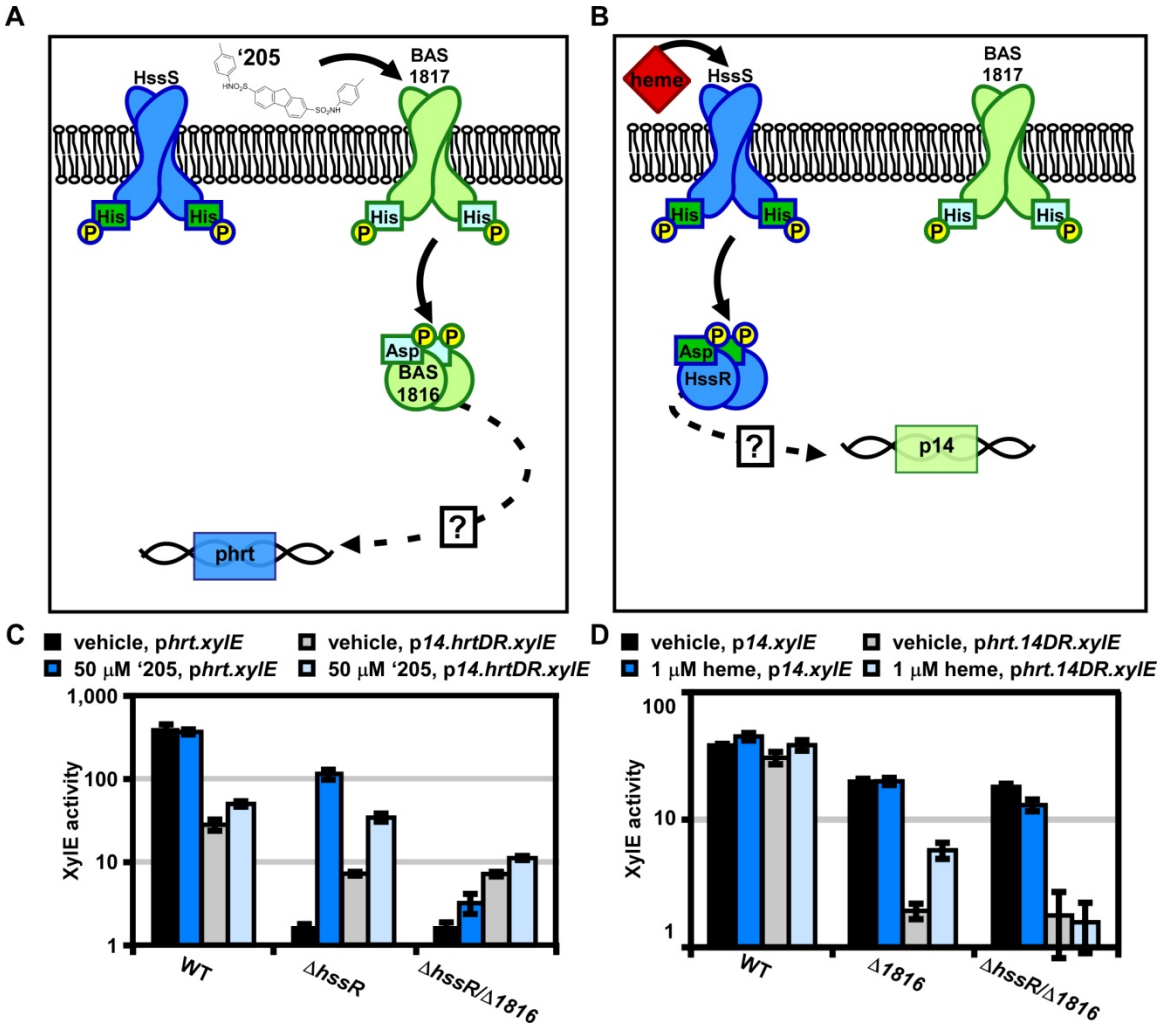

Figure 22. Cross-signaling at the response regulator-direct repeat level. ***A.*** and ***B.*** Shown are schema of the experimental design in panels *C.* and *D.*, respectively. ***C.*** Wildtype (WT) *B. anthracis*, Δ*hssR,* and Δ*hssR*/Δ*1816* were transformed with the *hrt* promoter fused to the *xylE* reporter gene (p*hrt.xylE*) and the *hrt* DR swapped into the *BAS1814* promoter (p*14.hrtDR.xylE*). The six strains were each treated with either 50 μM '205 or an equivalent volume of the vehicle DMSO. Cultures were grown for 24 h and harvested. Cells were lysed and XylE activity was quantified. ***D.*** Wildtype (WT) *B. anthracis*, Δ*1816,* and Δ*hssR*/Δ*1816* were transformed with the *BAS1814* promoter fused to the *xylE* reporter gene (p*14.xylE*) and the *BAS1814* DR swapped into the *hrt* promoter (p*hrt.14DR.xylE*). The six strains were each treated with either 1 μM heme or an equivalent volume of the vehicle 0.1 M NaOH. Cultures were grown for 24 h and harvested. Cells were lysed and XylE activity was quantified. In all instances, data are averaged from at least two independent experiments performed with biological triplicates. Error bars represent the standard error of the mean. Strains were generated by DLS.

The conserved residues predicted to be required for phosphorelay were identified in BAS1816 and BAS1817 using the NCBI protein viewer. The conserved aspartate at amino acid position 56 in the receiver domain of BAS1816 was mutated to an asparagine and the conserved histidine at amino acid position 137 in the DHp domain of BAS1817 was mutated to an alanine (Figure 23A and B). The analogous HssS and HssR wildtype and phosphorelay-deficient proteins were also purified as described previously (Figure 23A and B) (83).

First the ability of each histidine kinase to autophosphorylate was determined by incubating the purified HKs in the presence of γ-^{32}P labeled ATP and then resolving the proteins on an SDS-PAGE gel. Each HK was autophosphorylated in the presence of ATP and these activities required the conserved phosphate-accepting histidines (Figure 23C).

Next the ability of each HK to transfer the phosphate to each RR was investigated. The HKs were first autophosphorylated and then co-incubated with each RR for 5 min. The phosphorylation state of each protein was visualized by resolving each HK-RR pair on an SDS-PAGE gel and exposing the samples to a phosphorscreen (Figure 23D). The percent of phosphotransfer from each HK to each RR was quantified (Figure 23E). Each HK preferentially phosphorylates its cognate RR, although there is significant cross-phosphorylation to each non-cognate RR. It does not seem that HssS and BAS1817 are generally capable of phosphorylating any RR as the *E. coli* QseB RR is unable to be phosphorylated by either HK (data not shown). This suggests that it may be the similarity between HssR and BAS1816 that may permit cross-phosphorylation by the HKs.

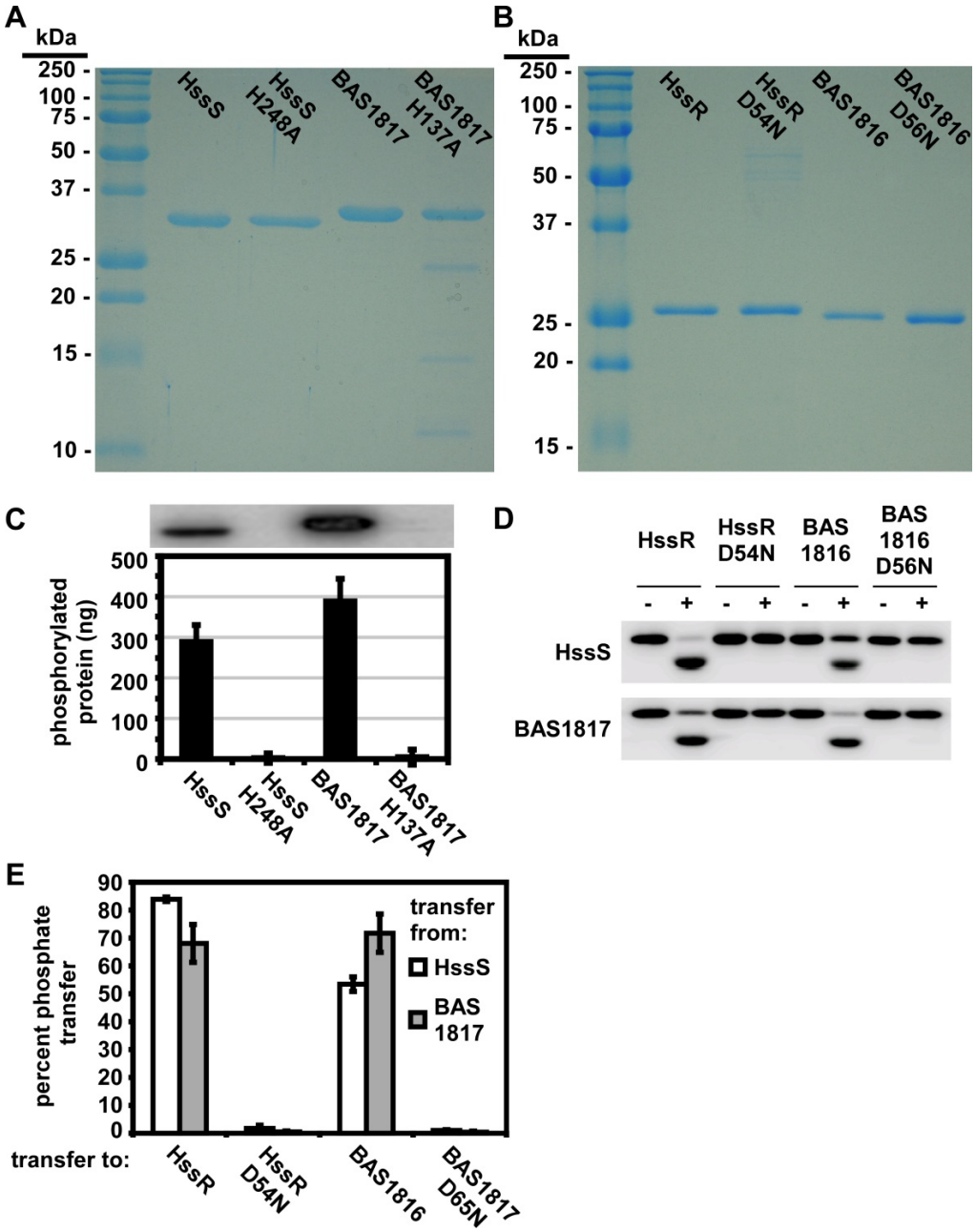

Figure 23. BAS1816-17 and HssRS are two-component systems that cross-phosphorylate. Each HK (***A***) and RR (***B***) was expressed in *E. coli* and purified by Ni-affinity purification. The dialyzed elutions were run on an SDS-PAGE gel to assess purity. ***C.*** Autophosphorylation of the histidine kinases and the corresponding histidine mutants. Each protein was incubated with ATP [γ-^{32}P] for 30 minutes, sampled for SDS-PAGE analysis (top) and quantified by phosphorimager analysis (bottom). Shown is the average of four replicates and the error bars represent the standard deviation. (***D*** and ***E***) Each histidine kinase phosphorylates each response regulator. Histidine kinases were autophosphorylated as described in *C* and then co-incubated with the indicated response regulator for 5 minutes, sampled for SDS-PAGE analysis in *D*, and quantified by phosphorimager analysis in *E*. Shown in *E* is the average of three replicates and the error bars represent one standard deviation from the mean. These experiments were performed by DLS and JC.

The hierarchy of HssS and BAS1817 phosphotransfer to each response regulator. To further delineate the relative preference each HK has for each RR, the concentration of each RR was diluted over a concentration range of 2-logs. Each RR concentration was then incubated with auto-phosphorylated HssS or BAS1817 for 30 sec and then resolved on an SDS-PAGE gel (Figure 24A). The percent of phosphotransfer was quantified by dividing the intensity of the P~RR band over the intensity of the total density in each lane. Plotting the percent of phosphotransfer against the RR concentration identifies a clear hierchary in the preference for phosphorelay *in vitro*, such that the phosphotransfer of BAS1817 to BAS1816 is most efficient, followed by HssS to HssR, then BAS1817 to HssR, and finally HssS to BAS1816 (Figure 24B). The question now remains if any cross-phosphorylation occurs *in vivo* and if so, if the cross-phosphorylation events have a biological function in the adaptation of *B. anthracis* to environmental changes.

Selective cross-talk at the histidine kinase-response regulator level *in vivo.* Since cross-phosphorylation between each HK to each RR is observed *in vitro*, the presence of HK-RR cross-signaling *in vivo* was next investigated. To study the influence of BAS1817 phosphorylation on HssR activity *in vivo,* an Δ*hssS/*Δ*1816* double knock-out strain was generated to eliminate any influence HssS or BAS1816 may have on HssR or BAS1817 (Figure 25A). This Δ*hssS/*Δ*1816* double knock-out strain was transformed with p*hrt.xylE* and p*14.hrtDR.xylE*, which has the p*hrt* DR inserted in p*14*. If phosphotransfer from BAS1817 to HssR occurs *in vivo*, then activation of p*hrt.xylE* is predicted to be observed in Δ*hssS/*Δ*1816* upon '205 treatment (Figure 25A). This is not the case (Figure 25C). When BAS1817 is stimulated by compound '205 p*hrt* is not activated in Δ*hssS/*Δ*1816*, which indicates that despite observing strong phosphotransfer from BAS1817 to HssR *in vitro*, BAS1817 to HssR phosphorelay does not occur *in vivo* (Figure 25C). The mechanism for maintaining this signaling purity in the absence of HssS and BAS1816 remains unclear.

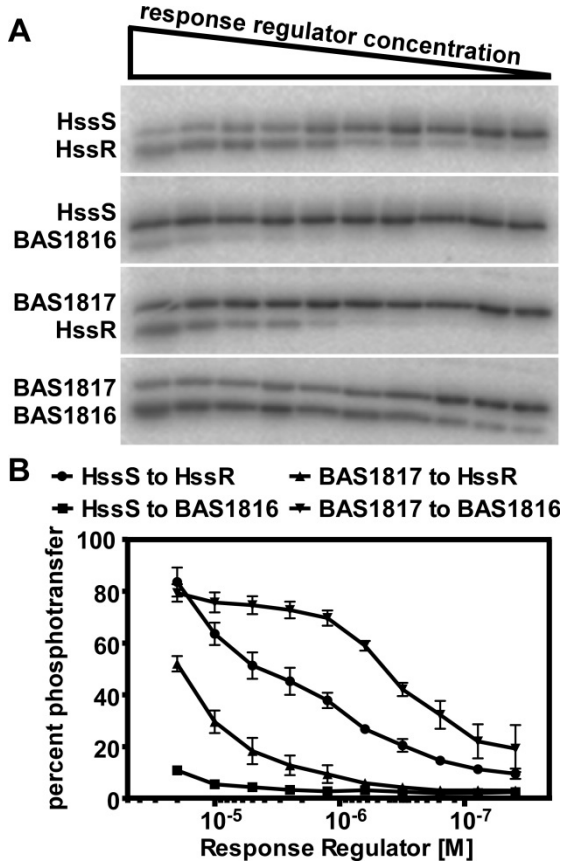

Figure 24. Each histidine kinase preferentially phosphorylates its cognate response regulator *in vitro*. A serial dilution of response regulator concentrations ranging from 20 μM to 39 nM was prepared. Each histidine kinase was autophosphorylated as described earlier and then mixed with each response regulator concentration for 30 sec. Phosphotransfer reactions were quenched with SDS-PAGE loading buffer and resolved on a gel. A representative image is shown in ***A***. Data from at least 4 replicates were average and plotted in ***B***. Error bars represent one standard deviation from the mean. Experiments were performed by DLS and JC.

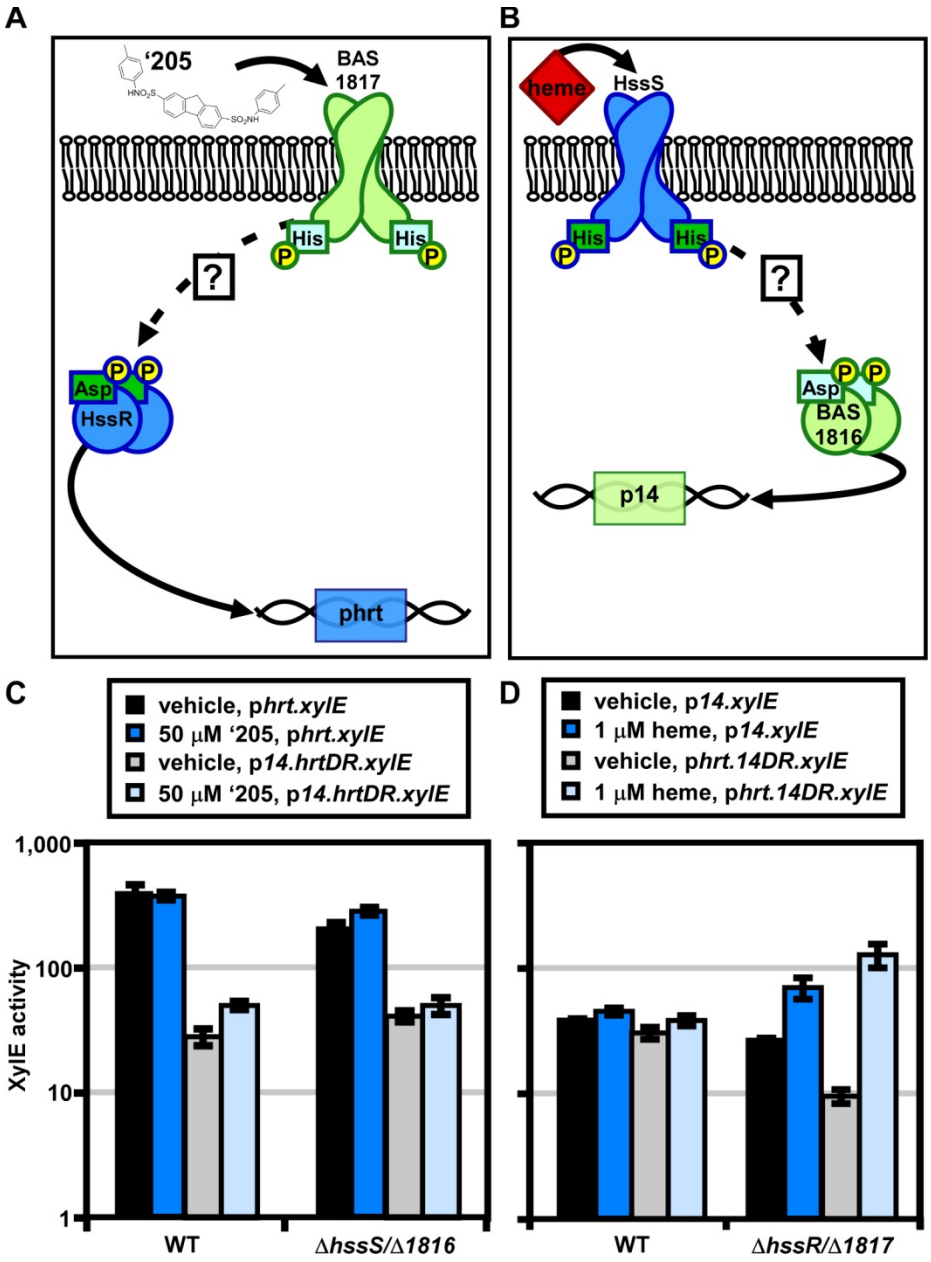

Figure 25. Cross-signaling at the histidine kinase-response regulator level. *A.* and ***B.*** Shown are schema of the experimental design in panels *C.* and *D.*, respectively. ***C.*** Wildtype (WT) *B. anthracis* and Δ*hssS/*Δ*1816* were transformed with the *hrt* promoter fused to the *xylE* reporter gene (p*hrt.xylE*) and the *hrt* DR swapped into the *BAS1814* promoter (p*14.hrtDR.xylE*). The four strains were each treated with either 50 μM '205 or an equivalent volume of the vehicle DMSO. Cultures were grown for 24 h and harvested. Cells were lysed and XylE activity was quantified. ***D.*** Wildtype (WT) *B. anthracis* and Δ*hssR/*Δ*1817* were transformed with the *14* promoter fused to the *xylE* reporter gene (p*14.xylE*) and the *14* DR swapped into the *hrt* promoter (p*hrt.14DR.xylE*). The four strains were each treated with either 1 μM heme or an equivalent volume of the vehicle 0.1 M NaOH. Cultures were grown for 24 h and harvested. Cells were lysed and XylE activity was quantified. In all instance, data are averaged from at least two independent experiments performed with biological triplicates. Error bars represent the standard error of the mean.

The analogous phosphotransfer from HssS to BAS1816 was tested by the same strategy. A Δ*1817/*Δ*hssR* double knock-out strain was generated and transformed with p*14.xylE* and p*hrt.14DR.xylE*, which has the p*14* DR inserted in p*hrt*. If phosphotransfer from HssS to BAS1816 occurs *in vivo*, then the p*14.xylE* is predicted to be activated in Δ*1817/*Δ*hssR* in the presence of heme (Figure 25B). This does indeed occur, suggesting that *in vivo* HssS may cross-phosphorylate BAS1816 to stimulate activation of p*14* (Figure 25B and D). These data suggest that at low heme concentrations the signaling integrity of HssRS activation of p*hrt* may be maintained by the higher phosphotransfer preference of HssS to HssR (Figure 24), the enhanced activity of HssR at p*hrt* (Figure 21), and perhaps even phosphatase activity of BAS1817 on BAS1816. However, at higher heme concentrations the mechanism by which heme activates p*14* may occur either through cross-phosphorylation from HssS to BAS1816 (Figure 24) or activation of p*14* by HssR (Figure 22B). It is intriguing that the 'least preferred' cross-phosphorylation from HssS to BAS1816 *in vitro* is observed *in vivo*, but the parallel cross-phosphorylation from BAS1817 to HssR is not. Perhaps there is a certain threshold of HK activation that must be achieved in order to observe cross-phosphorylation. It is possible that heme-induced activation of HssS exceeds this threshold, but '205-induced stimulation of BAS1817 does not. Perhaps with more potent BAS1817 activators cross-phosphorylation from BAS1817 to HssR may be observed.

The identification of BAS1816-17 activators. Since compound '205 is not likely to be an environmental signal typically encountered by *B. anthracis,* the native function of BAS1816-17 was interrogated. Identifying the native function of BAS1816-17 would not only inform the potential function of the BAS1814-15 ABC transporter, but may also reveal why HssRS and BAS1816-17 interact. To identify other signals that activate BAS1816-17 a chemical biology approach was undertaken, this time employing the Biolog Phenotypic Microarray.

The first twenty 96 well plates (PM1-20) were purchased from Biolog's Phenotypic Microarray Library for Microbial Cells. Each well contains a different compound that may differentially impact the growth and behavior of bacteria. The first ten plates interrogate different nutrient environments (e.g. carbon sources) and the second ten plates probe different chemical sensitivities (e.g. antibiotics). Wildtype *B. anthracis* transformed with p*14.xylE* was grown in each of these plates and activation of p*14* was monitored by XylE assay. The screen was repeated twice and the twelve molecules that activated p*14.xylE* were repurchased from commercial vendors. The specific activation of BAS1816-17 was tested by exposing both wildtype and Δ*1816-17* p*14.xylE* to each compound in a concentration range that spanned at least 2-logs and did not inhibit bacterial growth. Four compounds exhibit specific activation of p*14.xylE* in a manner that requires BAS1816-17.

The most potent activator identified is nordihydroguaiaretic acid (NDGA), which is even more active than '205 (Figure 26A). NDGA is an antioxidant isolated from the creosote bush; the long life of the bush is attributed to the antimutagenic effects of NDGA (45). Several other activities have been ascribed to the molecule as well including anti-inflammatory and antiviral activities (45).

The second best activator of BAS1816-17 identified in the phenotypic microarray is chlorpromazine (Figure 26B). Chlorpromazine is used to treat allergies and psychoses in humans, but it also sensitizes humans to light (15). This effect is thought to result from photoactivation of chlorpromazine and subsequent intercalation into DNA (54). Not surprisingly, chlorpromazine is

mutagenic in the Ames test (55). Chlorpromazine uncouples oxidative phosphorylation and has also been implicated in disrupting passive transport across mitochondrial membranes (65, 81). In bacteria, most work has been focused on the chemorepellent activity of chlorpromazine to *Bacillus subtilis* (56). Though one study notes that chlorpromazine inhibits cell wall biogenesis in *Bacillus megaterium* (38).

Both low concentrations of vancomycin and high concentrations of sodium phosphate (pH 7) were found to weakly activate BAS1816-17 (Figure 26D and E). The concentration range of vancomycin is limited due to the antibiotic nature of the compound. Vancomycin is best known for inhibiting Gram positive cell biosynthesis, but at low concentrations it has also been shown to disrupt membrane integrity (95). The anion sodium phosphate only showed weak activity at high concentrations, beyond which significant growth defects were observed.

The description of the biological activity of each of these compounds in the literature, leads to the hypothesis that BAS1816-17 may be activated by cell envelope stressors. Recently, a small molecule inhibitor of *S. aureus* wall techoic acid (WTA) synthesis called targocil was identified (89). Targocil inhibits the transport of the nascent WTA from inside the membrane to the outer surface. This not only results in a loss of cell wall integrity, but may also cause an accumulation of negative charges near the inner leaflet due to the accumulation of poly(ribitol-phosphate) components of WTA inside the cell (89). The activity of targocil on the Gram positive cell envelope indicated that this small molecule may also activate BAS1816-17. To test this hypothesis the activation of p*14.xylE* in wildtype and Δ*1816-17 B. anthracis* in response to targocil was investigated. Targocil does specifically activate the *BAS1814* promoter in a manner that requires BAS1816-17 (Figure 26C). A microarray performed on targocil treated *S.aureus* revealed the transcriptional up-regulation of *hrtAB* 12-fold (10). This was the second most up-regulated operon next *cwrA* a small peptide of unknown function that is a reporter of cell wall stress (10).

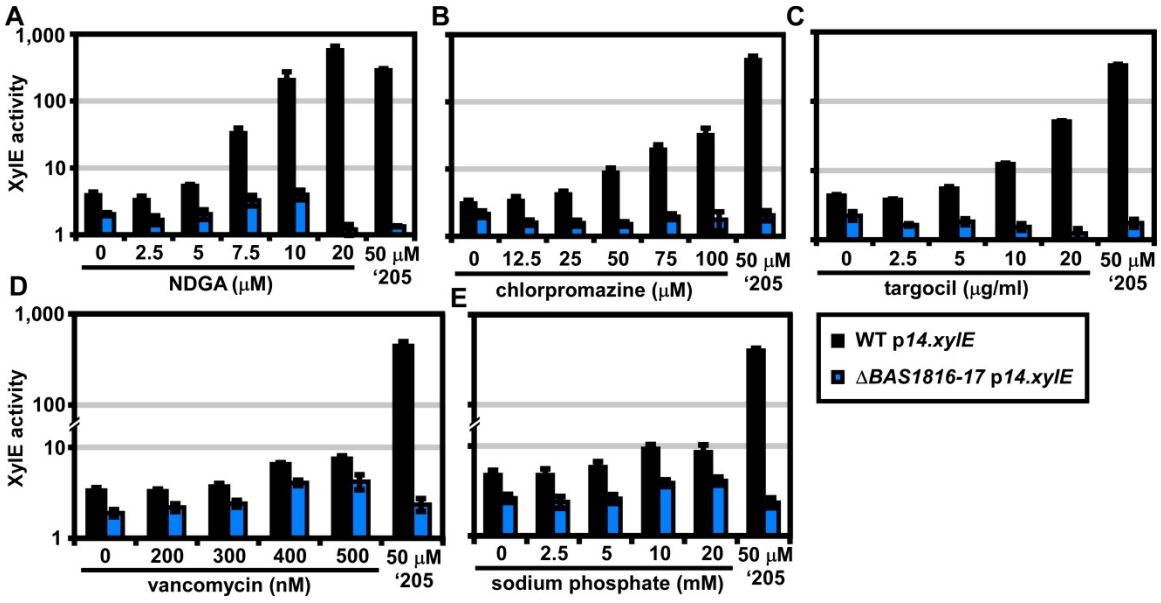

Figure 26. Five novel activators of BAS1816-17. Wildtype (WT) *B. anthracis* and Δ*BAS1816-17* were transformed with the *14* promoter fused to the *xylE* reporter gene (p*14.xylE*). The strains were treated with either 50 μM '205 or a range of concentrations of the following compounds: ***A.*** nordihydroguaiaretic acid (NDGA), ***B.*** chlorpromazine, ***C.*** targocil, ***D.*** vancomycin, and ***E.*** sodium phosphate pH 7. Cultures were grown for 6 h and harvested. Cells were lysed and XylE activity was quantified. In all instances, data are averaged from at least two independent experiments performed with biological triplicates. Error bars represent the standard error of the mean. The primary Biolog screen was performed by PB.

In summary, five novel activators of BAS1816-17 have been identified, including one compound, NDGA, that is more potent than ‘205. The common mechanism by which these molecules activate BAS1816-17 remains to be determined. The current understanding of the mode of action of each of these compounds, points to the hypothesis that BAS1816-17 may be activated by alterations in the cell envelope, perhaps disruptions in the electrochemical potential across the membrane. To identify common cellular events that result in BAS1816-17 activation, RNASeq analysis of *B. anthracis* treated with vehicle, ‘205, NDGA, chlorpromazine and targocil will be employed. Theoretically, there should be shared transcriptional responses to each of the BAS1816-17 activators since they all stimulate this new TCS. Identifying common transcriptional changes upon treatment with these compounds will provide insight to the native cellular signal that activates BAS1816-17.

Discussion

In this chapter a small molecule activator of *S. aureus* HssRS was used to identify a new TCS in *B. anthracis*. This TCS BAS1816-17 recognizes a DR in p*14* that differs from the p*hrt* DR by four nucleotides. These four nucleotides are the primary source of differential regulation between p*hrt* and p*14*. It is not surprising then, in the absence of HssR, BAS1816-17 activates expression of both p*14* and p*hrt*. Through both *in vitro* and *in vivo* experiments BAS1816-17 has been determined to regulate p*hrt* at the RR-DR level, while HssRS impacts expression at p*14* either through HK-RR or RR-DR interactions. The interactions between HssRS and BAS1816-17 are summarized in Figure 27.

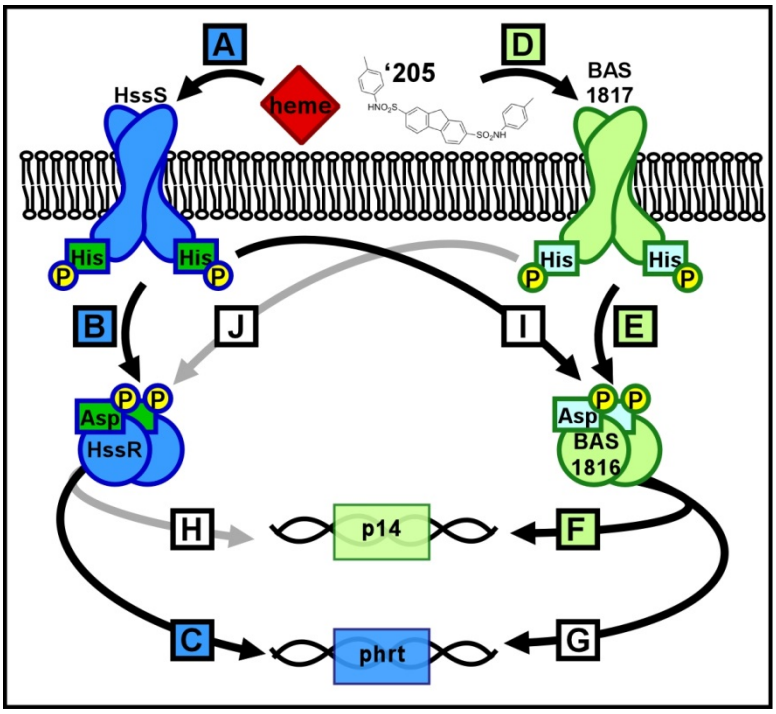

Figure 27. A summary of cross-talk observed between HssRS and BAS1816-17 in *B. anthracis*. *A-C.* HssRS was previously shown to be stimulated by heme to activate p*hrt* (83). ***D-F.*** Here a second TCS BAS1816-17 has been identified to be stimulated by '205 to activate p*14*. ***G.*** and ***H.*** At the RR-DR level BAS1816 can recognize the p*hrt* DR but HssR only recognizes the p*14* DR only in the context of p*hrt*. ***I.*** and ***J.*** At the HK-RR level HssS can cross-phosphorylate BAS1816 both *in vitro* and *in vivo*, while BAS1817 has only been observed to cross-phosphorylate HssR *in vitro*.

In addition, five new activators of BAS1816-17 were identified and will be used to determine the native function of BAS1816-17 and the nature of BAS1816-17 cross-talk with HssRS. Here, the impact of each of these new activators on BAS1816-17 mediated stimulation of p*14* was investigated. In order to more fully dissect the mechanisms of TCS cross-talk, the impact of each of these small molecules on p*hrt* activation should be determined. Such studies may reveal how these compounds activate BAS1816-17 and further dissect the cross-talk between BAS1816-17 and HssRS. Without this panel of non-native small molecule activators of BAS1816-17, the studies presented here characterizing this new TCS and its mechanisms of cross-talk with HssRS would have been impossible. Delineating the activity and function of many TCSs is limited by a lack of known activators. The success of the Biolog Phenotypic MicroArray for identifying activators of BAS1816-17 is applicable to any TCS and may be a powerful new chemical biology based strategy that will improve the tools available for studying TCSs.

The known activities of the six BAS1816-17 activating compounds lead to the hypothesis that BAS1816-17 may be activated by perturbations in the cell envelope, potentially even alterations in the electrochemical gradient across the membrane. The lipophilic nature of the protoporphyrin IX ring, which coordinates iron, disrupts the cell membrane of erythrocytes (1). This causes hemolysis by a colloid-osmotic mechanism as the cells no longer maintain ion gradients and water enters the cell. In addition, *S. aureus* heme-iron preferentially accumulates in the cell membranes (77). It is possible that HssRS is activated when heme disrupts the membrane. This model is supported by the previous observation that targocil, which prevents translocation of WTA to the outer leaflet of the cell membrane, activates HssRS in *S. aureus* (10, 89). It is possible that general membrane stress activates BAS1816-17 and is alleviated by activation of p*14*. The function of the putative ABC transporter BAS1814-15 is unknown. Perhaps it transports an osmoprotectant which could more generally protect against any membrane stress, even heme. The coordinated expression of *hrtAB* and *BAS1814-15* may enable *B. anthracis* to better cope with heme-induced membrane stress.

Cross-regulation between HssRS and BAS1816-17 could exist if the activation of both p*hrt* and p*14* help alleviate heme toxicity. In *Lactococcus lactis* HrtAB has been shown to efflux heme (42). In wildtype *B. anthracis* p*14* is activated in the presence of high concentrations of heme; meanwhile, activation of p*hrt* in the presence of '205 has not been consistently observed. This suggests that some cross-regulation may exist from HssRS to BAS1816-17 and that BAS1814-15 may help alleviate heme toxicity. The lack of cross- talk from BAS1816-17 to HssRS upon '205 treatment suggests that HrtAB may not be needed upon BAS1816-17 activation or that '205 is not a strong enough activator of BAS1816-17 to achieve cross-talk. It would be worthwhile to investigate whether cross- talk from BAS1816-17 to HssRS occurs in the presence of the more potent activator NDGA.

In a more general sense, the interactions between HssRS and BAS1816-17 suggest that *B. anthracis* may be able to integrate multiple signals to better adapt and survive in diverse environments. BAS1814-17 is only conserved in the *Bacillus* genus, it is not found in other *hssRS* encoding bacteria outside this genus. Perhaps this is due to the unique coordination of a sporulation program which the *Bacilli* must integrate with signals from diverse niches including soil, water, plant surfaces, and various insect and mammalian hosts. Alternatively, the cross-signaling between HssRS and BAS1816-17 may occur to supplement HssRS-mediated heme tolerance. *B. anthracis* HssRS is more active than *S. aureus* HssRS and Δ*hrtA B. anthracis* is more sensitive to heme toxicity than Δ*hrtA S. aureus* (83). These data suggest that *B. anthracis* has differential sensitivities and responses to heme toxicity and it is possible that *BAS1814-17* contributes to *Bacilli* adapting to heme stress.

BAS1816-17 and HssRS are more closely related to each other than any of the 45 other TCSs in *B. anthracis*. Moreover, the DR recognized by each RR differs by only four nucleotides. BAS1816-17 is only found in the *Bacillus* genus. These observations suggest that perhaps BAS1816-17 is a paralogous HssRS system in the *Bacillus* genus and that the two TCSs have not

diverged enough to completely eliminate cross-talk. The question remains whether the cross-talk between the TCSs is beneficial to the bacteria and therefore selectively maintained.

One of the most interesting results observed here is the re-engineering of p*14* to be strongly responsive to heme exposure. Upon deletion of HssR and BAS1817, the stimulation of HssS with heme presumably results in the phosphotransfer from HssS to BAS1816 and subsequent activation of p*14*. These results rejoin an idea proposed by Laub and Goulian who stated that:

> "...the ultimate test of whether we understand the specificity of protein-protein interactions throughout two-component pathways will be whether we can redesign or rationally engineer these systems. Can pathways, in effect, be rewired to execute novel functions (41)?"

In this chapter, the dissection of cross-talk between HssRS and BAS1816-17 has in fact allowed us to rewire the *B. anthracis* response to heme toxicity. This provides an exciting foundation for controlling *B. anthracis* signaling networks and potentially manipulating the bacterial response to its environment.

CHAPTER VI

SUMMARY

Conclusions

S. aureus and *B. anthracis* are two closely related pathogens. The pathogenesis of each of these organisms often consists of a significant blood component. While the blood is relatively devoid of free iron, both *S. aureus* and *B. anthracis* are capable of lysing red blood cells and acquiring heme-coordinated iron from host hemoglobin (50, 51, 58). This heme can be degraded to release free iron or trafficked to the cell membrane, presumably for use intact as a protein co-factor (75-77). An overabundance of heme is toxic, but these pathogens can alleviate heme toxicity by activating the heme regulated transporter (HrtAB) through the heme sensing system (HssRS) (85, 90). The *hssRS*/*hrtAB* systems are conserved across Gram positive pathogens as a mechanism for overcoming the heme paradox (1, 90). Identifying the mechanisms by which HssRS senses heme toxicity will provide insight into the mechanisms by which many Gram positive pathogens successfully adapt to the mammalian host.

Here a chemical genetics approach was utilized for dissecting the mechanisms of HssRS activation. An HTS for small molecule activators of *S. aureus* HssRS resulted in the identification of approximately fifteen small molecules that activate HssRS. These top compounds were then screened for activity in *B. anthracis* and several were also able to stimulate the *hrt* promoter (p*hrt*) in *B. anthracis*. This chemical genetics approach to probing TCS biology has yielded new models for how bacteria regulate heme homeostasis, innovative strategies for targeting bacterial energy production during infection, and a deeper understanding of how bacterial signaling networks are integrated to enable adaptation to complex environments.

Identified in the VICB small molecule library, compound ‘882, was the most potent activator of *S. aureus* HssRS. To dissect the mechanism of ‘882-induced HssRS activation, the

residues required for heme sensing by HssS were compared to the residues required for ‘882 sensing and found to be similar. This suggested a common mechanism of HssS activation by both ‘882 and heme. The simplest hypothesis is that ‘882 stimulates endogenous heme biosynthesis to activate HssS. This is indeed the case as HssS is not activated by ‘882 in a strain lacking endogenous heme biosynthesis and ‘882 treatment results in the accumulation of intracellular heme. Since ‘882 stimulates endogenous heme this indicates that HssS actually senses intracellular heme stress. These studies neither rule out the possibility that HssS may directly sense heme, nor that a product of heme toxicity is the ligand of HssS.

The stimulation of endogenous heme biosynthesis by ‘882 is unprecedented and provides an excellent probe for studying the regulation of endogenous heme biosynthesis. To study how *S. aureus* regulates heme biosynthesis, genes that contribute to ‘882 sensing were identified in a transposon screen. Many genes involved in central metabolism contributed to the activation of HssRS by ‘882. In fact, when multiple metabolic parameters of *S. aureus* energy production were monitored, it was determined that ‘882 suppresses fermentation. This suggests that heme biosynthesis may, in part, be regulated by the metabolic state of the cell. This is intuitive as heme is a critical co-factor for enzymes involved in energy homeostasis, most notably the cytochromes in the electron transport chain.

The hypothesis that heme biosynthesis is integrated with energy homeostasis is bolstered by the observation that suppressing upper glycolysis coordinately suppressed heme biosynthesis. While it is clear that the energetic state of the bacterial cell impacts the regulation of heme biosynthesis, the exact cellular signals and factors that form the interface between these two cellular processes remain elusive. Further studies utilizing ‘882 and knowledge gained here may help tease apart these fundamental aspects of *S. aureus* physiology.

The noted impact of ‘882 treatment on fermentative processes evoked the intriguing possibility that ‘882 may adversely affect *S. aureus* under conditions where the bacteria are generating energy solely by fermentation. This proved to be correct as growth of *S. aureus* in an

anaerobic chamber dramatically lowers the IC_{50} of ‘882 for wildtype *S. aureus*. The IC_{50} is further reduced for the two lab generated SCV strains *hemB::ermC* and Δ*menB*, which rely on fermentation to generate energy. These data, along with other data presented in Chapter III, indicate that ‘882 is specifically toxic to fermenting *S. aureus*.

No known antibiotics specifically target energy production in bacteria, especially fermentation, despite it being thought to be an important component of infection. Furthermore, identifying fermentation inhibitors by HTS is difficult to perform due to the required outfitting of an anaerobic chamber with HTS equipment. Thus, compound ‘882 presents a unique tool for investigating the importance of fermentation in bacterial pathogenesis and antibiotic resistance.

In dual therapy, ‘882 prevents the outgrowth of antibiotic resistance to gentamicin, reaffirming that fermentation is required for resistance to aminoglycosides. Furthermore, gentamicin is not used in monotherapy to treat *S. aureus* infections due to the high association of antibiotic resistance; it is sometimes used in a combination with a β-lactam or vancomycin, which is synergistic. The prevention of resistance to gentamicin by ‘882 has exciting potential to expand the current strategies used to treat *S. aureus* infections by repurposing an already approved antibiotic. This strategy is analogous to the antibiotic coctail amoxicillin-clavulanate, which combines a β-lactam with a β-lactamase inhibitor. This combination therapy prevents bacterial β-lactamases from inactivating amoxicillin and successfully treats many bacterial infections.

In monotherapy, ‘882 enhances neutrophil mediated killing of *S. aureus ex vivo*, and *in vivo* the ‘882 derivative, ‘373, reduces bacterial and abscess burdens in the liver. These exciting observations indicate that fermentation is important *in vivo*. That is, at certain points during pathogenesis *S. aureus* must rely on fermentation to successfully colonize the host. These processes most likely include resisting phagocytosis and forming absecesses. Since fermentation is a branched process, and since ‘882 seems to target fermentation in general, these data provide an insight into the role of fermentation in pathogenesis which cannot be provided with traditional genetic techniques.

Fermentation is likely to be important in pathogenesis more generally. Many pathogens including the *Clostridia* and the *Streptococci* genera only ferment, but most pathogens are more akin to *S. aureus* in that they are metabolically flexible and can generate energy through both fermentation and respiration. Since many pathogens utilize fermentation, it is possible that targeting this important energy generating process may be a new antibiotic strategy. This is supported by the observation that ‘882 is also toxic to *C. diphtheriae in vitro*. Further work investigating the anaerobic toxicity of ‘882 toward other pathogens or screening for other small molecules that target fermenting bacteria may provide valuable tools to the medical community for broadening the therapeutic strategies used to combat recalcitrant pathogens. As highlighted at the beginning of this section, compounds that manipulate energy homeostasis may also be powerful probes for understanding basic bacterial physiology.

The sensitivity of *S. aureus* to ‘882 under anaerobic conditions indicates that there are processes absolutely critical to anaerobic growth. Identifying the source of ‘882 toxicity would allow future studies to develop small molecules with better activity either through SAR improvements of ‘882 or the identification of other inhibitors by HTS. In order to identify the source of ‘882 toxicity, spontaneously ‘882-resistant strains were isolated and determined to have genetic mutations that result in lost SaeRS activity. Studying the ‘882 sensitivity profiles of a series of isogenic *sae* operon mutants revealed that it is the hyperactivity of *S. aureus* strain Newman SaeS that results in anaerobic ‘882 toxicity.

Although it is possible that a detrimental cross-talk event between the SaeRS and HssRS TCSs could be the source of toxicity, our current hypothesis is that a cellular factor impacted by SaeRS function is the source of ‘882 toxicity. The current model is that ‘882 interacts with a protein up-regulated by SaeRS activity to generate a toxic by-product that cannot be tolerated in anaerobic conditions. Ablating SaeRS activity could titrate that target to low levels which may prevent ‘882 toxicity from occurring. Identifying the source of anaerobic ‘882 toxicity will provide insight into *S. aureus* physiology and point to potential antibacterial drug targets.

Work presented here highlights the utility of '882 as a probe of *S. aureus* cell biology and identifies new therapeutic strategies for treating *S. aureus* infections. At the most basic level, '882 has revealed that bacterial heme sensors may generally sense intracellular heme, not only extracellular heme as previously thought. To determine if any of the hits from the HTS may also prove to be powerful probes of HssRS activity and provide additional insights into basic bacterial biology in other species, the top hits from the HTS were screened for p*hrt* activation in *B. anthracis.*

Compound '205 was identified to activate p*hrt* independent of HssRS. This is due to the activation of a previously uncharacterized TCS BAS1816-17. BAS1816-17 was predicted to regulate a DR in p*14*, which is similar to the p*hrt* DR recognized by HssR (12). Using '205 to stimulate BAS1816-17 enabled the dissection of a complex signaling network between BAS1816-17 and HssRS. The four nucleotides that differentiate the p*hrt* and p*14* DRs are sufficient to determine the response of each promoter to heme or '205. The exception is that the high basal activity of the p*hrt* promoter requires the p*hrt* DR, but the p*hrt* DR is not sufficient to induce high basal activation of the p*14* promoter. In all, the high basal activity of p*hrt* requires the p*hrt* DR, HssR, and the approximately 200 bp that encompass p*hrt.* This implicates other *cis*- or *trans*-acting cellular factors in the high basal level of p*hrt* activation. Despite the high basal activity of p*hrt*, it is clear that BAS1816-17 can interact with p*hrt* at the RR-DR level. Correspondingly, p*14* is activated in high concentrations of heme and this may occur at either the HK-RR or RR-DR level.

The activation of p*14* by heme-stimulated HssRS in wildtype *S. aureus* indicates that there is natural cross-talk between these systems. The function of BAS1814-15 and why it is activated in the presence of heme remains unclear. To better understand the function of BAS1814-15 and the natural conditions that activate BAS1816-17, Biolog Phenotypic Microarray plates were used to identify four other activators of BAS1816-17. Although none of these activators have a known function in *B. anthracis*, studies on the activity of the compounds in

other organisms suggest that BAS1816-17 may be activated by cell envelope stress or alterations in the electrochemical potential across the cell membrane. This hypothesis is further supported by the identification of a sixth BAS1816-17 activator, targocil. Targocil inhibits the transport of WTAs to the outer leaflet of the *S. aureus* cell membrane, resulting in cell envelope stress and the accumulation of WTA on the inner leaflet of the membrane (89). Since WTA is polyanionic, targocil may not only disrupt the cell envelope but may also disrupt the electrochemical potential across the membrane. Confirming the natural function of BAS1816-17 is essential for understanding if the cross-talk between HssRS and BAS1816-17 is a relic of evolutionary similarity between the TCSs or a beneficial event that enables *Bacilli* to adapt to multiple environmental perturbations. If cross-regulation between HssRS and BAS1816-17 is indeed advantageous, identifying the ligand of each HK and the substrate of each ABC transporter (HrtAB and BAS1814-15) may clarify the mechanisms of heme toxicity and tolerance in Gram positive pathogens.

Future directions

Elaborate the mechanisms by which heme homeostasis and energy metabolism are coordinated. Studies presented here point to the coordination of *S. aureus* heme biosynthesis with energy homeostasis. Inhibiting upper glycolysis suppresses heme biosynthesis while repressing fermentation stimulates heme biosynthesis. These observations suggest that a metabolic signal produced between upper glycolysis and fermentation regulates heme biosynthesis. The model is that inhibiting upper glycolysis decreases the metabolic signal and coordinately reduces heme biosynthesis, while inhibiting fermentation results in a build-up in the metabolic signal, which stimulates heme biosynthesis.

In order to identify the metabolic signal that regulates heme biosynthesis, a combined genetic and chemical biology approach may continue to provide insights. Each step in glycolysis and fermentation may be systematically inhibited either by genetically ablating each gene or

chemical targeting each step. The effect of manipulating each step in glycolysis and fermentation on heme biosynthesis may reveal the source of the metabolic signal.

Alternatively, a primarily chemistry driven strategy may be employed to delineate the mechanisms by which central metabolism impacts heme biosynthesis. SAR studies on ‘882 have identified chemical moieties on ‘882 that tolerate permutation. At these points, compound ‘882 may be modified to include probe-based elements. These elements can then be used to cross-link ‘882 to cellular binding partners, which may then be identified by mass spectrometry. Identifying the true binding partners of ‘882 may help elucidate the mechanisms by which ‘882 is exerting its effects on both heme biosynthesis and anaerobic toxicity.

Identify the source of ‘882 toxicity. The importance of identifying the source of anaerobic ‘882 toxicity hinges on extending the utility of ‘882 from a probe of basic bacterial physiology to one that provides direction for the development of antibacterial agents. Presumably ‘882 is manipulating *S. aureus* metabolism in a way that is incompatible with fermentative growth. Understanding what *S. aureus* cannot tolerate under anaerobic conditions will aid in improving ‘882 activity or identifying more effective molecules that target bacterial energy production.

Current efforts to identify the source of anaerobic ‘882 toxicity are focused on determining the role of SaeRS regulated gene targets in providing resistance to ‘882 or sensitivity to anaerobic growth. Approximately 80% of the genes predicted to be regulated by SaeRS under anaerobiosis are available in the NARSA *S. aureus* defined transposon library. Since the other 20% are not identified in the NARSA library, this suggests that they may be essential. The genes available in the NARSA library will be transduced into *S. aureus* strain Newman and then assessed for ‘882 sensitivity. If none of those genes prove to be the source of anaerobic toxicity, this will narrow the list of potential targets to the other 20% of the SaeRS regulatory targets. Either chemical inhibitors or siRNAs may be used to titrate levels of the remaining putative targets and subsequently investigate their role in anaerobic growth and ‘882 toxicity.

Correspondingly, each remaining gene of interest could be cloned under a constitutive promoter to assess the effect of overexpression of these putative targets on ‘882 toxicity and anaerobic growth.

Since ‘882 suppressor strains arose at a mutation rate of 1 in 10^7 bacteria and all have non-functional SaeRS TCSs, this indicates that mutation of the *sae* operon happens at a rate similar to most other genes in the genome. Viable mutations in the true target of ‘882 may occur at a much lower frequency if they affect bacterial fitness. In order to try to identify other genetic loci involved in ‘882 resistance, the *saePQRS* operon will be integrated into the *hlb* locus of *S. aureus* strain Newman (5). This will yield a merediploid strain of *S. aureus* carrying two copies of the *sae* locus. ‘882 suppressor colonies could then be isolated in this strain. Since there will be two copies of *sae*, the likelihood of isolating a strain with mutations at both *sae* loci will be lower and may permit the identification of other loci involved in providing resistance to ‘882. The mutations can be identified by whole genome sequencing. The role each mutation plays in anaerobic growth and ‘882 toxicity could then be further assessed to determine if it affects the cellular target of ‘882 and may serve as a suitable therapeutic target.

Define the native function of BAS1814-17. BAS1814 and BAS1815 comprise the predicted ABC transporter regulated by the TCS BAS1816-17. The p*14* promoter is activated in the presence of ‘205 by BAS1816-17 and high heme concentrations by HssRS. The impact this cross-talk has on *B. anthracis* heme toxicity and tolerance remains to be explored. Identifying the native function of BAS1814-17 may reveal whether there is a biological benefit of HssRS/BAS1816-17 cross-talk

Currently, six BAS1816-17 activators have been identified. Their known activity in other systems suggests that BAS1816-17 may be sensing perturbations in the cell envelope, perhaps changes in the electrochemical gradient. To identify common cellular events that trigger BAS1816-17 activation, RNASeq could be employed. An RNASeq analysis comparing genes

altered in *B. anthracis* upon exposure to each BAS1816-17 activator may reveal transcriptional changes induced by multiple compounds. Identifying common transcriptional changes that precede BAS1816-17 activation may either confirm that cell envelope stress is indeed a likely activator of BAS1816-17 or may generate other hypotheses about the native function of BAS1816-17. If the activation of BAS1814-17 by heme does have a biological purpose then understanding the native function of this new TCS and ABC transporter will provide insights into the mechanisms by which Gram positive bacteria overcome the heme paradox during infection.

APPENDIX

List of Publications

1. **Mike LA**, Dutter BF, Stauff DL, Moore JL, Vitko NP, Aranmolate O, Kehl-Fie TE, Sullivan S, Reid PR, DuBois JL, Richardson AR, Caprioli RM, Sulikowski GA, Skaar EP. "Activation of heme biosynthesis by a small molecule that is toxic to fermenting *Staphylococcus aureus.*" *PNAS 110 (20),* (2013): 8206-11.

2. Wakeman CA, Hammer ND, Stauff DL, Attia AS, **Anzaldi LL**, Dikalov SI, Calcutt MW, Skaar EP. "Menaquinone biosynthesis potentiates haem toxicity to *Staphylococcus aureus*." *Molecular Microbiology 86,* (2012):1376-92.

3. **Anzaldi LL**, Skaar EP. **"**The evolution of a superbug: How *Staphylococcus aureus* overcomes its unique susceptibility to polyamines." *Molecular Microbiology 82,* (2011): 1-3.

4. **Anzaldi LL**, Skaar EP. **"**Overcoming the heme paradox: Heme toxicity and tolerance in bacterial pathogens." *Infection & Immunity 78,* (2010): 4977-89.

REFERENCES

1. **Anzaldi, L. L., and E. P. Skaar.** 2010. Overcoming the heme paradox: heme toxicity and tolerance in bacterial pathogens. Infect. Immun. **78:**4977-4989.

2. **Bae, T., E. M. Glass, O. Schneewind, and D. Missiakas.** 2008. Generating a collection of insertion mutations in the *Staphylococcus aureus* genome using *bursa aurealis*. Methods Mol Biol **416:**103-16.

3. **Barker, K. D., K. Barkovits, and A. Wilks.** 2012. Metabolic flux of extracellular heme uptake in *Pseudomonas aeruginosa* is driven by the iron-regulated heme oxygenase (HemO). Journal of Biological Chemistry **287:**18342-18350.

4. **Beenken, K. E., P. M. Dunman, F. McAleese, D. Macapagal, E. Murphy, S. J. Projan, J. S. Blevins, and M. S. Smeltzer.** 2004. Global gene expression in *Staphylococcus aureus* biofilms. J Bacteriol **186:**4665-84.

5. **Boles, B. R., M. Thoendel, A. J. Roth, and A. R. Horswill.** 2010. Identification of genes involved in polysaccharide-independent *Staphylococcus aureus* biofilm formation. PLoS ONE **5:**e10146.

6. **Bryan, L. E., and S. Kwan.** 1981. Aminoglycoside-resistant mutants of *Pseudomonas aeruginosa* deficient in cytochrome d, nitrite reductase, and aerobic transport. Antimicrob Agents Chemother **19:**958-64.

7. **Burka, L. T., K. D. Washburn, and R. D. Irwin.** 1991. Disposition of [^{14}C]furan in the male F344 rat. J Toxicol Environ Health **34:**245-57.

8. **Cai, S. J., and M. Inouye.** 2002. EnvZ-OmpR interaction and osmoregulation in *Escherichia coli*. J Biol Chem **277:**24155-61.

9. **Calvin, M.** 1961. Chemical evolution. Oregon State System of Higher Education, Eugene, OR.

10. **Campbell, J., A. K. Singh, J. G. Swoboda, M. S. Gilmore, B. J. Wilkinson, and S. Walker.** 2012. An antibiotic that inhibits a late step in wall teichoic acid biosynthesis induces the cell wall stress stimulon in *Staphylococcus aureus*. Antimicrob Agents Chemother **56:**1810-20.

11. **Cheng, A. G., A. C. DeDent, O. Schneewind, and D. Missiakas.** 2011. A play in four acts: *Staphylococcus aureus* abscess formation. Trends Microbiol **19:**225-32.

12. **de Been, M., M. J. Bart, T. Abee, R. J. Siezen, and C. Francke.** 2008. The identification of response regulator-specific binding sites reveals new roles of two-component systems in *Bacillus cereus* and closely related low-GC Gram-positives. Environ Microbiol **10:**2796-809.

13. **DeLeo, F. R., B. A. Diep, and M. Otto.** 2009. Host defense and pathogenesis in *Staphylococcus aureus* infections. Infectious disease clinics of North America **23:**17-34.

14. **Doss, M., and W. K. Philipp-Dormston.** 1973. Regulatory link between lactate dehydrogenase and biosynthesis of porphyrin and heme in microorganisms. Enzyme **16**.

15. **Drucker, A. M., and C. F. Rosen.** 2011. Drug-induced photosensitivity. Drug Safety **34:**821-837.

16. **Duthie, E. S., and L. L. Lorenz.** 1952. Staphylococcal coagulase: mode of action and antigenicity. J Gen Microbiol **6:**95-107.

17. **Duwat, P., S. Sourice, B. Cesselin, G. Lamberet, K. Vido, P. Gaudu, Y. Le Loir, F. Violet, P. Loubiere, and A. Gruss.** 2001. Respiration capacity of the fermenting bacterium *Lactococcus lactis* and its positive effects on growth and survival. J Bacteriol **183:**4509-16.

18. **Fernandez, A., D. Lechardeur, A. Derre-Bobillot, E. Couve, P. Gaudu, and A. Gruss.** 2010. Two coregulated efflux transporters modulate intracellular heme and protoporphyrin IX availability in *Streptococcus agalactiae*. PLoS Pathog **6:**e1000860.

19. **Fitzpatrick, T. B., N. Amrhein, B. Kappes, P. Macheroux, I. Tews, and T. Raschle.** 2007. Two independent routes of *de novo* vitamin B6 biosynthesis: not that different after all. Biochem J **407:**1-13.

20. **Frankenberg-Dinkel, N.** 2004. Bacterial heme oxygenases. Antioxid Redox Signal **6:**825-34.

21. **Frazier, A. A., T. J. Franks, and J. R. Galvin.** 2006. Inhalational Anthrax. Journal of Thoracic Imaging **21:**252-258 10.1097/01.rti.0000213570.71161.84.

22. **Frunzke, J., C. Gatgens, M. Brocker, and M. Bott.** 2011. Control of heme homeostasis in *Corynebacterium glutamicum* by the two-component system HrrSA. J Bacteriol **193:**1212-21.

23. **Fuller, J. R., N. P. Vitko, E. F. Perkowski, E. Scott, D. Khatri, J. S. Spontak, L. R. Thurlow, and A. R. Richardson.** 2011. Identification of a lactate-quinone oxidoreductase in *Staphylococcus aureus* that is essential for virulence. Front Cell Infect Microbiol **1:**19.

24. **Geiger, T., C. Goerke, M. Mainiero, D. Kraus, and C. Wolz.** 2008. The virulence regulator Sae of *Staphylococcus aureus*: promoter activities and response to phagocytosis-related signals. J Bacteriol **190:**3419-28.

25. **Giraudo, A. T., A. L. Cheung, and R. Nagel.** 1997. The *sae* locus of *Staphylococcus aureus* controls exoprotein synthesis at the transcriptional level. Arch Microbiol **168:**53-8.

26. **Giraudo, A. T., C. G. Raspanti, A. Calzolari, and R. Nagel.** 1994. Characterization of a Tn551-mutant of *Staphylococcus aureus* defective in the production of several exoproteins. Can J Microbiol **40:**677-81.

27. **Gorwitz, R. J., D. Kruszon-Moran, S. K. McAllister, G. McQuillan, L. K. McDougal, G. E. Fosheim, B. J. Jensen, G. Killgore, F. C. Tenover, and M. J. Kuehnert.** 2008. Changes in the prevalence of nasal colonization with *Staphylococcus aureus* in the United States, 2001-2004. Journal of Infectious Diseases **197:**1226-1234.

28. **Groban, E. S., E. J. Clarke, H. M. Salis, S. M. Miller, and C. A. Voigt.** 2009. Kinetic buffering of cross talk between bacterial two-component sensors. Journal of Molecular Biology **390:**380-393.

29. **Grzegorzewicz, A. E., H. Pham, V. A. Gundi, M. S. Scherman, E. J. North, T. Hess, V. Jones, V. Gruppo, S. E. Born, J. Kordulakova, S. S. Chavadi, C. Morisseau, A. J. Lenaerts, R. E. Lee, M. R. McNeil, and M. Jackson.** 2012. Inhibition of mycolic acid transport across the *Mycobacterium tuberculosis* plasma membrane. Nat Chem Biol **8:**334-41.

30. **The Human Microbiome Project Consortium.** 2012. Structure, function and diversity of the healthy human microbiome. Nature **486:**207-214.

31. **Horton, R. M., Z. L. Cai, S. N. Ho, and L. R. Pease.** 1990. Gene splicing by overlap extension: tailor-made genes using the polymerase chain reaction. Biotechniques **8:**528-35.

32. **Jeong, D. W., H. Cho, M. B. Jones, K. Shatzkes, F. Sun, Q. Ji, Q. Liu, S. N. Peterson, C. He, and T. Bae.** 2012. The auxiliary protein complex SaePQ activates the phosphatase activity of sensor kinase SaeS in the SaeRS two-component system of *Staphylococcus aureus*. Mol Microbiol **86:**331-48.

33. **Johansson, P., and L. Hederstedt.** 1999. Organization of genes for tetrapyrrole biosynthesis in Gram-positive bacteria. Microbiology **145:**529-538.

34. **Jurtshuk, P. J.** 1996. Bacterial Metabolism. *In* S. Baron (ed.), Medical Microbiology, 4th ed. University of Texas Medical Branch at Galveston, Galveston

35. **Kahl, B. C., A. Duebbers, G. Lubritz, J. Haeberle, H. G. Koch, B. Ritzerfeld, M. Reilly, E. Harms, R. A. Proctor, M. Herrmann, and G. Peters.** 2003. Population dynamics of persistent *Staphylococcus aureus* isolated from the airways of cystic fibrosis patients during a 6-year prospective study. J Clin Microbiol **41:**4424-7.

36. **Kehl-Fie, T. E., S. Chitayat, M. I. Hood, S. Damo, N. Restrepo, C. Garcia, K. A. Munro, W. J. Chazin, and E. P. Skaar.** 2011. Nutrient metal sequestration by calprotectin inhibits bacterial superoxide defense, enhancing neutrophil killing of *Staphylococcus aureus*. Cell Host Microbe **10:**158-64.

37. **Kim, H. S., D. Sherman, F. Johnson, and A. I. Aronson.** 2004. Characterization of a major *Bacillus anthracis* spore coat protein and its role in spore inactivation. J Bacteriol **186:**2413-7.

38. **Klubes, P., P. J. Fay, and I. Cerna.** 1971. Effects of chlorpromazine on cell wall biosynthesis and incorporation of orotic acid into nucleic acids in *Bacillus megaterium*. Biochemical Pharmacology **20:**265-277.

39. **Koo, S. P., A. S. Bayer, H. G. Sahl, R. A. Proctor, and M. R. Yeaman.** 1996. Staphylocidal action of thrombin-induced platelet microbicidal protein is not solely dependent on transmembrane potential. Infect Immun **64:**1070-4.

40. **Krell, T., J. Lacal, A. Busch, H. Silva-Jimenez, M. E. Guazzaroni, and J. L. Ramos.** 2010. Bacterial sensor kinases: diversity in the recognition of environmental signals. Annu Rev Microbiol **64:**539-59.

41. **Laub, M. T., and M. Goulian.** 2007. Specificity in two-component signal transduction pathways. Annu Rev Genet **41:**121-45.

42. **Lechardeur, D., B. Cesselin, U. Liebl, M. H. Vos, A. Fernandez, C. Brun, A. Gruss, and P. Gaudu.** 2012. Discovery of intracellular heme-binding protein HrtR, which controls heme efflux by the conserved HrtB-HrtA transporter in *Lactococcus lactis*. J Biol Chem **287:**4752-8.

43. **Liang, X., C. Yu, J. Sun, H. Liu, C. Landwehr, D. Holmes, and Y. Ji.** 2006. Inactivation of a two-component signal transduction system, SaeRS, eliminates adherence and attenuates virulence of *Staphylococcus aureus*. Infect Immun **74:**4655-65.

44. **Lin, H., and J. Everse.** 1987. The cytotoxic activity of hematoheme: evidence for two different mechanisms. Anal Biochem **161:**323-31.

45. **Lu, J. M., J. Nurko, S. M. Weakley, J. Jiang, P. Kougias, P. H. Lin, Q. Yao, and C. Chen.** 2010. Molecular mechanisms and clinical applications of nordihydroguaiaretic acid (NDGA) and its derivatives: an update. Med Sci Monit **16:**RA93-100.

46. **Luong, T. T., K. Sau, C. Roux, S. Sau, P. M. Dunman, and C. Y. Lee.** 2011. *Staphylococcus aureus* ClpC divergently regulates capsule via *sae* and *codY* in strain Newman but activates capsule via *codY* in strain UAMS-1 and in strain Newman with repaired *saeS*. J Bacteriol **193:**686-94.

47. **Macias, R. I., J. J. Marin, and M. A. Serrano.** 2009. Excretion of biliary compounds during intrauterine life. World J Gastroenterol **15:**817-828.

48. **Malik, Z., H. Ladan, Y. Nitzan, and B. Ehrenberg.** 1990. The bactericidal activity of a deuteroporphyrin--hemin mixture on gram-positive bacteria. A microbiological and spectroscopic study. Journal of Photochemistry and Photobiology B: Biology **6:**419-430.

49. **Manier, M. L., M. L. Reyzer, A. Goh, V. Dartois, L. E. Via, C. E. Barry, 3rd, and R. M. Caprioli.** 2011. Reagent precoated targets for rapid in-tissue derivatization of the anti-tuberculosis drug isoniazid followed by MALDI imaging mass spectrometry. J Am Soc Mass Spectrom **22:**1409-19.

50. **Maresso, A. W., G. Garufi, and O. Schneewind.** 2008. *Bacillus anthracis* secretes proteins that mediate heme acquisition from hemoglobin. PLoS Pathog **4:**e1000132.

51. **Mazmanian, S. K., E. P. Skaar, A. H. Gaspar, M. Humayun, P. Gornicki, J. Jelenska, A. Joachmiak, D. M. Missiakas, and O. Schneewind.** 2003. Passage of heme-iron across the envelope of *Staphylococcus aureus*. Science **299:**906-9.

52. **McIllmurray, M. B., and J. Lascelles.** 1970. Anaerobiosis and the activity of enzymes of pyrimidine biosynthesis of *Staphylococcus aureus*. J Gen Microbiol **64**.

53. **Mike, L. A., B. F. Dutter, D. L. Stauff, J. L. Moore, N. P. Vitko, O. Aranmolate, T. E. Kehl-Fie, S. Sullivan, P. R. Reid, J. L. Dubois, A. R. Richardson, R. M. Caprioli, G. A. Sulikowski, and E. P. Skaar.** 2013. Activation of heme biosynthesis by a small molecule that is toxic to fermenting Staphylococcus aureus. Proc Natl Acad Sci U S A **110:**8206-11.

54. **Ni, Y., D. Lin, and S. Kokot.** 2005. Synchronous fluorescence and UV-vis spectrometric study of the competitive interaction of chlorpromazine hydrochloride and Neutral Red with DNA using chemometrics approaches. Talanta **65:**1295-1302.

55. **Obaseiki-Ebor, E. E., and J. O. Akerele.** 1988. The mutagenic activity of chlorpromazine. Mutat Res **208:**33-8.

56. **Ordal, G. W.** 1976. Recognition sites for chemotactic repellents of *Bacillus subtilis*. J Bacteriol **126:**72-9.

57. **Panek, H., and M. R. O'Brian.** 2002. A whole genome view of prokaryotic haem biosynthesis. Microbiology **148:**2273-2282.

58. **Papaparaskevas, J., D. P. Houhoula, M. Papadimitriou, G. Saroglou, N. J. Legakis, and L. Zerva.** 2004. Ruling out *Bacillus anthracis*. Emerg Infect Dis **10:**732-5.

59. **Park, M. K., R. A. M. Myers, and L. Marzella.** 1992. Oxygen tensions and infections: modulation of microbial growth, activity of antimicrobial agents, and immunologic responses. Clinical Infectious Diseases **14:**720-740.

60. **Pattee, P. A., and D. S. Neveln.** 1975. Transformation analysis of three linkage groups in *Staphylococcus aureus*. J Bacteriol **124:**201-11.

61. **Pedersen, M. B., C. Garrigues, K. Tuphile, C. Brun, K. Vido, M. Bennedsen, H. Mollgaard, P. Gaudu, and A. Gruss.** 2008. Impact of aeration and heme-activated respiration on *Lactococcus lactis* gene expression: identification of a heme-responsive operon. J Bacteriol **190:**4903-11.

62. **Podgornaia, A. I., and M. T. Laub.** 2013. Determinants of specificity in two-component signal transduction. Curr Opin Microbiol **16:**156-62.

63. **Proctor, R. A., C. von Eiff, B. C. Kahl, K. Becker, P. McNamara, M. Herrmann, and G. Peters.** 2006. Small colony variants: a pathogenic form of bacteria that facilitates persistent and recurrent infections. Nat Rev Microbiol **4:**295-305.

64. **Proctor, R. A., and A. von Humboldt.** 1998. Bacterial energetics and antimicrobial resistance. Drug Resist Updat **1:**227-35.

65. **Quastel, J. H.** 1965. Effects of drugs on metabolism of the brain *in vitro*. Br Med Bull **21:**49-56.

66. **Reniere, M. L., and E. P. Skaar.** 2008. *Staphylococcus aureus* haem oxygenases are differentially regulated by iron and haem. Mol Microbiol **69:**1304-15.

67. **Reniere, M. L., V. J. Torres, and E. P. Skaar.** 2007. Intracellular metalloporphyrin metabolism in *Staphylococcus aureus*. Biometals **20:**333-45.

68. **Reniere, M. L., G. N. Ukpabi, S. R. Harry, D. F. Stec, R. Krull, D. W. Wright, B. O. Bachmann, M. E. Murphy, and E. P. Skaar.** 2010. The IsdG-family of haem oxygenases degrades haem to a novel chromophore. Mol Microbiol **75:**1529-38.

69. **Richardson, A. R., S. J. Libby, and F. C. Fang.** 2008. A nitric oxide-inducible lactate dehydrogenase enables *Staphylococcus aureus* to resist innate immunity. Science **319:**1672-6.

70. **Schafer, D., T. T. Lam, T. Geiger, M. Mainiero, S. Engelmann, M. Hussain, A. Bosserhoff, M. Frosch, M. Bischoff, C. Wolz, J. Reidl, and B. Sinha.** 2009. A point mutation in the sensor histidine kinase SaeS of *Staphylococcus aureus* strain Newman alters the response to biocide exposure. J Bacteriol **191:**7306-14.

71. **Schenkman, J. B., and I. Jansson.** 1998. Spectral Analyses of Cytochromes P450, p. 25-34. *In* I. R. Phillips and E. A. Shephard (ed.), Cytochrome P450 Protocols vol. 107. Humana Press, Totowa, New Jersey.

72. **Schmitt, J., I. Joost, E. P. Skaar, M. Herrmann, and M. Bischoff.** 2012. Haemin represses the haemolytic activity of *Staphylococcus aureus* in an Sae-dependent manner. Microbiology **158:**2619-31.

73. **Schmitt, M. P.** 1999. Identification of a two-component signal transduction system from *Corynebacterium diphtheriae* that activates gene expression in response to the presence of heme and hemoglobin. J Bacteriol **181:**5330-40.

74. **Schneewind, O., P. Model, and V. A. Fischetti.** 1992. Sorting of protein A to the staphylococcal cell wall. Cell **70:**267-81.

75. **Skaar, E. P., A. H. Gaspar, and O. Schneewind.** 2006. *Bacillus anthracis* IsdG, a heme-degrading monooxygenase. J Bacteriol **188:**1071-80.

76. **Skaar, E. P., A. H. Gaspar, and O. Schneewind.** 2004. IsdG and IsdI, heme-degrading enzymes in the cytoplasm of *Staphylococcus aureus*. J Biol Chem **279:**436-43.

77. **Skaar, E. P., M. Humayun, T. Bae, K. L. DeBord, and O. Schneewind.** 2004. Iron-source preference of *Staphylococcus aureus* infections. Science **305:**1626-8.

78. **Skerker, J. M., B. S. Perchuk, A. Siryaporn, E. A. Lubin, O. Ashenberg, M. Goulian, and M. T. Laub.** 2008. Rewiring the specificity of two-component signal transduction systems. Cell **133:**1043-54.

79. **Skerker, J. M., M. S. Prasol, B. S. Perchuk, E. G. Biondi, and M. T. Laub.** 2005. Two-component signal transduction pathways regulating growth and cell cycle progression in a bacterium: a system-level analysis. PLoS Biol **3:**e334.

80. **Somerville, G. A., and R. A. Proctor.** 2009. At the crossroads of bacterial metabolism and virulence factor synthesis in *Staphylococci*. Microbiol Mol Biol Rev **73:**233-48.

81. **Spirites, M. A., and P. S. Guth.** 1963. Effects of chlorpromazine on biological membranes-I.: Chlorpromazine-induced changes in liver mitochondria. Biochemical Pharmacology **12:**37-46.

82. **Stauff, D. L., D. Bagaley, V. J. Torres, R. Joyce, K. L. Anderson, L. Kuechenmeister, P. M. Dunman, and E. P. Skaar.** 2008. *Staphylococcus aureus* HrtA is an ATPase required for protection against heme toxicity and prevention of a transcriptional heme stress response. J Bacteriol **190:**3588-96.

83. **Stauff, D. L., and E. P. Skaar.** 2009. *Bacillus anthracis* HssRS signalling to HrtAB regulates haem resistance during infection. Molecular Microbiology **72:**763-778.

84. **Stauff, D. L., and E. P. Skaar.** 2009. The heme sensor system of *Staphylococcus aureus*. Contrib Microbiol **16:**120-135.

85. **Stauff, D. L., V. J. Torres, and E. P. Skaar.** 2007. Signaling and DNA-binding activities of the *Staphylococcus aureus* HssR-HssS two-component system required for heme sensing. J Biol Chem **282:**26111-26121.

86. **Stephenson, K., and J. A. Hoch.** 2002. Evolution of signalling in the sporulation phosphorelay. Mol Microbiol **46:**297-304.

87. **Sterne, M.** 1937. Avirulent anthrax vaccine. Onderstepoort J Vet Sci Animal Ind **21:**41–43.

88. **Stocker, R., Y. Yamamoto, A. F. McDonagh, A. N. Glazer, and B. N. Ames.** 1987. Bilirubin is an antioxidant of possible physiological importance. Science **235:**1043-6.

89. **Swoboda, J. G., T. C. Meredith, J. Campbell, S. Brown, T. Suzuki, T. Bollenbach, A. J. Malhowski, R. Kishony, M. S. Gilmore, and S. Walker.** 2009. Discovery of a small molecule that blocks wall teichoic acid biosynthesis in *Staphylococcus aureus*. ACS Chem Biol **4:**875-83.

90. **Torres, V. J., D. L. Stauff, G. Pishchany, J. S. Bezbradica, L. E. Gordy, J. Iturregui, K. L. Anderson, P. Dunman, S. Joyce, and E. P. Skaar.** 2007. A *Staphylococcus aureus* regulatory system that responds to host heme and modulates virulence. Cell Host & Microbe **1:**109-119.

91. **von Eiff, C., D. Bettin, R. A. Proctor, B. Rolauffs, N. Lindner, W. Winkelmann, and G. Peters.** 1997. Recovery of small colony variants of *Staphylococcus aureus* following gentamicin bead placement for osteomyelitis. Clin Infect Dis **25:**1250-1.

92. **von Eiff, C., C. Heilmann, R. A. Proctor, C. Woltz, G. Peters, and F. Gotz.** 1997. A site-directed *Staphylococcus aureus hemB* mutant is a small-colony variant which persists intracellularly. J Bacteriol **179:**4706-12.

93. **Wakeman, C. A., N. D. Hammer, D. L. Stauff, A. S. Attia, L. L. Anzaldi, S. I. Dikalov, M. W. Calcutt, and E. P. Skaar.** 2012. Menaquinone biosynthesis potentiates haem toxicity in *Staphylococcus aureus*. Mol Microbiol.

94. **Wang, F., D. Sambandan, R. Halder, J. Wang, S. M. Batt, B. Weinrick, I. Ahmad, P. Yang, Y. Zhang, J. Kim, M. Hassani, S. Huszar, C. Trefzer, Z. Ma, T. Kaneko, K. E. Mdluli, S. Franzblau, A. K. Chatterjee, K. Johnson, K. Mikusova, G. S. Besra, K. Futterer, W. R. Jacobs, Jr., and P. G. Schultz.** 2013. Identification of a small molecule with activity against drug-resistant and persistent tuberculosis. Proc Natl Acad Sci U S A **110:**E2510-7.

95. **Watanakunakorn, C.** 1984. Mode of action and *in-vitro* activity of vancomycin. J Antimicrob Chemother **14 Suppl D:**7-18.

96. **Weinberg, E. D.** 2009. Iron availability and infection. Biochimica et Biophysica Acta (BBA) - General Subjects **1790:**600-605.

97. **Wick, A. N., D. R. Drury, H. I. Nakada, J. B. Wolfe, and with the technical assistance of B. Britton, and R. Grabowski.** 1957. Localization of the primary metabolic block produced by 2-deoxyglucose. Journal of Biological Chemistry **224:**963-969.

98. **Yamamoto, Y., C. Poyart, P. Trieu-Cuot, G. Lamberet, A. Gruss, and P. Gaudu.** 2006. Roles of environmental heme, and menaquinone, in *Streptococcus agalactiae*. Biometals **19:**205-10.

99. **Youngman, P. J., J. B. Perkins, and R. Losick.** 1983. Genetic transposition and insertional mutagenesis in *Bacillus subtilis* with *Streptococcus faecalis* transposon Tn*917*. Proc Natl Acad Sci U S A **80:**2305-9.

100. **Zhu, W., A. Wilks, and I. Stojiljkovic.** 2000. Degradation of heme in gram-negative bacteria: the product of the *hemO* gene of *Neisseriae* is a heme oxygenase. J. Bacteriol. **182:**6783-6790.